Article:
Duncan, LC, Watling, DP, Connors, RD et al. (2022) Choice set robustness and internal consistency in correlation-based logit stochastic user equilibrium models. Transportmetrica A: Transport Science. ISSN: 2324-9935

https://doi.org/10.1080/23249935.2022.2063969

Choice set robustness and internal consistency in correlation-based logit stochastic user equilibrium models

Lawrence Christopher DUNCAN [a,b] *, David Paul WATLING [b], Richard Dominic CONNORS [b,c], Thomas Kjær RASMUSSEN [a], Otto Anker NIELSEN [a]

[a] Department of Technology, Management and Economics, Technical University of Denmark
Bygningstorvet 116B, 2800 Kgs. Lyngby, Denmark.
[b] Institute for Transport Studies, University of Leeds
36-40 University Road, Leeds, LS2 9JT, United Kingdom.
[c] University of Luxembourg, Faculté des Sciences, des Technologies et de Médecine,
Maison du Nombre, 6 Avenue de la Fonte, L-4364, Esch-sur-Alzette, Luxembourg.

* corresponding author:
Department of Technology, Management and Economics, Technical University of Denmark
Bygningstorvet 116B, 2800 Kgs. Lyngby, Denmark.
E-mail: lawdun@dtu.dk

Abstract
The Stochastic User Equilibrium (SUE) traffic assignment model is a well-known approach for investigating the behaviours of travellers on congested road networks. SUE compensates for driver/modelling uncertainty of the route travel costs by supposing the costs include stochastic terms. Two key challenges for SUE modelling, however, are capturing route correlations and dealing with unrealistic routes. Numerous correlation-based SUE models have been proposed, but issues remain over both internal consistency and choice set robustness. This paper develops internally consistent versions of correlation-based logit SUE models, and assesses their choice set robustness and computational feasibility for obtaining internally consistent solutions. We formulate internally consistent SUE formulations for GEV structure and correction term logit route choice models, where the functional forms in the correlation components are based upon generalised, flow-dependent congested costs, rather than e.g. length / free-flow travel time as done typically. The paper proves solutions exist for the SUE models developed. Numerical experiments are then conducted on the Sioux Falls and Winnipeg networks, where computational performance, choice set robustness, and internal consistency are compared. SUE solution uniqueness is explored numerically where results suggest that uniqueness conditions exist.

Key Words: internal consistency, choice set robustness, stochastic user equilibrium, correlation, fixed-point

1 Introduction

The Stochastic User Equilibrium (SUE) traffic assignment model proposed by Daganzo & Sheffi (1977) is a well-known approach for investigating the behaviours of travellers on congested road networks. SUE relaxes the perfect information assumption of the Deterministic User Equilibrium model by supposing that route choice is based on costs that include stochastic terms. This accounts for the differing perceptions travellers have of the attractiveness of routes. A specific challenge when developing a route choice model for SUE is capturing correlations between overlapping routes. There is a trade-off: accurately capturing route correlation in a behaviourally realistic way requires a more complex route choice model, but this results in computational challenges for solving for SUE (e.g. long computation times). Theoretically undesirable trade-offs are thus often made to improve computational performance, but issues with internal consistency and choice set robustness arise. This paper explores and addresses both internal consistency and choice set robustness for correlation-based SUE models.

Different stochastic route cost terms proposed in the literature give rise to different types of correlation-based route choice models that have been applied to SUE. The current study focuses on two of such types: GEV structure models (e.g. Cross-Nested Logit (CNL), Generalised Nested Logit (GNL), Paired Combinatorial Logit (PCL)) and correction term models (e.g. C-Logit (CL), Path Size Logit (PSL), Path Size Weibit (PSW), Path Size Hybrid (PSH)). For detailed reviews of correlation-based route choice models see Prashker & Bekhor (2004) and Duncan et al (2020,2021). SUE and equivalent Mathematical Programming (MP) formulations as well as solution algorithms for GEV structure and correction term models can be found in the following. Equivalent MP formulations for CNL, GNL, and PCL are given by Bekhor & Prashker (1999,2001). Bekhor & Prashker (2001), Chen et al (2003) and Bekhor et al (2008a) provide path-based partial linearization algorithms for solving GNL SUE, PCL SUE, and CNL SUE, respectively. Zhou et al (2012) give equivalent MP and variational inequality formulations for Length-based CL SUE (LCL SUE) and Congestion-based CL SUE (CCL SUE), where length and congestion based refers to whether the correction term is computed using length

or congestion-dependent travel cost. Chen et al (2012a), Kitthamkesorn & Chen (2013), and Xu et al (2015) give equivalent MP formulations for PSL SUE, PSW SUE, and PSH SUE, respectively. Chen et al (2012a) present a path-based partial linearization algorithm for solving LCL SUE and PSL SUE. Zhou et al (2012) present a path-based Gradient Projection algorithm for solving LCL SUE and CCL SUE, and Xu et al (2012) and Chen et al (2013) assess the computational trade-off for different step-size strategies. Kitthamkesorn & Chen (2013) develop a path-based partial linearization algorithm for solving PSW SUE, and Kitthamkesorn & Chen (2014) propose a link-based algorithm.

Although GEV structure models have closed-form probability expressions, due to their multi-level tree structure the choice probabilities and in particular MP formulations are complex to compute, where the computational burden escalates significantly as the scale of network / choice set sizes increase. Correction term models on-the-other-hand have simple closed-form expressions, meaning the route choice probabilities and MP formulations are generally easy and quick to compute; more complex models can capture correlations more accurately, though. Theoretically undesirable trade-offs are often made for GEV structure and correction term models, however, to improve computational performance of applicable algorithms. There are two common types of such trade-offs.

The first trade-off is between desirable behavioural features for the SUE model and the ability to solve it more efficiently. An SUE model is *internally consistent* if the same definition of generalised cost is used in all components of the specification. This is often overlooked in the SUE formulations of GEV structure and correction term models so that solution methods are simpler/quicker to implement. In SUE application where the travel costs within the deterministic utilities are flow-dependent (congested), for consistency, the route similarity features (PCL, CL) or link-route prominence features (CNL, GNL, PSL, PSW, PSH) in the correlation components should also be based upon the congested cost. Most studies use topological length or uncongested cost (free-flow travel time) for these features, however this may be inaccurate behaviourally since a short route can have a large congested travel cost, and vice versa.

The second trade-off is between the sizes of the choice sets generated (pre or column generated) and the ability to solve efficiently. Typical road networks have many very costly routes that should be considered unrealistic and excluded from route choice. In large-scale case studies, choice sets are typically generated to be large enough that one can be fairly certain the realistic alternatives are present, regardless of how many unrealistic routes are generated. However, for many GEV structure and correction term SUE models, the computational burden of solution algorithms increases dramatically as the number of routes increases, which limits how large the choice sets can be generated. Furthermore, many of the models have poor choice set robustness, and results are thus negatively influenced by the presence of unrealistic routes as well as highly sensitive to the choice set generation method adopted (Bovy et al, 2008; Bliemer & Bovy, 2008; Ramming, 2002; Ben-Akiva & Bierlaire, 1999; Duncan et al, 2020,2021). The *choice set robustness* of a model is a measure of how sensitive the route choice probability / route flow results are to the set of routes generated, i.e. a model that has poor choice set robustness may be affected significantly by small changes to the choice set, such as the unintentional inclusion of unrealistic routes.

Motivated by the above challenges, we set out to develop a correlation-based SUE model that addresses both internal consistency and choice set robustness, and is computationally feasible in large-scale network applications. Zhou et al (2012), Xu et al (2012), and Chen et al (2013) explore an internally consistent SUE formulation for the CL model (CCL SUE), where the CCL commonality factors capture the similarity between routes according to their shared flow-dependent congested cost. However, internally consistent SUE formulations are yet to be explored for other GEV structure and correction term models. A novel contribution of this paper is thus addressing this by formulating, proving solution exist of, and solving internally consistent SUE formulations for the CNL, GNL, PCL, and PSL models, where the route similarity or link-route prominence features are based upon generalised, flow-dependent congested cost. We assess the choice set robustness for these models (including CCL SUE), and evaluate their computational performances, including for different sizes of choice sets and scale of network.

None of these models, however, have explicit mechanisms for dealing with unrealistic routes within the adopted choice sets, and thus there are questions over how well these models perform in terms of choice set robustness. For the PSL model, a mechanism has been proposed for dealing with unrealistic routes: to weight the contributions of routes to path size terms, with path size contribution factors. Generalised Path Size Logit (GPSL) (Ramming, 2002) proposes a path size contribution factor based upon travel cost ratios, while Adaptive Path Size Logit (APSL) (Duncan et al, 2020) proposes a factor based upon choice probability ratios – ensuring internal consistency within the specification of the choice model. GPSL and APSL are yet to be applied to SUE, however, and we therefore also formulate, prove solutions exist to, and solve SUE formulations of GPSL and APSL (that are internally consistent), and compare choice set robustness / computational performance. Note that since the APSL choice probabilities are themselves a solution to a fixed-point problem, then embedding APSL within a SUE framework (an outer-loop fixed-point problem) and solving APSL SUE requires special attention. In the paper we formulate an alternative APSL SUE model and develop solution techniques to improve computational performance.

The structure of the paper is as follows. In Section 2 we introduce congested network notation. In Section 3 we detail the internally consistent SUE formulations for the correlation-based route choice models, and prove solution existence. In Section 4 we conduct numerical experiments to assess computational performance and choice set robustness, examine internal consistency, and investigate solution uniqueness. In Section 5 we conclude the paper.

Table 1 lists the abbreviations used throughout the remainder of the paper.

Abbreviation	Definition
MNL	Multinomial Logit
PSL	Path Size Logit
GPSL	Generalised Path Size Logit
APSL	Adaptive Path Size Logit
APSL′	Adaptive Path Size Logit alternative formulation
CL	C-Logit
CNL	Cross-Nested Logit
GNL	Generalised Nested Logit
PCL	Paired Combinatorial Logit
SUE	Stochastic User Equilibrium
FAA	Flow-Averaging Algorithm
FPIM	Fixed-Point Iteration Method
RMSE	Root Mean Squared Error
NRMSE	Normalised Root Mean Squared Error
MP	Mathematical Programming
MSWA	Method of Successive Weighted Averages

Table 1. Abbreviations.

2 Congested Network Notation

A road network consists of link set A and $m = 1, \dots, M$ OD movements. R_m is the choice set of all simple routes (no cycles) for OD movement m of size $N_m = |R_m|$, where $N = \sum_{m=1}^{M} N_m$ is the total number of routes. $A_{m,i} \subseteq A$ is the set of links belonging to route $i \in R_m$, and $\delta_{a,m,i} = \begin{cases} 1 & if\ a \in A_{m,i} \\ 0 & otherwise \end{cases}$.

The travel demand for OD movement m is $q_m \geq 0$, and $\boldsymbol{Q}_m$ is the $N_m \times N_m$ diagonal matrix of the travel demand for OD movement m (i.e. with q_m on each diagonal element). The flow on route $i \in R_m$ is $f_{m,i}$, and $\boldsymbol{f}_m$ is the N_m-length vector of route flows for OD movement m. $\boldsymbol{f}$ is the N-length vector of all OD movement route flow vectors such that $\boldsymbol{f} = (\boldsymbol{f}_1, \dots, \boldsymbol{f}_M)$, where $f_{m,i}$ refers to element number $i + \sum_{k=1}^{m-1} N_k$ in $\boldsymbol{f}$. F denotes the set of all demand-feasible non-negative universal route flow vector solutions:

$$F = \left\{ \boldsymbol{f} \in \mathbb{R}_+^N : \sum_{i \in R_m} f_{m,i} = q_m, m = 1, \dots, M \right\}.$$

Furthermore, x_a denotes the flow on link $a \in A$, and $\boldsymbol{x} = (x_1, x_2, \dots, x_{|A|})$ is the vector of all link flows. X denotes the set of all demand-feasible non-negative link flow vectors:

$$X = \left\{ \boldsymbol{x} \in \mathbb{R}_+^{|A|} : \sum_{m=1}^{M} \sum_{i \in R_m} \delta_{a,m,i} f_{m,i} = x_a, \forall a \in A, \boldsymbol{f} \in F \right\}.$$

For link $a \in A$ experiencing a flow of x_a, denote the generalised travel cost for that link as $t_a(x_a)$, where $\boldsymbol{t}(\boldsymbol{x})$ is the vector of all generalised link travel cost functions. In vector/matrix notation, let $\boldsymbol{x}$ and $\boldsymbol{f}$ be column vectors, and define $\boldsymbol{\Delta}$ as the $|A| \times N$-dimensional link-route incidence matrix. Then the relationship between link and route flows may be written as $\boldsymbol{x} = \boldsymbol{\Delta f}$. Supposing that the travel cost for a route can be attained through summing up the total cost of its links, then the generalised travel cost for route $i \in R_m$, $c_{m,i}$, can be computed as follows: $c_{m,i}\big(\boldsymbol{t}(\boldsymbol{\Delta f})\big) = \sum_{a \in A_{m,i}} t_a(\boldsymbol{\Delta f})$, where $\boldsymbol{c}_m\big(\boldsymbol{t}(\boldsymbol{\Delta f})\big)$ is the vector of generalised travel cost functions for OD movement m.

Let the route choice probability for route $i \in R_m$ be $P_{m,i}$, where $\boldsymbol{P}_m = \big(P_{m,1}, P_{m,2}, \dots, P_{m,N_m}\big)$ is the vector of route choice probabilities for OD movement m, and D_m is the domain of possible route choice probability vectors for OD movement m, $m = 1, \dots, M$.

3 Internally Consistent SUE Formulations for Correlation-Based Logit Route Choice Models

In this section, we detail the congestion-based C-Logit SUE model proposed by Zhou et al (2012), and develop the new internally consistent SUE formulations for the other correction term and GEV structure correlation-based logit route choice models. We then prove the existence of solutions.

3.1 Correction Term Models

Correction term models capture correlations between overlapping routes by including heuristic correction terms within the deterministic utilities. The deterministic utility of route $i \in R_m$ is thus $V_{m,i} = -\theta c_{m,i}(\boldsymbol{t}) + \kappa_{m,i}$, where $\theta > 0$ is the Logit scaling parameter and $\kappa_{m,i} \leq 0$ is the correction term for route $i \in R_m$. The choice probability for route $i \in R_m$ is then:

$$P_{m,i}(\boldsymbol{c}_m(\boldsymbol{t}), \boldsymbol{\kappa}_m) = \frac{e^{-\theta c_{m,i}(\boldsymbol{t}) + \kappa_{m,i}}}{\sum_{j \in R_m} e^{-\theta c_{m,j}(\boldsymbol{t}) + \kappa_{m,j}}}.$$

3.1.1 Regular Path Size Logit SUE Models

Regular Path Size Logit models propose that the correction terms adopt the form $\kappa_{m,i} = \beta \ln(\gamma_{m,i})$, where $\beta \geq 0$ is the path size scaling parameter, and $\gamma_{m,i} \in (0,1]$ is the path size term for route $i \in R_m$. A distinct route with no shared links has a path size term equal to 1, resulting in no penalisation. Less distinct routes have smaller path size terms and incur greater penalisation. The path size terms are often based upon link lengths and thus $\gamma_{m,i}$ (in those cases) is not dependent upon the link/route generalised travel costs. However, this leads to internal inconsistency (as we discuss in more detail below) and in this study we base the path size terms upon on generalised link travel costs (i.e. $\gamma_{m,i} = \gamma_{m,i}(\boldsymbol{t})$), which in SUE application are congested, flow-dependent costs. The choice probability for route $i \in R_m$ is thus:

$$P_{m,i}\big(\boldsymbol{c}_m(\boldsymbol{t}), \boldsymbol{\gamma}_m(\boldsymbol{t})\big) = \frac{e^{-\theta c_{m,i}(\boldsymbol{t}) + \beta \ln\left(\gamma_{m,i}(\boldsymbol{t})\right)}}{\sum_{j \in R_m} e^{-\theta c_{m,j}(\boldsymbol{t}) + \beta \ln\left(\gamma_{m,j}(\boldsymbol{t})\right)}} = \frac{\left(\gamma_{m,i}(\boldsymbol{t})\right)^{\beta} e^{-\theta c_{m,i}(\boldsymbol{t})}}{\sum_{j \in R_m} \left(\gamma_{m,j}(\boldsymbol{t})\right)^{\beta} e^{-\theta c_{m,j}(\boldsymbol{t})}}. \quad (1)$$

The general form for the path size term of route $i \in R_m$ is as follows:

$$\gamma_{m,i}(\boldsymbol{t}) = \sum_{a \in A_{m,i}} \frac{t_a}{c_{m,i}(\boldsymbol{t})} \frac{1}{\sum_{k \in R_m} \left(\frac{W_{m,k}(\boldsymbol{t})}{W_{m,i}(\boldsymbol{t})}\right) \delta_{a,m,k}}, \quad (2)$$

where $W_{m,k}(\boldsymbol{t}) > 0$ is the path size contribution weighting of route $i \in R_m$ to path size terms (different for each model), so that the contribution of route $k \in R_m$ to the path size term of route $i \in R_m$ (the path size contribution factor) is $\frac{W_{m,k}(\boldsymbol{t})}{W_{m,i}(\boldsymbol{t})}$. To dissect the path size term: each link a in route $i \in R_m$ is penalised (in terms of decreasing the path size term and hence the utility of the route) according to the number of routes in the choice set that also use that link $\left(\sum_{k \in R_m} \delta_{a,m,k}\right)$, where each contribution is weighted (i.e. $\sum_{k \in R_m} \left(\frac{W_{m,k}(\boldsymbol{t})}{W_{m,i}(\boldsymbol{t})}\right) \delta_{a,m,k}$), and the significance of the penalisation is also weighted according to how prominent link a is in route $i \in R_m$, i.e. the cost of route a in relation to the total cost of route $i \in R_m$ $\left(\frac{t_a}{c_{m,i}(\boldsymbol{t})}\right)$.

The Path Size Logit (PSL) model (Ben-Akiva & Bierlaire, 1998) proposes that $W_{m,k}(\boldsymbol{t}) = 1$ so that all routes contribute equally to path size terms. This is problematic with the mis-generation of realistic route choice sets, however, as the correction terms and thus the choice probabilities of realistic routes are affected by link sharing with unrealistic routes. To combat this, Ramming (2002) proposed the Generalised Path Size Logit (GPSL) model where $W_{m,k}(\boldsymbol{t}) = \left(c_{m,k}(\boldsymbol{t})\right)^{-\lambda}$, $\lambda \geq 0$, and routes contribute according to travel cost ratios, so that routes with large travel costs have a diminished impact upon the correction terms of routes with small travel costs, and consequently the choice probabilities of those routes.

Most studies of PSL SUE, or of SUE models with PSL path size terms, suppose that the link-route prominence feature is represented as the ratio of link-route length, i.e. $\frac{t_a}{c_{m,i}(\boldsymbol{t})} = \frac{l_a}{L_{m,i}}$, where l_a and $L_{m,i}$ are the lengths of link $a \in A$ and route $i \in R_m$, respectively. However, this may be inaccurate in how travellers perceive the prominence of links in a route: a short link may be highly congested and have a greater travel time than a long link that is uncongested, and hence the timely, short link may be perceived as more prominent in the route than the long, quick link. A similar argument can be made for using other uncongested costs, e.g. free-flow travel time. Thus, for internal consistency, the path size term defined in (2) above considers generalised travel cost for the link-route prominence feature.

In the context of SUE, the generalised travel costs include congested cost and are thus flow-dependent. Adopting generalised, flow-dependent congested costs for the link-route prominence features, SUE for a Path Size Logit model can be formulated as follows:

Path Size Logit model SUE: A universal route flow vector $\boldsymbol{f}^* \in F$ is an SUE solution for a Path Size Logit model iff the route flow vector for OD movement m, $\boldsymbol{f}_m^*$, is a solution to the fixed-point problem

$$\boldsymbol{f}_m = \boldsymbol{Q}_m \boldsymbol{P}_m\left(\boldsymbol{c}_m\left(\boldsymbol{t}(\boldsymbol{\Delta f})\right), \boldsymbol{\gamma}_m\left(\boldsymbol{t}(\boldsymbol{\Delta f}), \boldsymbol{W}_m\left(\boldsymbol{t}(\boldsymbol{\Delta f})\right)\right)\right), \qquad m = 1, \dots, M, \tag{3}$$

where $P_{m,i}$ and $\gamma_{m,i}$ are as in (1) and (2) for route $i \in R_m$, respectively, given the universal route flow vector $\boldsymbol{f}$. $\boldsymbol{Q}_m$ is travel demand diagonal matrix for OD movement m so that $\boldsymbol{f}_m = \boldsymbol{Q}_m \boldsymbol{P}_m$ results in $f_{m,i} = q_m P_{m,i}$, $\forall i \in R_m$.

3.1.2 Adaptive Path Size Logit SUE

As shown in Duncan et al (2020), the APSL model provides an internally consistent approach to reducing the negative effects unrealistic routes have on the correction terms (and thus choice probabilities) of realistic routes. To do this, path size contributions are weighted according to ratios of choice probability, and APSL is consequently naturally expressed as a fixed-point problem. APSL is thus not a 'regular' Path Size Logit model in that it does not assume the form in (1) and (2).

Since at SUE the route flow proportions and route choice probabilities are equal, APSL SUE can be defined in two different ways. These two definitions are equal at equilibrium, but not equal for any other route flow vector. We define and discuss each definition in turn below.

3.1.2.1 Definition 1: APSL SUE

Formulation of the APSL model was complicated by the desire to establish existence and uniqueness of solutions. To circumvent issues with the standard APSL formulation, a modified version was proposed where solutions are guaranteed to exist and are unique under determinable conditions. Moreover, the standard formulation can be approximated to arbitrary precision. We thus provide here the definition of and establish SUE conditions for the final proposed definition of APSL, see Duncan et al (2020) for more details on its derivation.

The APSL route choice probabilities for OD movement m, $\boldsymbol{P}_m^*$, (for a choice set of size N_m) are a solution to the fixed-point problem $\boldsymbol{P}_m = \boldsymbol{G}_m\left(\boldsymbol{g}_m\left(\boldsymbol{c}_m(\boldsymbol{t}), \boldsymbol{\gamma}_m^{APS}(\boldsymbol{t}, \boldsymbol{P}_m)\right)\right)$, where:

$$G_{m,i}\left(g_{m,i}\left(\boldsymbol{c}_m(\boldsymbol{t}), \boldsymbol{\gamma}_m^{APS}(\boldsymbol{t}, \boldsymbol{P}_m)\right)\right) = \tau_m + (1 - N_m\tau_m) \cdot g_{m,i}\left(\boldsymbol{c}_m(\boldsymbol{t}), \boldsymbol{\gamma}_m^{APS}(\boldsymbol{t}, \boldsymbol{P}_m)\right), \tag{4}$$

$$g_{m,i}\left(\boldsymbol{c}_m(\boldsymbol{t}), \boldsymbol{\gamma}_m^{APS}(\boldsymbol{t}, \boldsymbol{P}_m)\right) = \frac{\left(\gamma_{m,i}^{APS}(\boldsymbol{t}, \boldsymbol{P}_m)\right)^{\beta} e^{-\theta c_{m,i}(\boldsymbol{t})}}{\sum_{j \in R_m}\left(\gamma_{m,j}^{APS}(\boldsymbol{t}, \boldsymbol{P}_m)\right)^{\beta} e^{-\theta c_{m,j}(\boldsymbol{t})}}, \tag{5}$$

$$\gamma_{m,i}^{APS}(\boldsymbol{t}, \boldsymbol{P}_m) = \sum_{a \in A_{m,i}} \frac{t_a}{c_{m,i}(\boldsymbol{t})} \frac{P_{m,i}}{\sum_{k \in R_m} P_{m,k}\delta_{a,m,k}} = \sum_{a \in A_{m,i}} \frac{t_a}{c_{m,i}(\boldsymbol{t})} \frac{1}{\sum_{k \in R_m}\left(\frac{P_{m,k}}{P_{m,i}}\right)\delta_{a,m,k}}, \tag{6}$$

$$\forall i \in R_m, \qquad \forall \boldsymbol{P}_m \in D_m^{(\tau_m)}, \qquad D_m^{(\tau_m)} = \left\{\boldsymbol{P}_m \in \mathbb{R}_{>0}^{N_m} : \tau_m \le P_{m,i} \le (1 - (N_m - 1)\tau_m), \forall i \in R_m, \sum_{j=1}^{N_m} P_{m,j} = 1\right\}.$$

$\theta > 0$ is the Logit scaling parameter, $\beta \ge 0$ is the path size scaling parameter, and $0 < \tau_m \le \frac{1}{N_m}$, $m = 1, \dots, M$, are the perturbation parameters. $\gamma_{m,i}^{APS}$ is the APSL path size term function, $g_{m,i}$ is the choice probability function, and $G_{m,i}$ is the probability adjustment function.

As shown in (6), for a choice probability solution $\boldsymbol{P}_m^*$, the contribution of route k to the path size term of route i is weighted according to the ratio of choice probabilities between the routes $\left(\frac{P_{m,k}^*}{P_{m,i}^*}\right)$, and hence unrealistic route alternatives with very low choice probabilities have a diminished contribution to the path size terms of realistic routes with relatively large choice probabilities. The APSL model is thus internally consistent as the probability relation and path size terms both define a route as unrealistic if it has a relatively unattractive combination of travel cost and distinctiveness. Moreover, unlike GPSL, an additional parameter to scale the path size contributions is not required as this is done implicitly and consistently through the scaling of the probabilities with θ and β. This has practical and behavioural estimation benefits compared to GPSL (Duncan et al, 2020).

The APSL model is not closed-form since the choice probabilities for each OD movement are the solution to a fixed-point problem. The τ_m parameters are not model parameters that require estimating, they are simply a mathematical construct that ensure solutions to the APSL model exist and can be unique; specifically, they ensure that the probability domain $D_m^{(\tau_m)}$ for the fixed-point function $\boldsymbol{G}_m$ is closed and bounded, while avoiding issues occurring from zero choice probabilities. Duncan et al (2020) recommend that only very small values for τ_m are used so that the

fixed-point solution obtained is negligibly different to the fixed-point solution if $\tau_m = 0$ (where one would exist). We thus set $\tau_m = 10^{-16}$, $m = 1, \dots, M$, throughout this paper.

APSL SUE – where for internal consistency the link-route prominence feature considers flow-dependent, congested cost – can be formulated as follows:

APSL SUE: A universal route flow vector $\boldsymbol{f}^* \in F^{(\boldsymbol{\tau})}$ is an APSL SUE solution iff the route flow vector for OD movement m, $\boldsymbol{f}_m^*$, is a solution to the fixed-point problem

$$\boldsymbol{f}_m = \boldsymbol{Q}_m \boldsymbol{P}_m^*\big(\boldsymbol{t}(\boldsymbol{\Delta f})\big), \qquad m = 1, \dots, M, \tag{7}$$

where $\boldsymbol{P}_m^*$ is a route choice probability solution for OD movement m in $\boldsymbol{Y}_m$ to the fixed-point problem

$$\boldsymbol{Y}_m = \boldsymbol{G}_m\left(\boldsymbol{g}_m\left(\boldsymbol{c}_m\big(\boldsymbol{t}(\boldsymbol{\Delta f})\big), \boldsymbol{\gamma}_m^{APS}(\boldsymbol{t}(\boldsymbol{\Delta f}), \boldsymbol{Y}_m)\right)\right), \tag{8}$$

given the universal route flow vector $\boldsymbol{f}$, where $G_{m,i}$, $g_{m,i}$, and $\gamma_{m,i}^{APS}$ are as in (4), (5), and (6) for route $i \in R_m$, respectively, and

$$F^{(\boldsymbol{\tau})} = \left\{\boldsymbol{f} \in \mathbb{R}_{>0}^{N} : \tau_m \le \frac{f_{m,i}}{q_m} \le (1 - (N_m - 1)\tau_m), \forall i \in R_m, \sum_{i \in R_m} f_{m,i} = q_m, m = 1, \dots, M\right\}.$$

APSL SUE is derived directly by utilising APSL as the underlying route choice model and applying flow-dependent link travel costs. For a given route flow vector and hence setting of the link costs, the APSL fixed-point system must be re-solved, so that the path size contribution factors are consistent with the relative attractiveness of the routes. This ensures that the choice model is internally consistent for all route flow vectors.

The APSL model restricts the domain for the route choice probabilities so that the probabilities for OD movement m must belong to the domain $D_m^{(\tau_m)}$, where $P_{m,i} \ge \tau_m$, $\forall i \in R_m$. Consequently, the set of all demand-feasible universal route flow vector solutions for the APSL SUE model, $F^{(\boldsymbol{\tau})}$, is also restricted, where $f_{m,i} \ge \tau_m q_m$, $\forall i \in R_m$, $m = 1, \dots, M$.

3.1.2.2 Definition 2: APSL′ SUE

APSL SUE Definition 2 (APSL′ SUE) is derived indirectly by utilising a new underlying route choice model, that is equivalent to APSL at SUE, but only at SUE. By the definition of SUE, the route flow proportions and route choice probabilities equate at equilibrium. Therefore, APSL′ SUE supposes that the path size contribution factors consider route flow proportion ratios, instead of choice probability. The underlying route choice model, APSL′, proposes that the choice probability for route $i \in R_m$ is:

$$P_{m,i}\left(g_{m,i}\left(\boldsymbol{c}_m(\boldsymbol{t}), \boldsymbol{\gamma}_m^{APS'}(\boldsymbol{t}, \boldsymbol{f}_m)\right)\right) = \tau_m + (1 - N_m\tau_m) \cdot g_{m,i}\left(\boldsymbol{c}_m(\boldsymbol{t}), \boldsymbol{\gamma}_m^{APS'}(\boldsymbol{t}, \boldsymbol{f}_m)\right), \tag{9}$$

$$g_{m,i}\left(\boldsymbol{c}_m(\boldsymbol{t}), \boldsymbol{\gamma}_m^{APS'}(\boldsymbol{t}, \boldsymbol{f}_m)\right) = \frac{\left(\gamma_{m,i}^{APS'}(\boldsymbol{t}, \boldsymbol{f}_m)\right)^{\beta} e^{-\theta c_{m,i}(\boldsymbol{t})}}{\sum_{j \in R_m}\left(\gamma_{m,j}^{APS'}(\boldsymbol{t}, \boldsymbol{f}_m)\right)^{\beta} e^{-\theta c_{m,j}(\boldsymbol{t})}}, \tag{10}$$

$$\gamma_{m,i}^{APS'}(\boldsymbol{t}, \boldsymbol{f}_m) = \sum_{a \in A_{m,i}} \frac{t_a}{c_{m,i}(\boldsymbol{t})} \frac{f_{m,i}/q_m}{\sum_{k \in R_m}(f_{m,k}/q_m)\delta_{a,m,k}} = \sum_{a \in A_{m,i}} \frac{t_a}{c_{m,i}(\boldsymbol{t})} \frac{f_{m,i}}{\sum_{k \in R_m} f_{m,k}\delta_{a,m,k}}, \tag{11}$$

$$\forall \boldsymbol{f}_m \in F_m^{>0}, \qquad F_m^{>0} = \left\{\boldsymbol{f}_m \in \mathbb{R}_{>0}^{N_m} : \sum_{i \in R_m} f_{m,i} = q_m\right\}.$$

The model parameters are again $\theta > 0$, $\beta \ge 0$, and $0 < \tau_m \le \frac{1}{N_m}$, $m = 1, \dots, M$. As shown in (11), the contribution of route $k \in R_m$ to the path size term of route $i \in R_m$ is weighted according to the ratio of flow between the routes $\left(\frac{f_{m,k}}{f_{m,i}}\right)$, and hence unrealistic route alternatives with very low use/flow have a diminished contribution to the path size terms of realistic routes with relatively high use/flow.

The APSL′ choice model is closed-form and hence choice probability solutions for a given route flow vector are guaranteed to exist and be unique, assuming every route has a non-zero flow. Stipulating that the flows for OD movement m $\boldsymbol{f}_m$ belong to the set $F_m^{>0}$ ensures that: a) no routes have zero flow; b) the route flows are demand-feasible; and, c) the path size contribution factors consider ratios of route flow proportion. The APSL′ choice model need not only

be considered in an SUE application; regardless of whether the link costs are flow-dependent or fixed, if information is available on the route flow proportions then the path size contribution factors can utilise this for route choice prediction.

Adopting generalised, flow-dependent congested costs for the link-route prominence features, APSL′ SUE is formulated as follows:

APSL′ SUE: A universal route flow vector $\boldsymbol{f}^* \in F^{(\boldsymbol{\tau})}$ is an APSL SUE solution iff the route flow vector for OD movement m, $\boldsymbol{f}_m^*$, is a solution to the fixed-point problem

$$\boldsymbol{f}_m = \boldsymbol{Q}_m \boldsymbol{P}_m \left(\boldsymbol{g}_m \left(\boldsymbol{c}_m\big(\boldsymbol{t}(\boldsymbol{\Delta f})\big), \boldsymbol{\gamma}_m^{APS'}\big(\boldsymbol{t}(\boldsymbol{\Delta f}), \boldsymbol{f}_m\big) \right) \right), \qquad m = 1, \dots, M, \tag{12}$$

where $P_{m,i}$, $g_{m,i}$, and $\gamma_{m,i}^{APS'}$ are as in (9), (10), and (11) for route $i \in R_m$, respectively, given the universal route flow vector $\boldsymbol{f}$, and

$$F^{(\boldsymbol{\tau})} = \left\{ \boldsymbol{f} \in \mathbb{R}_{>0}^{N} : \tau_m \leq \frac{f_{m,i}}{q_m} \leq (1 - (N_m - 1)\tau_m), \forall i \in R_m, \sum_{i \in R_m} f_{m,i} = q_m, m = 1, \dots, M \right\}.$$

The APSL′ choice model is only internally consistent for route flow vectors at SUE, since for all other route flow vectors, the relative attractiveness of routes as defined in the path size contribution factors does not match the relative attractiveness in the probability relation.

3.1.3 C-Logit SUE

C-Logit (CL) proposes that the correction terms adopt the form $\kappa_{m,i} = \ln\big(\sigma_{m,i}\big)$, where $\upsilon \leq 0$ is the commonality scaling parameter, and $\sigma_{m,i} \in [1, \infty)$ is the commonality factor for route $i \in R_m$. The choice probability for route $i \in R_m$ is thus:

$$P_{m,i}\big(\boldsymbol{c}_m(\boldsymbol{t}), \boldsymbol{\sigma}_m(\boldsymbol{t})\big) = \frac{e^{-\theta c_{m,i}(\boldsymbol{t}) + \upsilon \ln\left(\sigma_{m,i}(\boldsymbol{t})\right)}}{\sum_{j \in R_m} e^{-\theta c_{m,j}(\boldsymbol{t}) + \upsilon \ln\left(\sigma_{m,j}(\boldsymbol{t})\right)}} = \frac{\left(\sigma_{m,i}(\boldsymbol{t})\right)^{\upsilon} e^{-\theta c_{m,i}(\boldsymbol{t})}}{\sum_{j \in R_m} \left(\sigma_{m,j}(\boldsymbol{t})\right)^{\upsilon} e^{-\theta c_{m,j}(\boldsymbol{t})}}. \tag{13}$$

Routes not similar in any way to any other route have commonality factors equal to 1 (similar only to itself) and no penalisation is incurred. Routes that are more similar to other routes (in terms of shared congested travel cost) have greater commonality factors and incur greater penalisation. Cascetta et al (1996) proposed several functional forms for the commonality factor, however the congestion-based functional form adopted by Zhou et al (2012), and thus adopted in this paper, is as follows for route $i \in R_m$:

$$\sigma_{m,i}(\boldsymbol{t}) = \sum_{k \in R_m} \frac{\sum_{a \in A_{m,i}} t_a \delta_{a,m,i} \delta_{a,m,k}}{\sqrt{c_{m,i}(\boldsymbol{t})} \cdot \sqrt{c_{m,k}(\boldsymbol{t})}}, \tag{14}$$

where $\sum_{a \in A_{m,i}} t_a \delta_{a,m,i} \delta_{a,m,k}$ is the shared congested travel cost between routes $i \in R_m$ and $k \in R_m$.

CL SUE can thus be formulated as follows:

CL SUE: A universal route flow vector $\boldsymbol{f}^* \in F$ is a CL SUE solution iff the route flow vector for OD movement m, $\boldsymbol{f}_m^*$, is a solution to the fixed-point problem

$$\boldsymbol{f}_m = \boldsymbol{Q}_m \boldsymbol{P}_m \left(\boldsymbol{c}_m\big(\boldsymbol{t}(\boldsymbol{\Delta f})\big), \boldsymbol{\sigma}_m\big(\boldsymbol{t}(\boldsymbol{\Delta f})\big) \right), \qquad m = 1, \dots, M, \tag{15}$$

where $P_{m,i}$ and $\sigma_{m,i}$ are as in (13) and (14) for route $i \in R_m$, respectively, given the universal route flow vector $\boldsymbol{f}$.

3.2 GEV Structure Models

GEV structure models are those that are based on the Generalized Extreme Value (GEV) theory (McFadden, 1978), which use a multi-level tree structure to capture the similarity among routes through the random error component of the utility function.

3.2.1 Cross-Nested Logit SUE

The Cross-Nested Logit (CNL) model was adapted to the context of route choice by Prashker & Bekhor (1998) and Bekhor & Prashker (1999). Their adaptation uses a two-level nesting structure in which the upper level (nests) includes all the links in the network. The lower level consists of all the routes in the choice set R_m for OD movement m, and each of the routes is allocated to all the link nests that that route consists of. The nest inclusion parameters $\alpha_{a,m,i}$ represent the proportion of link a used by alternative $i \in R_m$. For more than a handful of routes and links, however, the number of

independent nest inclusion parameters becomes very large, making estimation difficult. Seeking to address this, Prashker & Bekhor (1998) proposed a functional form for these parameters based on the network topology. These link-route prominence features are represented in terms of length or free-flow travel time however, which is not internally consistent. Addressing this so that the nest inclusion parameters $\alpha_{a,m,i}(\boldsymbol{t})$ are based upon flow-dependent congested cost, the choice probability for route $i \in R_m$ is:

$$P_{m,i}(\boldsymbol{t}) = \sum_{a \in A_{m,i}} P_{m,(a)}(\boldsymbol{t}) \cdot P_{m,(i|a)}(\boldsymbol{t}), \tag{16}$$

where

$$P_{m,(i|a)}(\boldsymbol{t}) = \frac{\left(\alpha_{a,m,i}(\boldsymbol{t}) \exp\left(-\theta c_{m,i}(\boldsymbol{t})\right)\right)^{1/\mu}}{\sum_{j \in R_m}\left(\alpha_{a,m,j}(\boldsymbol{t}) \exp\left(-\theta c_{m,j}(\boldsymbol{t})\right)\right)^{1/\mu}}, \tag{17}$$

and

$$P_{m,(a)}(\boldsymbol{t}) = \frac{\left(\sum_{k \in R_m}\left(\alpha_{a,m,k}(\boldsymbol{t}) \exp\left(-\theta c_{m,k}(\boldsymbol{t})\right)\right)^{1/\mu}\right)^{\mu}}{\sum_{b \in A}\left(\sum_{k \in R_m}\left(\alpha_{b,m,k}(\boldsymbol{t}) \exp\left(-\theta c_{m,k}(\boldsymbol{t})\right)\right)^{1/\mu}\right)^{\mu}}, \tag{18}$$

where $\alpha_{a,m,i}(\boldsymbol{t}) = \frac{t_a}{c_{m,i}(\boldsymbol{t})} \cdot \delta_{a,m,i}$, and $\mu \in (0,1]$ indicates the degree of nesting such that when $\mu = 1$ CNL collapses to MNL.

CNL SUE can thus be formulated as follows:

CNL SUE: A universal route flow vector $\boldsymbol{f}^* \in F$ is a CNL SUE solution iff the route flow vector for OD movement m, $\boldsymbol{f}^*_m$, is a solution to the fixed-point problem

$$\boldsymbol{f}_m = \boldsymbol{Q}_m \boldsymbol{P}_m\big(\boldsymbol{t}(\boldsymbol{\Delta f})\big), \qquad m = 1, \dots, M, \tag{19}$$

where $P_{m,i}$ is as in (16)-(18) for route $i \in R_m$, respectively, given the universal route flow vector $\boldsymbol{f}$.

3.2.2 Generalised Nested Logit SUE

Bekhor & Prashker (2001) generalise CNL by introducing a functional form for the nesting coefficient μ, to be a parameterised average value of the nest inclusion coefficients. With congestion-based inclusion coefficients, the Generalised Nested Logit (GNL) model proposes that the choice probability for route $i \in R_m$ is as in (16)-(18), where the nesting coefficient μ for link nest a and OD movement m is: $\mu_{a,m}(\boldsymbol{t}) = \left(1 - \frac{\sum_{i \in R_m} \alpha_{a,m,i}(\boldsymbol{t})}{\sum_{i \in R_m} \delta_{a,m,i}}\right)^{\lambda}$, $\lambda \geq 0$. GNL SUE is thus as in (19) but with flow-dependent nesting coefficients as above. Note that routes consisting of a single link between the origin and destination result in the nesting coefficient $\mu_{a,m}(\boldsymbol{t})$ for that link being equal to 0, since $\sum_{i \in R_m} \alpha_{a,m,i}(\boldsymbol{t}) = \sum_{i \in R_m} \delta_{a,m,i} = 1$. This results in the GNL model being undefined.

3.2.3 Paired Combinatorial Logit SUE

The Paired Combinatorial Logit (PCL) model was adapted to the context of route choice by Prashker & Bekhor (1998). Here, each pair of routes in a choice set form a nest and routes are chosen from each nest. Within each nest, $\sigma_{m,i,j}$ is the similarity index between routes $i \in R_m$ and $j \in R_m$. Like CNL/GNL, individually estimating each of these parameters for each nest becomes infeasible for more than a handful of routes. Instead, Prashker & Bekhor (1998) propose a functional form for these similarity indexes, proposing that the similarity between routes is measured according to the C-Logit commonality factor. These commonality factors are formulated in terms of shared length / uncongested travel cost however, which is not internally consistent. Addressing this so that the similarity index parameters $\sigma_{m,i,j}(\boldsymbol{t})$ are based upon flow-dependent congested cost, the choice probability for route $i \in R_m$ is

$$P_{m,i}(\boldsymbol{t}) = \sum_{j \in R_m; j \neq i} P_{m,(i,j)}(\boldsymbol{t}) \cdot P_{m,(i|i,j)}(\boldsymbol{t}), \tag{20}$$

where

$$P_{m,(i|i,j)}(\boldsymbol{t}) = \frac{\exp\left(\frac{-\theta c_{m,i}(\boldsymbol{t})}{1-\sigma_{m,i,j}(\boldsymbol{t})}\right)}{\exp\left(\frac{-\theta c_{m,i}(\boldsymbol{t})}{1-\sigma_{m,i,j}(\boldsymbol{t})}\right)+\exp\left(\frac{-\theta c_{m,j}(\boldsymbol{t})}{1-\sigma_{m,i,j}(\boldsymbol{t})}\right)}, \tag{21}$$

and

$$P_{m,(i,j)}(\boldsymbol{t}) = \frac{\left(1-\sigma_{m,i,j}(\boldsymbol{t})\right)\cdot\left(\exp\left(\frac{-\theta c_{m,i}(\boldsymbol{t})}{1-\sigma_{m,i,j}(\boldsymbol{t})}\right)+\exp\left(\frac{-\theta c_{m,j}(\boldsymbol{t})}{1-\sigma_{m,i,j}(\boldsymbol{t})}\right)\right)^{1-\sigma_{m,i,j}(\boldsymbol{t})}}{\sum_{k=1}^{N_m-1}\sum_{l=k+1}^{N_m}\left(1-\sigma_{m,k,l}(\boldsymbol{t})\right)\cdot\left(\exp\left(\frac{-\theta c_{m,k}(\boldsymbol{t})}{1-\sigma_{m,k,l}(\boldsymbol{t})}\right)+\exp\left(\frac{-\theta c_{m,l}(\boldsymbol{t})}{1-\sigma_{m,k,l}(\boldsymbol{t})}\right)\right)^{1-\sigma_{m,k,l}(\boldsymbol{t})}}, \tag{22}$$

where $\sigma_{m,i,j}(\boldsymbol{t}) = \left(\frac{\sum_{a\in A_{m,i}} t_a \delta_{a,m,i}\delta_{a,m,j}}{\sqrt{c_{m,i}(\boldsymbol{t})}\cdot\sqrt{c_{m,j}(\boldsymbol{t})}}\right)^{\lambda}$, $\lambda \geq 0$, is the similarity index between routes $i \in R_m$ and $j \in R_m$. PCL collapses to MNL when similarity indexes are all equal to zero.

PCL SUE can thus be formulated as follows:

PCL SUE: A universal route flow vector $\boldsymbol{f}^* \in F$ is a PCL SUE solution iff the route flow vector for OD movement m, $\boldsymbol{f}_m^*$, is a solution to the fixed-point problem

$$\boldsymbol{f}_m = \boldsymbol{Q}_m \boldsymbol{P}_m\big(\boldsymbol{t}(\boldsymbol{\Delta f})\big), \qquad m = 1, \dots, M, \tag{23}$$

where $P_{m,i}$ is as in (20)-(22) for route $i \in R_m$, respectively, given the universal route flow vector $\boldsymbol{f}$.

3.3 Existence of Solutions

Zhou et al (2012) prove existence for the congestion-based CL SUE model formulated above, and in a similar vein, in this subsection we prove that solutions are guaranteed to exist to all of the other SUE models developed above. Proving existence for most of the models is straightforward, however existence for APSL/APSL′ SUE requires a little more thought. We will therefore first provide a generic proof which can be applied to the non-APSL/ APSL′ SUE models, and then independently prove the existence of APSL/APSL′ SUE solutions.

We begin by defining an important function: the SUE fixed-point function. Let $H_{m,i}(\boldsymbol{f}) = q_m P_{m,i}(\boldsymbol{f})$, where $P_{m,i}(\boldsymbol{f})$ is the choice probability for route $i \in R_m$ given by either (1), (16), or (20) for the appropriate model, dependent upon $\boldsymbol{f}$. It is clear from (3), (19), and (23) that a route flow solution $\boldsymbol{f}^*$ is an SUE solution iff $H_{m,i}(\boldsymbol{f}^*) = f_{m,i}^*, \forall i \in R_m$, $m = 1, \dots, M$. Let $\boldsymbol{H}(\boldsymbol{f})$ be the vector of all SUE fixed-point functions $H_{m,i}$, with the same ordering as $\boldsymbol{f}$.

Proposition 1: If the link cost function $\boldsymbol{t}(\boldsymbol{\Delta f})$ is a continuous function for all $\boldsymbol{f} \in F$, then at least one SUE fixed-point route flow solution, $\boldsymbol{f}^* \in F$, is guaranteed to exist for the SUE fixed-point systems in (3), (19), and (23).

Proof. From the assumption that $\boldsymbol{t}(\boldsymbol{\Delta f})$ is a continuous function for all $\boldsymbol{f} \in F$, (and thus $\boldsymbol{H}$ is continuous), and given that F is a nonempty, convex, and compact set, and $\boldsymbol{H}$ maps F into itself, then by Brouwer's Fixed-Point Theorem at least one solution $\boldsymbol{f}^*$ exists such that $\boldsymbol{H}(\boldsymbol{f}^*) = \boldsymbol{f}^*$, and hence solutions are guaranteed to exist for the SUE fixed-point systems in (3), (19), and (23).

■

For APSL/APSL′ SUE, we prove that solutions are guaranteed to exist to the APSL′ SUE fixed-point system as defined in (12), and thus the APSL SUE fixed-point system defined in (7)-(8), due to equivalence in equilibrium.

Now, let $H_{m,i}(\boldsymbol{f}) = q_m P_{m,i}\left(g_{m,i}\left(\boldsymbol{c}_m\big(\boldsymbol{t}(\boldsymbol{\Delta f})\big), \boldsymbol{\gamma}_m^{APS'}(\boldsymbol{t}(\boldsymbol{\Delta f}), \boldsymbol{f}_m)\right)\right)$, where $P_{m,i}$, $g_{m,i}$, and $\gamma_{m,i}^{APS'}$ are as in (9), (10), and (11), respectively, for route $i \in R_m$. It is clear from (12) that a route flow solution $\boldsymbol{f}^*$ is an APSL′ SUE solution iff $H_{m,i}(\boldsymbol{f}^*) = f_{m,i}^*, \forall i \in R_m, m = 1, \dots, M$. Let $\boldsymbol{H}(\boldsymbol{f})$ be the vector of all APSL′ SUE fixed-point functions $H_{m,i}$, with the same ordering as $\boldsymbol{f}$.

We first clarify an important property of $\boldsymbol{H}(\boldsymbol{f})$ required for the proof of existence of APSL′ SUE solutions.

Property 1: $\boldsymbol{H}(\boldsymbol{f})$ maps $F^{(\tau)}$ into itself.

Proof. Let $Z_{m,i}(\boldsymbol{f}) = P_{m,i}\left(g_{m,i}\left(\boldsymbol{c}_m(\boldsymbol{t}), \boldsymbol{\gamma}_m^{APS'}(\boldsymbol{t}, \boldsymbol{f}_m)\right)\right), \forall i \in R_m, m = 1, \dots, M$, where $\boldsymbol{Z}(\boldsymbol{f})$ is the N-length vector of all $Z_{m,i}$, with the same ordering as $\boldsymbol{f}$. It is clear that $\boldsymbol{Z}(\boldsymbol{f})$ maps into

$$D^{(\boldsymbol{\tau})} = \left\{\boldsymbol{P} \in \mathbb{R}_{>0}^{N_m} : \tau_m \leq P_{m,i} \leq (1 - (N_m - 1)\tau_m), \forall i \in R_m, \sum_{j=1}^{N_m} P_{m,j} = 1, m = 1, \dots, M\right\}.$$

From inspection, it follows that $\boldsymbol{H}(\boldsymbol{f}) = \boldsymbol{Q}\boldsymbol{Z}(\boldsymbol{f})$ maps into $F^{(\boldsymbol{\tau})}$, since $f_{m,i} = q_m P_{m,i}, \forall i \in R_m, m = 1, \dots, M$.

■

Given $\boldsymbol{H}(\boldsymbol{f})$ and Property 1, we prove that APSL′ SUE solutions are guaranteed to exist.

Proposition 2: If the link cost function $\boldsymbol{t}(\boldsymbol{\Delta f})$ is a continuous function for all $\boldsymbol{f} \in F^{(\boldsymbol{\tau})}$, then at least one APSL′ SUE fixed-point route flow solution, $\boldsymbol{f}^* \in F^{(\boldsymbol{\tau})}$, is guaranteed to exist.

Proof. From the assumption that $\boldsymbol{t}(\boldsymbol{\Delta f})$ is a continuous function for all $\boldsymbol{f} \in F^{(\boldsymbol{\tau})}$, (and thus $\boldsymbol{c}_m$, $\boldsymbol{\gamma}_m^{APS'}$, $g_{m,i}$, $P_{m,i}$, and $\boldsymbol{H}$ are all continuous), and given that $F^{(\boldsymbol{\tau})}$ is a nonempty, convex, and compact set, and by Property 1 $\boldsymbol{H}$ maps $F^{(\boldsymbol{\tau})}$ into itself, then by Brouwer's Fixed-Point Theorem at least one solution $\boldsymbol{f}^*$ exists such that $\boldsymbol{H}(\boldsymbol{f}^*) = \boldsymbol{f}^*$, and hence APSL′ SUE solutions are guaranteed to exist.

■

Next, we clarify the equivalence of APSL SUE and APSL′ SUE.

Lemma 1: If $\boldsymbol{f}^* \in F^{(\boldsymbol{\tau})}$ is an APSL′ SUE solution, $\boldsymbol{f}^* \in F^{(\boldsymbol{\tau})}$ is also an APSL SUE solution.

Proof. This follows by inspection from the equivalence of (4), (5), and (6) with (9), (10), and (11), respectively, when $P_{m,i} = \frac{f_{m,i}}{q_m}, \forall i \in R_m, m = 1, \dots, M$, and hence for an APSL′ SUE solution $\boldsymbol{f}^* \in F^{(\boldsymbol{\tau})}$ where $P_{m,i} = \frac{f_{m,i}^*}{q_m}$.

■

What remains is to prove the existence of APSL SUE solutions.

Proposition 3: If the link cost function $\boldsymbol{t}(\boldsymbol{\Delta f})$ is a continuous function, then at least one APSL SUE fixed-point route flow solution, $\boldsymbol{f}^* \in F^{(\boldsymbol{\tau})}$, is guaranteed to exist.

Proof. It follows from Proposition 2 and Lemma 1 that since APSL′ SUE solutions are guaranteed to exist, and an APSL′ SUE solution is also always an APSL SUE solution, then at least one APSL SUE fixed-point route flow solution $\boldsymbol{f}^* \in F^{(\boldsymbol{\tau})}$ is guaranteed to exist.

■

4 Numerical Experiments

In this section, some numerical experiments are conducted to assess computational performance and choice set robustness for the internally consistent correlation-based SUE models detailed in Section 3. We also examine the two types of internal consistency in the paper and investigate solution uniqueness.

4.1 Experiment Setup

The computer used has a 2.10GHz Intel Xeon CPU and 512GB RAM, and the code was implemented in Python. In our implementation, we assume that a working set of routes is available in advance to solve the SUE models. The advantage of using a working route set (i.e. generated from a choice set generation scheme) is that it provides a common basis for the comparison of various models. Behaviourally, it has the advantage of identifying routes that would likely to be used (Cascetta et al, 1997; Bekhor et al 2008b). However, a column generation procedure (e.g. Chen et al, 2001) could also be used.

In our experiments, we consider two well-known networks: Sioux Falls and Winnipeg. The Sioux Falls network consists of 24 nodes, 76 links, and 528 OD movements (with positive demands), and the Winnipeg network consists of 1052 nodes, 2836 links, and 4345 OD movements.

In general, the generalised travel cost, $t_a(x_a)$, for link $a \in A$ may consist of several flow-dependent and flow-independent attributes, for example congested travel time, length, number of left turns, etc. However, for the numerical experiments in this section and for all networks, the travel cost of link $a \in A$ is specified as the flow-dependent travel

time $T_a(x_a)$ only, where the volume-delay link cost functions for all networks are based on the Bureau of Public Road (BPR) formula with link-specific parameters:

$$t_a(x_a) = T_a(x_a) = T_{0,a}\left(1 + D\left(\frac{x_a}{K_a}\right)^B\right),$$

where $T_{0,a}$ and K_a are the free-flow travel time and capacity of link $a \in A$, respectively, and $D, B \geq 0$. For the Sioux Falls and Winnipeg networks, the link-cost function values as well as the network and demand data are obtained from https://github.com/bstabler/TransportationNetworks.

In Bekhor et al (2008b), working choice sets for both the Sioux Falls and Winnipeg networks are generated by using a combination of the link elimination method (Azevedo et al, 1993) and link penalty method (De La Barra et al, 1993). These same choice sets are used in numerous other studies, e.g. Chen et al (2012b,2013,2014), Xu et al (2012), Zhou et al (2012). For Sioux Falls, the maximum and average generated choice set sizes for an OD movement were 13 and 6.3, respectively. For Winnipeg, 174,491 routes were generated in total, and the maximum and average choice set sizes for an OD movement were 50 and 40.1, respectively. It would definitely be a possibility to use the same route generation method to generate the route choice sets for this study, which would then facilitate comparisons across the studies. However, with this generation method, we believe the aim was to generate a set of realistic alternatives without any possibility of generating unrealistic routes. As discussed further in e.g. Watling et al (2015,2018); Duncan et al (2021), with this approach, it is difficult to say with any certainty that no realistic alternative has been left out, since the route generation criteria is not consistent with the calculation of the choice probabilities among chosen routes, i.e. a route found by the generation criteria may be considered unrealistic by the choice probability criteria, and vice versa.

Therefore, for the numerical experiments in this paper, we generated new working choice sets for the Sioux Falls and Winnipeg networks. From experimenting with different settings and generation methods, we ultimately generated as large choice sets as we deemed our computational resources would allow, in order to minimise the possibility that we had excluded what would later turn out to be a plausible route from the working choice set. For the Sioux Falls network, the working choice sets were obtained by generating all routes with a free-flow travel time less than 2.5 times greater than the free-flow travel time on the quickest route for each OD movement. This technique was not viable computationally for the Winnipeg network; instead, we utilised a simulation approach (Sheffi & Powell, 1982) where the link costs were drawn randomly from a truncated normal distribution with mean value being free-flow travel time and standard deviation being 0.6 times the mean. The link costs were simulated 150 times for each OD movement and for each simulation shortest path was conducted to generate a route, where a maximum of 100 unique routes were generated for each choice set. The average and maximum free-flow travel time relative deviations from the quickest route in each choice set were 1.14 and 3.2, respectively. For Sioux Falls, 42,976 routes were generated in total, and the maximum, average, and median choice set sizes for an OD movement were 898, 116, and 6, respectively. For Winnipeg, 305,005 routes were generated in total, and the maximum, average, and median choice set sizes for an OD movement were 100, 70, and 88, respectively. As can be seen, these choice sets are considerably larger than those generated in Bekhor et al (2008b). In Supplementary Material A&B and Section 4.4 we investigate how varying the choice set sizes effects computational performance and choice set robustness, respectively.

It is not expected that equivalent Mathematical Programming (MP) formulations can be derived for the internally consistent SUE formulations in this paper. This is due to the correlation components being flow-dependent, e.g. based upon the flow-dependent congested costs. For example, as Zhou et al (2012) explain for congestion-based CL SUE: since the CL commonality factors are nonlinear flow-dependent functions, CL SUE cannot be formulated as an equivalent MP formulation, and thus cannot be obtained through solving some convex optimisation problem. Instead, we use a standard Flow-Averaging Algorithm (FAA) to solve all SUE models, where a step-size scheme averages the route flows between the current flow vector and an auxiliary flow vector computed from the route choice probabilities of the underlying choice model. The FAA is as follows:

$$f_{m,i}^{(n)} = (1 - \eta_n) \cdot f_{m,i}^{(n-1)} + \eta_n \cdot q_m P_{m,i}\left(\boldsymbol{f}^{(n-1)}\right), \qquad n = 1,2,3 \ldots$$

such that

$$\lim_{n\to\infty} f_{m,i}^{(n)} = \lim_{n\to\infty} (1 - \eta_n) \cdot f_{m,i}^{(n-1)} + \eta_n \cdot q_m P_{m,i}\left(\boldsymbol{f}^{(n-1)}\right) = f_{m,i}^{*}, \qquad \forall i \in R_m, m = 1, \ldots, M, \qquad \boldsymbol{f}^{(0)} \in F,$$

where $f_{m,i}^{(n)}$ is the flow for route $i \in R_m$ at iteration n, η_n is the step-size at iteration n, and $P_{m,i}\left(\boldsymbol{f}^{(n-1)}\right)$ is the choice probability for route $i \in R_m$ at iteration n given the route flows from iteration $n-1$. For the APSL & APSL′ SUE models, the feasible set of route flows is $F^{(\boldsymbol{\tau})}$ rather than F.

The step-size scheme we adopt in this paper is the Method of Successive Weighted Averages (MSWA) (Liu et al, 2009), which is based upon the well-known Method of Successive Averages (MSA). While being pre-defined, the MSWA allows giving higher weight to auxiliary flow patterns from later iterations, and the step-size η_n at iteration n is defined as:

$$\eta_n = \frac{n^d}{\sum_{k=1}^{n} k^d},$$

where $d \geq 0$ is the MSWA parameter. Increasing the value of d moves more flow towards the auxiliary solution. The MSA is a special case of the MSWA, namely when $d = 0$.

Convergence of the FAA is measured by the Root Mean Squared Error (RMSE) between the final route flow vector and auxiliary route flow vector at iteration n:

$$RMSE^{(n)} = \sqrt{\frac{1}{N}\sum_{m=1}^{M}\sum\nolimits_{i\in R_m}\left(f_{m,i}^{(n)} - \bar{f}_{m,i}^{(n)}\right)^2},$$

where $f_{m,i}^{(n)}$ and $\bar{f}_{m,i}^{(n)}$ are the final route flow and auxiliary route flow for route $i \in R_m$ at iteration n, and N is the total number of routes. The route flows are thus said to have converged sufficiently to a route flow vector solution $\boldsymbol{f}^* = \boldsymbol{f}^{(n)}$ if $RMSE^{(n)} < 10^{-\zeta}$, where ζ is a predetermined flow convergence parameter.

For PSL, GPSL, APSL′, CL, CNL, GNL, & PCL SUE, the auxiliary flows are computed exactly since the probability relations are closed-form. For APSL SUE, however, the accuracy of the auxiliary flows is dependent upon the accuracy of the APSL fixed-point probabilities. To ensure that APSL SUE is reached, when the RMSE convergence criteria are said to have converged, we check by computing the RMSE between the final route flow vector and an auxiliary route flow vector calculated from APSL′ probabilities, which at iteration n is:

$$RMSE^{(n)} = \sqrt{\frac{1}{N}\sum_{m=1}^{M}\sum\nolimits_{i\in R_m}\left(f_{m,i}^{(n)} - q_m P_{m,i}\left(\boldsymbol{c}_m\left(\boldsymbol{t}(\boldsymbol{\Delta f}^{(n)}), \boldsymbol{\gamma}_m^{APS\prime}(\boldsymbol{t}(\boldsymbol{\Delta f}^{(n)}), \boldsymbol{f}^{(n)})\right)\right)\right)^2}.$$

We continue until this RMSE satisfies the convergence criterion, or it is clear that this convergence criterion will not be satisfied.

Computing the APSL **choice probabilities** (at each iteration of the FAA) also requires a fixed-point algorithm. In general, there are many fixed-point algorithms available for solving the APSL fixed-point system. In this study, we use the Fixed-Point Iteration Method (FPIM) (Isaacson & Keller, 1966), which Duncan et al (2020) also use. Other algorithms were considered, however the performance and convergence of the FPIM in our tests were sufficiently promising that we did not consider this worthwhile. The FPIM for solving the APSL choice probabilities for OD movement m at iteration n of the FAA is as follows:

$$P_{m,i}^{[s]} = G_{m,i}\left(g_{m,i}\left(\boldsymbol{c}_m\left(\boldsymbol{t}(\boldsymbol{\Delta f}^{(n)})\right), \boldsymbol{\gamma}_m^{APS}\left(\boldsymbol{t}(\boldsymbol{\Delta f}^{(n)}), \boldsymbol{P}_m^{[s-1]}\right)\right)\right), \qquad s = 1,2,3,\ldots$$

such that

$$\lim_{s\to\infty} P_{m,i}^{[s]} = \lim_{s\to\infty} G_{m,i}\left(g_{m,i}\left(\boldsymbol{c}_m\left(\boldsymbol{t}(\boldsymbol{\Delta f}^{(n)})\right), \boldsymbol{\gamma}_m^{APS}\left(\boldsymbol{t}(\boldsymbol{\Delta f}^{(n)}), \boldsymbol{P}_m^{[s-1]}\right)\right)\right) = P_{m,i}^*, \qquad \forall i \in R_m, \qquad \boldsymbol{P}_m^{(0)} \in D_m^{(\tau_m)},$$

where $G_{m,i}$, $g_{m,i}$, and $\gamma_{m,i}^{APS}$ are as in (4), (5), and (6), respectively, for route $i \in R_m$, and $\boldsymbol{f}^{(n)}$ is the route flow vector at iteration n of the FAA. The FPIM is said to have converged sufficiently to an OD movement m APSL choice probability solution $\boldsymbol{P}_m^* = \boldsymbol{P}_m^{[s]}$ if: $\sum_{i\in R_m}\left|P_{m,i}^{[s-1]} - P_{m,i}^{[s]}\right| < 10^{-\xi}$, where ξ is a predetermined APSL probability convergence parameter.

In the numerical experiments in this paper, we explore adopting two different initial conditions for the FPIM: *fixed* initial conditions where $P_{m,i}^{[0]} = \frac{1}{N_m}$, $\forall i \in R_m$, $m = 1, \ldots, M$, and *follow-on* initial conditions where $P_{m,i}^{[0]} = \frac{f_{m,i}^{(n-1)}}{q_m}$, $\forall i \in R_m$, $m = 1, \ldots, M$. The follow-on initial FPIM conditions utilise information from the previous FAA iteration route flows $\boldsymbol{f}^{(n-1)}$ to determine the FPIM initial conditions. The idea is to harness the useful relation between route flow proportions and route choice probabilities in SUE, where these equate at equilibrium. The hypothesis is that by utilising follow-on initial conditions, the numbers of fixed-point iterations required for APSL choice probability convergence (and thus computation time to perform each FAA iteration) should decrease as the algorithm progresses and the route flow proportions become closer to the APSL SUE route choice probabilities. This hypothesis is tested in Section 4.2.1.

Unless stated otherwise, the specifications are as follows. The initial SUE conditions are set as the even split route flows, i.e. $f_{m,i}^{(0)} = \frac{q_m}{N_m}$, $\forall i \in R_m$, $m = 1, \ldots, M$, and the SUE route flow convergence parameter is set as $\zeta = 3$. The MSWA parameter is set as $d = 15$. For computing APSL probabilities, the initial FPIM conditions are set as the fixed initial conditions, and the APSL probability convergence parameter is set as $\xi = 6$. The utilised model parameters for the

Sioux Falls network are $\theta = 0.3$, $\beta = 0.8$, $\upsilon = -0.8$, $\lambda^{GPSL} = 10$, $\mu = 0.25$. $\theta = 0.5$, $\beta = 0.8$, $\upsilon = -0.8$, $\lambda^{GPSL} = 10$, $\mu = 0.25$, and $\lambda^{GNL} = 1$ for the Winnipeg network.

Note that for the GNL SUE model as defined in Section 3.2.2, the model is undefined when there are routes consisting of a single link between the origin and destination. The Sioux Falls network contains numerous instances of such cases and thus we do not present results for GNL SUE on this network.

4.2 Computational Feasibility for Obtaining Internally Consistent Solutions

In this subsection, we assess computational feasibility for obtaining internally consistent solutions. If a SUE model has for example a very slow convergence rate such that it cannot be solved in feasible computation times, then in order to use the model one must settle for an insufficiently converged output. This is obviously problematic for numerous reasons, such as less reliable forecasts, discontinuous flow outputs etc. It may also mean that the output choice probabilities are not internally consistent. In the case of the APSL′ SUE model, for example, the route flows and thus the APSL′ path size contribution factors at the iteration the algorithm is stopped, may define a completely different set of routes as unrealistic to if the algorithm was continued an additional iteration. It is thus crucial that a SUE model can be solved in feasible computation times, in order to be able to provide internally consistent and thus more accurate / behaviourally realistic outputs.

To illustrate this point further, imagine you have a choice between two SUE models, where one model is believed to be more behaviourally realistic than the other, e.g. PSL SUE with flow-dependent path size terms vs flow-independent. If you have well-converged outputs from both the SUE models, then you will choose the output with greater perceived realism, i.e. in this case the flow-dependent model. But, if solving say flow-dependent PSL SUE had an extremely slow convergence rate such that the solution algorithm had to be terminated after a certain number of iterations, then one would probably choose to utilise the output from the well-converged model instead. This aligns with the trade-offs discussed in the introduction: if a model is not computationally feasible to solve, then features such as internal consistency are often compromised for computational efficiency.

Since (most of) the internally consistent correlation-based SUE models developed in this paper have not been solved before, the computational feasibility for doing so is currently unknown. We thus in this subsection conduct some numerical experiments to assess whether the models can be solved in feasible computation times, so that if one is to use the models, well-converged and thus internally consistent equilibrium solutions can be obtained in reasonable, practical times.

4.2.1 Techniques for Solving APSL SUE

We shall first pay particular attention to solving APSL SUE, which is more complicated than for the other SUE models. While the other SUE models all have closed-form choice probability functions, APSL SUE has a fixed-point probability function. Computing APSL *probabilities* thus requires solving a fixed-point problem, which has the potential to be computationally burdensome even when the travel costs are fixed. Therefore, before the following research was conducted, there was a question of whether it would be computationally feasible to implement APSL within an SUE framework, since it apparently needs to embed a fixed-point problem (for calculating choice probabilities) within another fixed-point problem (for equilibrating flows). As we shall now show, however, solution techniques exist that can improve computational performance for solving APSL SUE. As we explore, the useful relationship between choice probabilities and route flow proportions in SUE context allows for a considerable flexibility in solving APSL SUE, where one can trade-off the accuracy of APSL probabilities (and thus computation times of each iteration) with rate of SUE convergence.

The key features of solving the APSL SUE and APSL′ SUE models with the FAA are as follows. As demonstrated later on this section, and in the experience of the authors, while convergence rates (i.e. number if FAA iterations required for SUE convergence) for APSL SUE tend to be similar to PSL & GPSL SUE, total computation times are longer due to the fixed-point APSL probabilities. On-the-other-hand, while computing APSL′ probabilities is no more burdensome than for PSL & GPSL, the convergence rate of APSL′ SUE is comparatively slow, and thus total computational times are also longer. There are unique aspects of the APSL model however that allow for some flexibility in solving APSL SUE and consequent potential to improve computation times, as we show below.

The computational burden involved in computing APSL probabilities depends on numerous factors; some of which can be controlled by the modeller, for example the choice of fixed-point algorithm, and the fixed-point algorithm initial conditions and probability convergence parameter ξ. The current study focuses on the FPIM as the fixed-point algorithm (see Section 3.1.2.1).

Fig. 1A-B display for the Sioux Falls and Winnipeg networks, respectively, the cumulative computation times of the iterations during a single run of the FAA, for fixed and follow-on FPIM initial conditions. Fig. 2A-B shows the average number of fixed-point iterations per OD movement required for APSL choice probability convergence at each iteration of the FAA. As shown, utilising follow-on initial conditions can significantly improve overall computation time due to the reduction in the number of FPIM iterations required for APSL probability convergence as the FAA progresses. Note that it is not guaranteed that follow-on initial conditions will improve solution times compared to fixed initial conditions. As

can be seen in early iterations in Fig. 2A for Sioux Falls, due to large fluctuations in route flow between iterations, follow-on conditions requires greater numbers of FPIM iterations for APSL probability convergence than fixed conditions. Nonetheless, later on in the algorithm when the auxiliary and current route flow proportions (choice probabilities) become closer, fewer FPIM iterations are required with follow-on conditions.

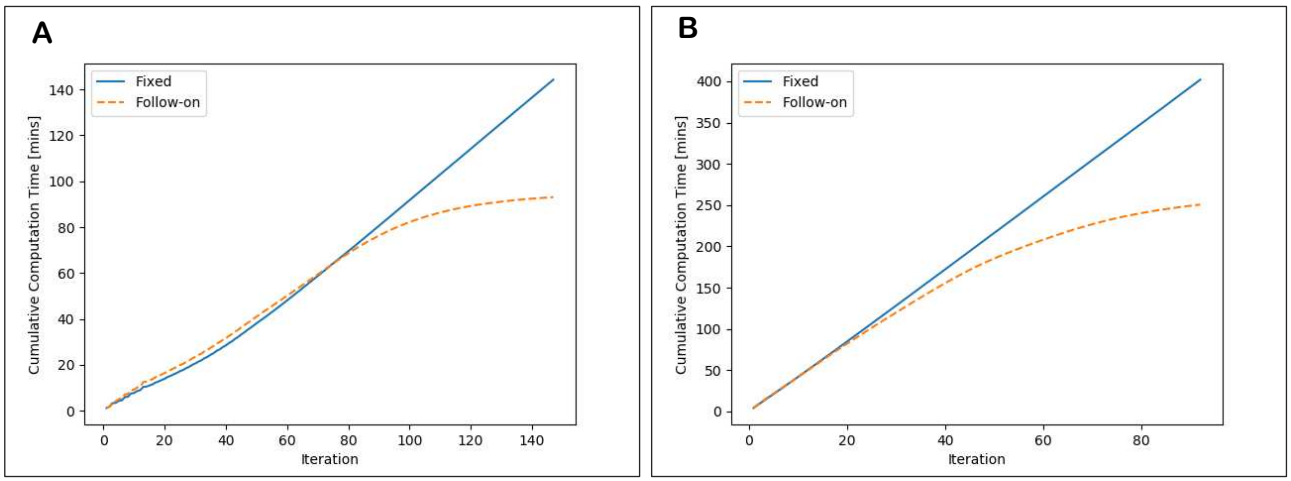

Fig. 1. Cumulative computation times of the iterations during a single run of the FAA solving APSL SUE with different FPIM initial conditions. **A:** Sioux Falls. **B:** Winnipeg.

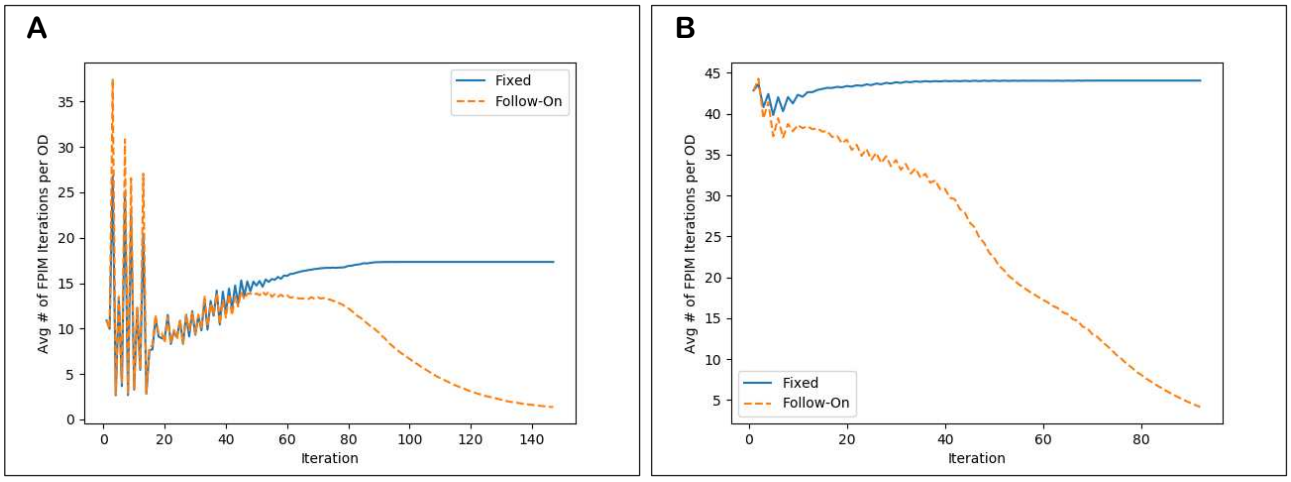

Fig. 2. Average number of APSL probability fixed-point iterations per OD movement at each iteration of the FAA solving APSL SUE with different FPIM initial conditions. **A:** Sioux Falls. **B:** Winnipeg.

Fig. 3A-B display for the Sioux Falls and Winnipeg networks, respectively, how the total computation time for solving APSL SUE varies as the FPIM probability convergence parameter ξ is increased, with follow-on and fixed FPIM initial conditions. Fig. 4A-B display how the average number of APSL fixed-point iterations and total number of FAA iterations vary as ξ is increased.

With fixed FPIM initial conditions, APSL SUE could not be solved for $\xi < 6$ due to the inaccuracies of the APSL probabilities. For $\xi \geq 6$, as shown, as ξ increases, while the number of iterations required for SUE convergence remains constant, greater numbers of FPIM iterations are required for APSL probability convergence and thus total computation times increase.

With follow-on FPIM initial conditions, APSL SUE could be solved for all ξ. This is because for $\xi = -1$, only single FPIM iterations are required for APSL probability convergence, and with follow-on initial FPIM conditions, solving APSL SUE this way simulates solving APSL$'$ SUE. Increasing ξ increases the number of FPIM iterations required for APSL probability convergence and the accuracy of the APSL probabilities, but the APSL SUE solution obtained is the same. As shown, convergence of APSL$'$ SUE (APSL SUE with small ξ & follow-on conditions) is slow, resulting in longer computation times. On-the-other-hand, large values of ξ result in comparatively quick APSL SUE convergence, but longer computation times at each iteration, also resulting in longer total computation times. There is thus an optimal, intermediate value of ξ whereby suitable SUE convergence meets suitable iteration computation times. As shown in Fig. 3A-B, the optimal values in these cases are approximately $\xi = 1$ and $\xi = 0$ for Sioux Falls and Winnipeg, respectively, yielding computation times of 32.68 minutes and 53.94 minutes, respectively.

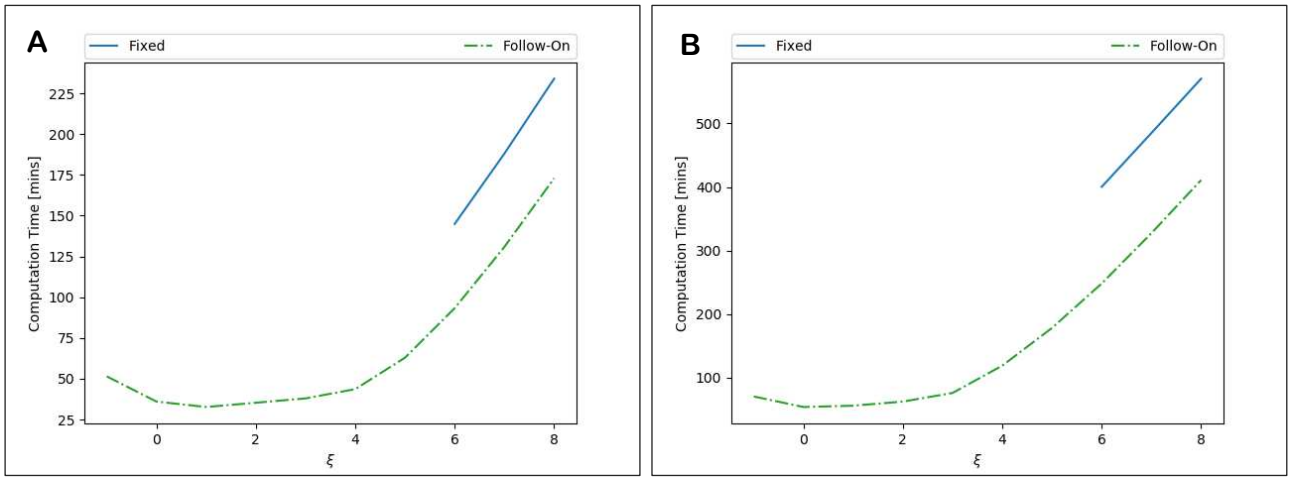

Fig. 3. Computation time for solving APSL SUE as the APSL probability convergence parameter ξ is increased, with fixed and follow-on initial FPIM conditions. **A:** Sioux Falls. **B:** Winnipeg.

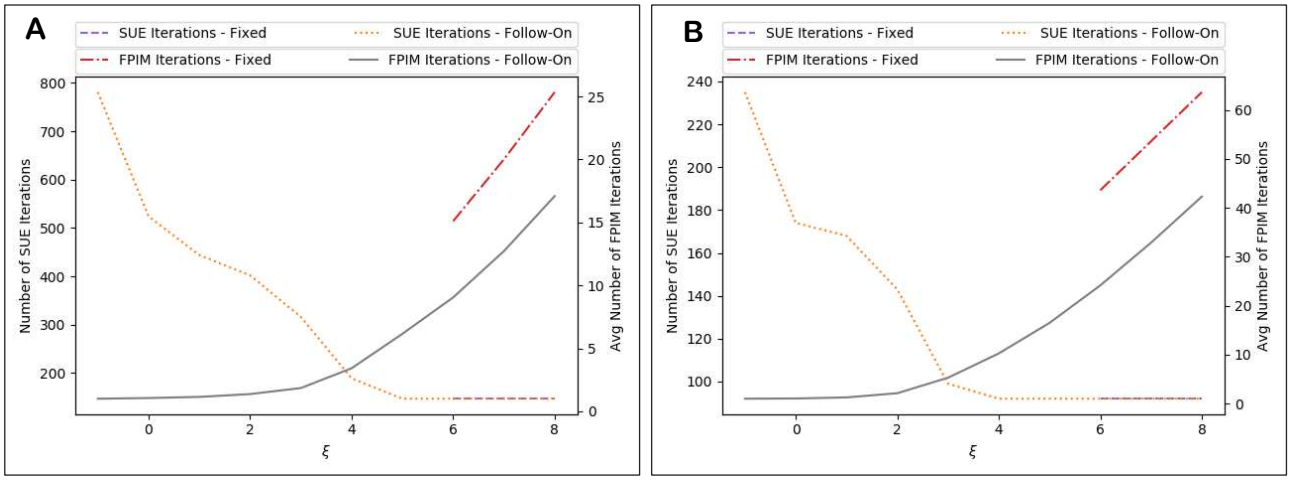

Fig. 4. Average number of APSL fixed-point iterations and total number of FAA iterations for solving APSL SUE as ξ is increased, with fixed and follow-on initial FPIM conditions. **A:** Sioux Falls. **B:** Winnipeg.

Alternatively, utilising follow-on conditions, one can stipulate a set number of FPIM iterations to perform at each FAA iteration. Supposing that h FPIM iterations are conducted, Fig. 5A-B display the total computation times and number of FAA iterations solving APSL SUE, for the Sioux Falls and Winnipeg networks, respectively. As shown, conducting just two FPIM iterations (instead of one) can significantly reduce the number of FAA iterations required for convergence, and thus total computation times. The optimal values for h appear to be 3 and 2 FPIM iterations, respectively, where suitable SUE convergence meets suitable iteration computation times. This yields computation times of 23.79 minutes for Sioux Falls and 47.17 minutes for Winnipeg.

One can also utilise a combination of both techniques for reducing APSL SUE total computation times and stipulate a maximum number of FPIM iterations to perform and a maximum level of APSL probability convergence, i.e. the FPIM is stopped if either a maximum of h iterations are conducted or the probabilities have converged sufficiently according to the set parameter ξ. This can potentially save computation times in latter FAA iterations where the stipulated amount of FPIM iterations unnecessarily overly-converges the APSL probabilities. Fig. 6A and Fig. 7A display for Sioux Falls how computation times and the number of FAA iterations / average number of FPIM iterations vary, respectively, for different settings of ξ, where a maximum of 3 FPIM iterations are conducted. Fig. 6B displays results for Winnipeg where a maximum of 2 FPIM iterations are conducted. As shown, optimal values of ξ with this technique are approximately $\xi = 5$ and $\xi = 4$ for Sioux Falls and Winnipeg, respectively, where a suitable number of FAA iterations meets a suitable average number of FPIM iterations. This yields computation times of 20.24 minutes for Sioux Falls and 42.25 minutes for Winnipeg.

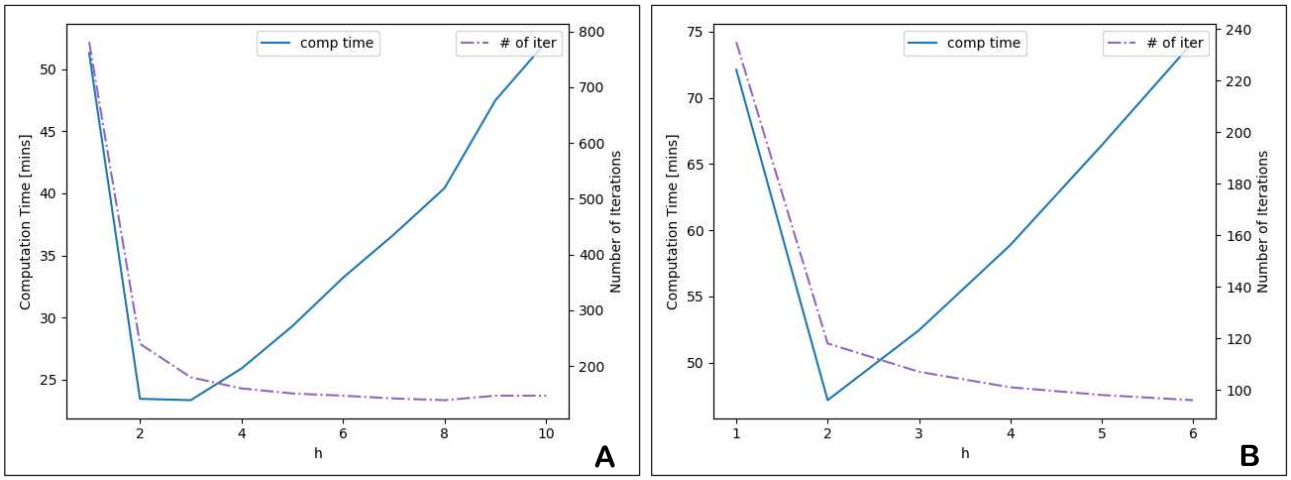

Fig. 5. Total computation times and number of FAA iterations for solving APSL SUE utilising follow-on conditions, with h FPIM iterations conducted. **A:** Sioux Falls. **B:** Winnipeg.

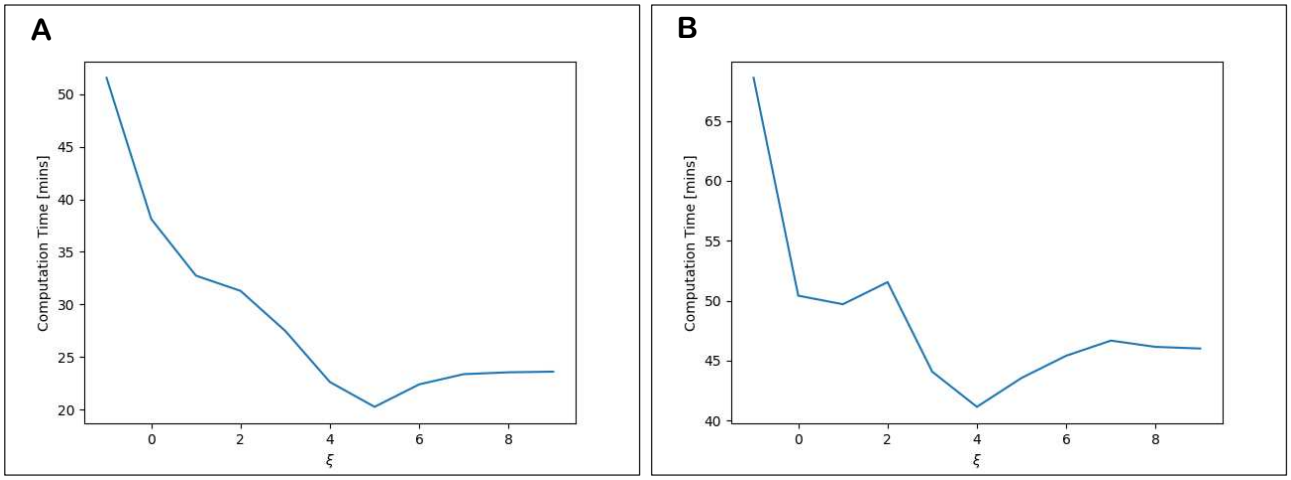

Fig. 6. Total computation times for solving APSL SUE utilising follow-on conditions as ξ is varied, with a max number of FPIM iterations conducted h. **A:** Sioux Falls ($h = 3$). **B:** Winnipeg ($h = 2$).

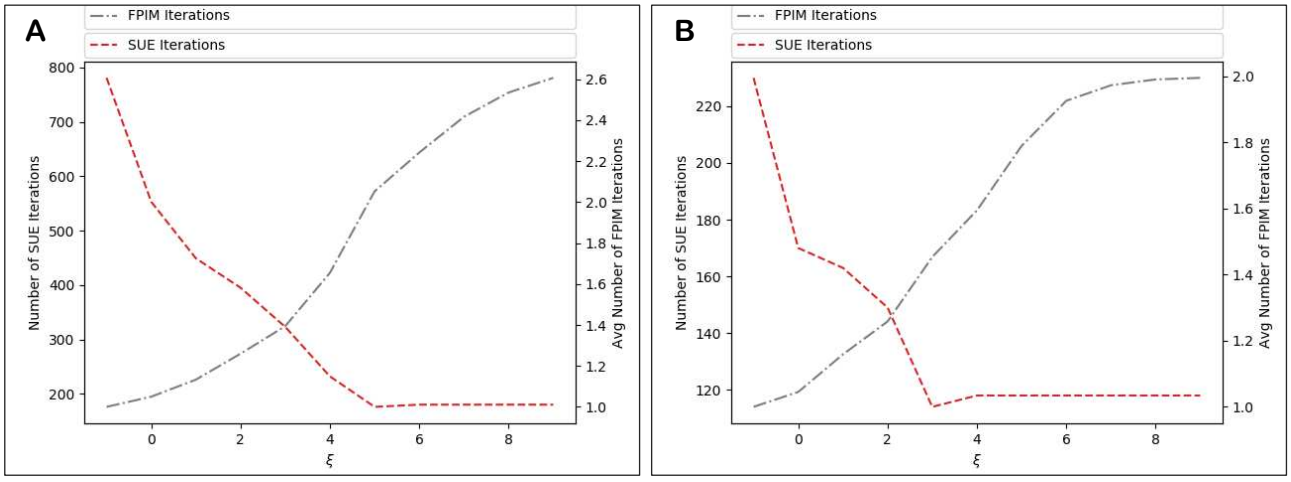

Fig. 7. Number of FAA iterations, and average number of FPIM iterations for solving APSL SUE utilising follow-on conditions as ξ is varied, with a max number of FPIM iterations conducted h. **A:** Sioux Falls ($h = 3$). **B:** Winnipeg ($h = 2$).

Considering the above results, for the remainder of the paper, unless stated otherwise, we solve APSL SUE by stipulating a maximum number of FPIM iterations to perform at each FAA iteration and a maximum level of APSL probability convergence. For Sioux Falls, a maximum of 3 FPIM iterations are conducted with $\xi = 5$. For Winnipeg, 2 FPIM iterations are used with $\xi = 4$. We label for reference this method APSL SUE*. This 'optimal' method for solving APSL SUE is of course particular to the network, model, and algorithm specifications, e.g. model parameters, adopted step-size

scheme, choice set sizes. However, by fixing the optimised values for that particular specification, and then varying the specifications, we will show that the method is robust in its effectiveness compared to solving APSL SUE in a standard way (i.e. where the APSL fixed-point probabilities are accurately solved with non-follow-on initial conditions).

Factors that affect the computational performance of APSL SUE, in terms of solving the APSL probability fixed-point problems, include the value of β and the choice set sizes. As shown in Duncan et al (2020), larger values of β result in a greater number of FPIM iterations being required for APSL convergence (increasing computation times). Moreover, the greater the choice set sizes, the more routes there are to capture the correlation between (escalating the computational burden involved in computing path size terms). In supplementary material, we thus investigate how the computation times for APSL SUE*, as well as for solving APSL SUE with follow-on and fixed initial FPIM conditions, vary as the β parameter is increased / the choice set sizes are increased. The results demonstrate the effectiveness of the APSL SUE* solution technique.

4.2.2 Computational Performance of All Models

We analyse here the computational performance of the FAA for solving the different internally consistent SUE models. Table 2 displays for all SUE models the average computation time to perform a single FAA iteration on the Sioux Falls and Winnipeg networks. Results are displayed for solving APSL SUE in a standard way (i.e. without APSL SUE*). As expected, MNL probabilities are the quickest to compute. PSL/GPSL/APSL′ probabilities all take a similar amount of time to compute, but longer than MNL due to the computation of path size terms. APSL probabilities take significantly longer than the other PSL models due to the requirement of having to solve APSL probability fixed-point problems. CL probabilities take longer to compute than CNL probabilities on the Sioux Falls network, while CNL & GNL take longer than CL on the Winnipeg network. This is because the Winnipeg network has greater network depth and the routes are made up of a greater number of links. The greater the number of links, the greater the number of nests for CNL & GNL, and hence the greater the complexity of the probability expression and longer the computation times. GNL takes longer than CNL due to the computation of nesting coefficients. For CL, the commonality factors evaluate the similarity between each pair of routes, and thus despite the smaller network depth of the Sioux Falls network, there are still many routes to compare, increasing the computational burden. Due to relatively large choice set sizes and thus extremely large number of route pairs and hence nests for PCL, the probabilities for Sioux Falls and Winnipeg are very computationally burdensome and could not be computed in computationally feasible times. Due to this, we do not present computation/flow results for PCL SUE.

	MNL	PSL	GPSL	APSL	APSL′	CL	CNL	GNL
Sioux Falls	0.006	0.038	0.038	0.920	0.038	0.562	0.196	-
Winnipeg	0.089	0.208	0.208	4.199	0.208	1.611	6.806	12.921

Table 2. Average computation time [mins] to perform a single FAA iteration on the Sioux Falls and Winnipeg networks.

Fig. 8A-B display for the Sioux Falls and Winnipeg networks, respectively, the number of FAA iterations required to obtain levels of SUE convergence. Fig. 9A-B the display computation time required. As shown, MNL SUE is the quickest to solve due to not having to compute path size terms, while PSL SUE takes less time than GPSL SUE due to fewer iterations. For Sioux Falls, iteration times are quicker for CNL than for CL, and thus despite fewer number of iterations required for CL SUE, CNL SUE takes less time overall. For Winnipeg, iteration times are quicker for CL than for CNL & GNL, and thus CNL & GNL SUE take more time overall, where GNL SUE takes longer than CNL SUE. Note that numerous studies have also found that flow-dependent CL SUE takes considerably longer to solve than MNL SUE, with different solution algorithms (e.g. Chen et al, 2013; Zhou et al, 2012).

As also shown, while APSL SUE requires a similar number of FAA iterations for convergence to PSL & GPSL SUE, total computation times are significantly longer due to the requirement of solving APSL probability fixed-point problems at each iteration, and hence longer iteration times. APSL′ SUE has the same iteration computation times as for PSL & GPSL SUE, but the slow convergence also results in longer total computation times. For APSL SUE*, the number of iterations required to obtain levels of convergence is now significantly less than for APSL′ SUE, though more than required for APSL SUE. Hence, since the iteration computation times of APSL SUE* are significantly less than for APSL SUE, total computation times are improved. Moreover, APSL SUE* outperforms CL, CNL, & GNL SUE – significantly on the larger-scale Winnipeg network.

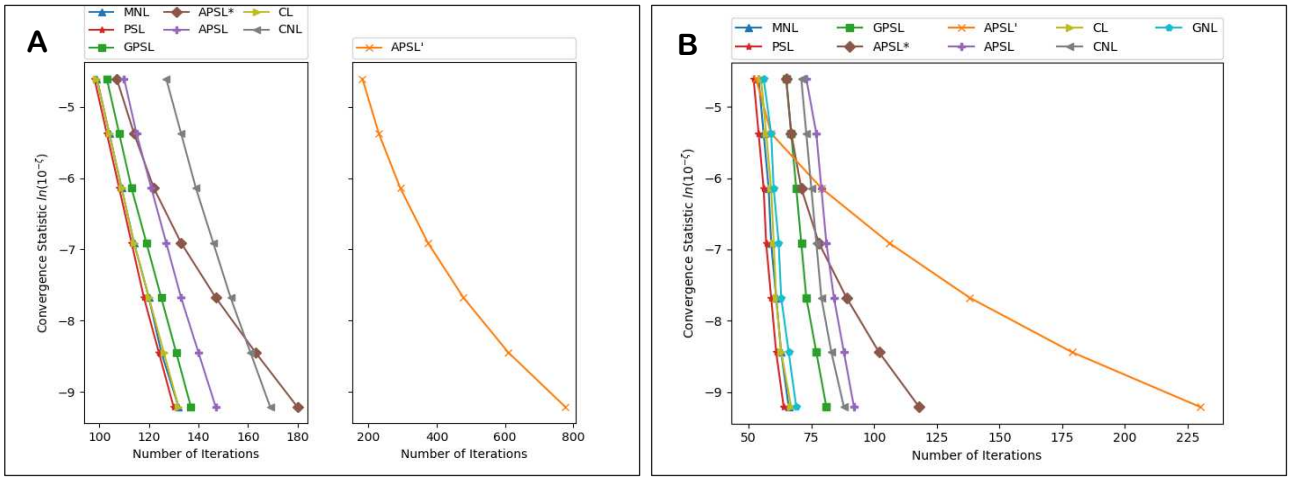

Fig. 8. Number of FAA iterations required to obtain levels of SUE convergence for the different SUE models, including the APSL SUE* solution method. **A:** Sioux Falls. **B:** Winnipeg.

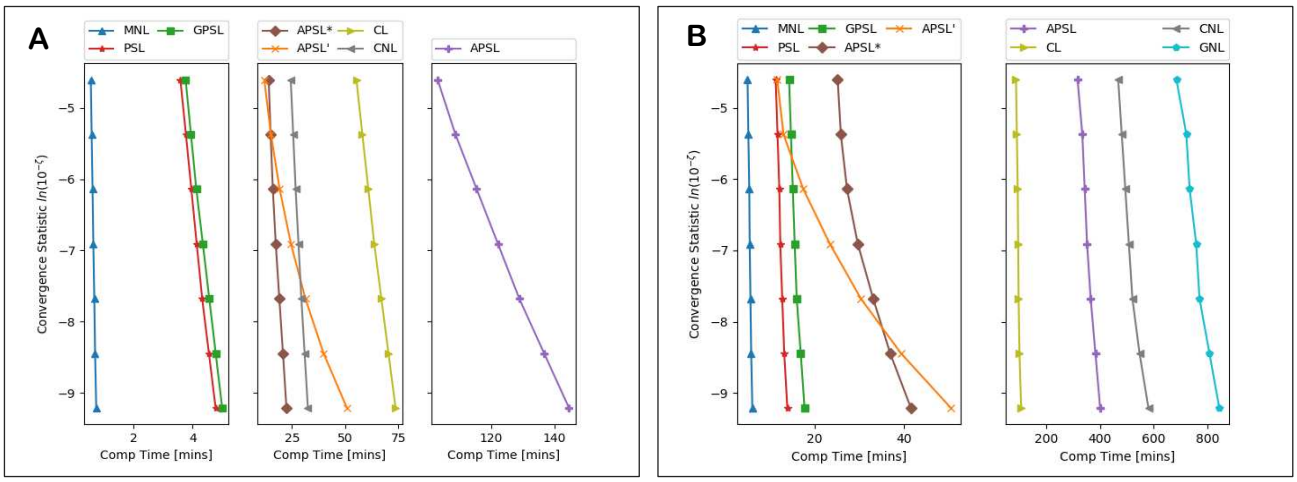

Fig. 9. Computation time [mins] required to obtain levels of SUE convergence for the different SUE models, including the APSL SUE* solution method. **A:** Sioux Falls. **B:** Winnipeg.

The computational performances of the different SUE models depend of course on, among other things, the sizes of the choice sets, the level of travel demand, and the model parameters. In real-life applications, model parameters are either estimated statistically or calibrated using e.g. observed link flows. Thus, since we do not have estimated/calibrated model parameters for this study, in supplementary material we include results from numerical experiments investigating the effects of choice set size and demand level on computational performance (and, in the following subsection, choice set robustness) for fixed parameter settings, then explore how varying the parameters effects results (with fixed choice sets / demand).

A summary for general networks is as follows. The computational performances of CNL & GNL SUE are affected most by network depth: the greater the number of links in a route, the greater the number of nests, and hence the greater the complexity of the probability expressions (at each SUE iteration). CL & PCL SUE, however, are affected most by choice set size. These models measure route correlation by evaluating the similarity between each pair of routes; thus, since the number of route pairings grows exponentially with choice set size, so do computation times for calculating the commonality factors (at each SUE iteration). For solving APSL SUE, choice set size affects the numbers of FPIM iterations required for computing the APSL probabilities (see Supplementary Material A) and thus computation times. For APSL SUE*, this means that more stringent FPIM convergence criteria (smaller ξ values) / greater maximum FPIM iterations (greater h values) are required to improve performance.

4.3 Choice Set Robustness

In this subsection we compare the choice set robustness of the different SUE models. To compare the flow results $\boldsymbol{f}^{*R1}$ and $\boldsymbol{f}^{*R2}$ for Result 1 and Result 2, respectively, we measure the Normalised Root Mean Squared Error (NRMSE):

$$NRMSE = \frac{RMSE}{\bar{y}},$$

where:

$$RMSE = \sqrt{\frac{1}{N}\sum_{m=1}^{M}\sum_{i\in R_m}\left(f_{m,i}^{*R1} - f_{m,i}^{*R2}\right)^2},$$

and $\bar{y}$ is the average value of $f_{m,i}^{*R1}$ and $f_{m,i}^{*R2}$, $\forall i \in R_m$, $m = 1, \dots, M$. N is the total number of routes. Note that for reference the RMSE between the previous and final route flows of the FAA converging to a SUE solution $\boldsymbol{f}^*$ were approximately of the order 10^{-5}. Moreover, the average route flow values on the Sioux Falls and Winnipeg networks were approximately 26-28 and 0.21, respectively.

To help the reader comprehend the numerical experiments below, Table 3 provides a summary description of the model parameters.

Parameter	Model	Name	Description
θ	All models	Logit scaling parameter	Scales the travel cost component in all Logit models. A small θ value corresponds to drivers being less aware of / less sensitive to differences in route travel cost, and a large θ corresponds to the opposite.
β	PSL, GPSL, APSL	Path size scaling parameter	Scales the path size correction factor. A small β value corresponds to drivers being less aware of route correlation / less sensitive to route distinctiveness, and a large β corresponds to the opposite.
λ^{GPSL}	GPSL	Path size contribution scaling parameter	Scales the travel cost ratio path size contribution factor in the GPSL path size term. Does not have a (sensible) behavioural interpretation (see Duncan et al 2020,2021), but increasingly reduces the path size contributions of costly routes for greater values of λ.
υ	CL	Commonality scaling parameter	Similar to the path size scaling parameter, scales the C-Logit correction factor.
μ	CNL	Nesting coefficient	Describes the degree of nesting, i.e. when $\mu = 1$ CNL is equivalent to MNL, and as $\mu \to 0$ CNL becomes probabilistic at the higher (link) level and deterministic at the lower (nest) level (Prashker & Bekhor, 1999)
λ^{GNL}	GNL	Similarity index	Scales the GNL nesting coefficient factor. $\lambda^{GNL} = 0$ results in $\mu = 1$ and thus GNL collapses to MNL, greater λ^{GNL} values move GNL away from MNL towards $\mu \to 0$.

Table 3. Summary description of the model parameters.

Fig. 10A-B display for the Sioux Falls and Winnipeg networks, respectively, the impact that varying the sizes of choice sets has on the route flow results from the different models. The choice sets are obtained by generating all routes (from the pre-generated choice sets) with a free-flow travel time less than φ times greater than the free-flow travel time on the quickest route for each OD movement, and it is assumed that $\varphi = 2$ are the true choice sets, i.e. flow results are compared between the $\varphi = 2$ generated routes only. As shown, PSL SUE is the most affected by expanding the choice sets, as the path size terms of the assumed true routes are adjusted significantly attempting to capture the correlation with the added high costing routes. GPSL & APSL SUE are the least affected (and affected significantly less than PSL SUE) due to the employment of path size contribution weighting techniques, reducing the impact of the added routes. Note that

the initial sharp increase in NRMSE is due to the fact that Sioux Falls and Winnipeg have integer free-flow travel times; there are many routes in the choice sets with free-flow travel times exactly e.g. two times greater than the quickest route.

Fig. 11A-B display for the Sioux Falls and Winnipeg networks, respectively, the impact varying the common θ parameter has on choice set robustness for the Path Size Logit SUE models, (we have omitted results for the other models in this figure in order to improve clarity of the most interesting findings, we look at each other model in more detail below). Flow results from the $\varphi = 2$ and $\varphi = 2.5$ choice sets are compared, where flows again are just compared between the $\varphi = 2$ generated routes. Choice set robustness improves for all models (including those not shown) as the θ parameter is increased. The key finding though is that, for low θ, the choice set robustness of APSL SUE is more similar to that for PSL SUE than GPSL SUE. This is more evident on the Winnipeg network, for that range of θ; it is less evident for Sioux Falls, but as will be clear from the discussion below it would be more evident if a lower more fine-grained range of θ was displayed. The reason this is the case is because for low θ routes are considered more evenly attractive (travellers are less sensitive to differences in travel cost), and hence the APSL SUE path size contribution factors are closer to 1 (the PSL SUE factors). Increasing θ (implying the routes are less evenly attractive) accentuates the travel cost differences within the factors moving them away from 1, thereby improving choice set robustness so that for larger θ APSL SUE is the most choice set robust.

For GPSL SUE, however, regardless of the θ value and consequent behavioural implications, the path size contribution factors accentuate the travel cost differences and GPSL SUE remains relatively insensitive to the inclusion of routes to the choice set. This demonstrates how APSL SUE is more internally consistent and adaptable than GPSL SUE, where APSL SUE is always consistent with the behavioural implications of the model parameters. For small θ values, the route choice probabilities / route flows are more evenly split due to the lower sensitivity to route cost differences. Therefore, if a route (with only marginally greater cost than the current routes) is added to the current choice set, due to the small θ parameter it will likely receive a non-small choice probability, implying it is not an unrealistic route according to the route choice criteria. However, the GPSL path size contribution factors will still define it as an unrealistic route, in which case GPSL is inconsistent. For more on the internal (in)consistency of GPSL/APSL, see Duncan et al (2020).

Fig. 12A-B display choice set robustness for the CNL SUE model as μ is varied. As shown, for Sioux Falls, choice set robustness improves for greater values of μ, where the probabilities are closer to the MNL model, thus implying that in this case MNL is more robust than the correlation-based models. For Winnipeg, however, choice set robustness worsens with μ, implying the opposite. Moreover, best choice set robustness occurs for μ close to 0, however as Bekhor & Prashker (2001) note, the extreme case for CNL where $\mu \to 0$ is suitable in the context of route choice only when the total route costs are equal, otherwise $\mu \to 0$ can lead to counter-intuitive results.

Fig. 13 display choice set robustness for the GNL SUE model as λ^{GNL} is varied. As shown, choice set robustness improves as λ^{GNL} increases: the nesting coefficients move away from 1 and closer 0, and thus since MNL SUE ($\mu = 1$ for CNL/GNL) on Winnipeg has poor robustness, robustness for GNL SUE improves for greater values of λ^{GNL}.

Fig. 14A-B display choice set robustness for the CL SUE model as υ is varied. As shown, for Sioux Falls, since MNL SUE is choice set robust, CL SUE is also choice set robust for low υ; however, as υ increases and the correlation component becomes more prominent, choice set robustness worsens dramatically. For Winnipeg, since MNL SUE is not robust, robustness actually improves for CL SUE as υ increases, up to a point where the correlation components become prominent enough that the adjustments from capturing similarities with new unrealistic routes begins to worsen robustness.

Fig. 15A-B display choice set robustness for the GPSL SUE model as λ^{GPS} is varied. As shown, and as expected, for both networks, choice set robustness is equivalent to that of PSL SUE for $\lambda^{GPS} = 0$ (where the models are equivalent), and robustness improves as λ^{GPS} increases from 0 and the path size contribution factors accentuate the cost differences more, resulting in the new more costly routes having reduced contributions and thus adjusting the realistic route probabilities less. A peak is reached in terms of choice set robustness, however, and increasing λ^{GPS} further worsens robustness.

Fig. 16A-B display choice set robustness for the PSL/GPSL/APSL SUE models as β is varied. As shown, for $\beta = 0$ the path size models are equal to MNL SUE, where robustness is good for Sioux Falls and bad for Winnipeg. As β increases for Sioux Falls, the increasing prominence of the correlation components worsens robustness, where the effects for PSL SUE are significantly worse than for the weighted path size contribution models. For Winnipeg, robustness improves as β increases for the weighted contribution models, but worsens for PSL SUE.

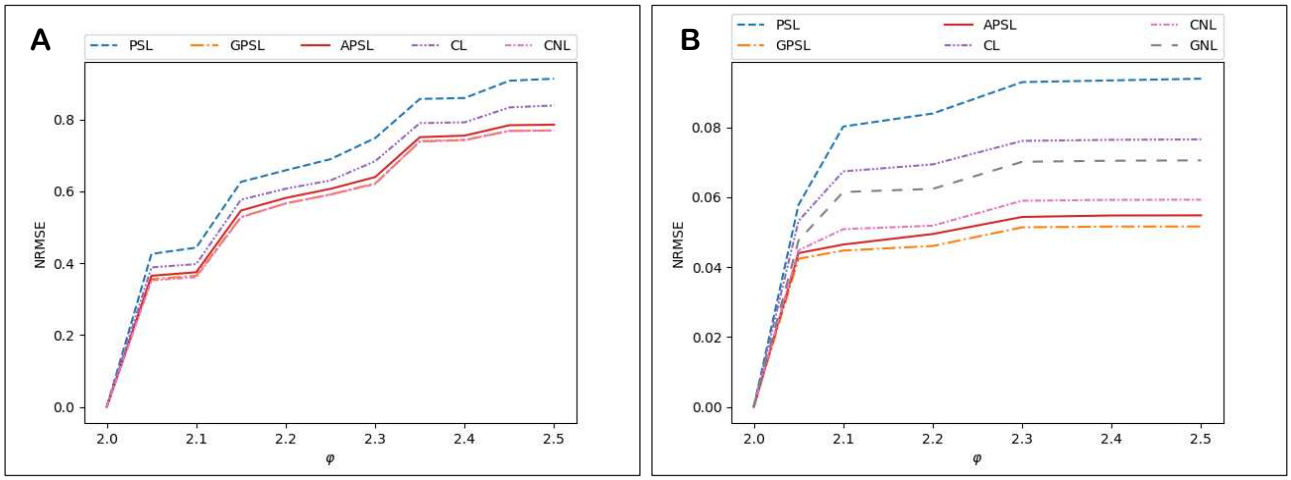

Fig. 10. Impact that varying the sizes of choice sets has on the route flow results of the different SUE models, scaled by φ. **A:** Sioux Falls ($\theta = 0.07$). **B:** Winnipeg.

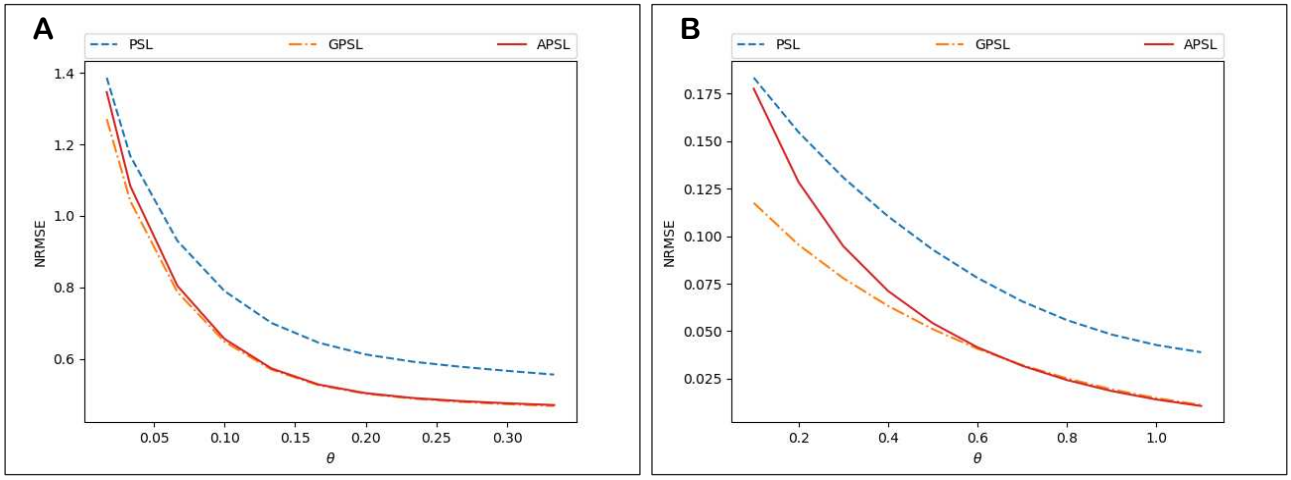

Fig. 11. Impact that varying the θ parameter has on choice set robustness for the different SUE models. **A:** Sioux Falls. **B:** Winnipeg.

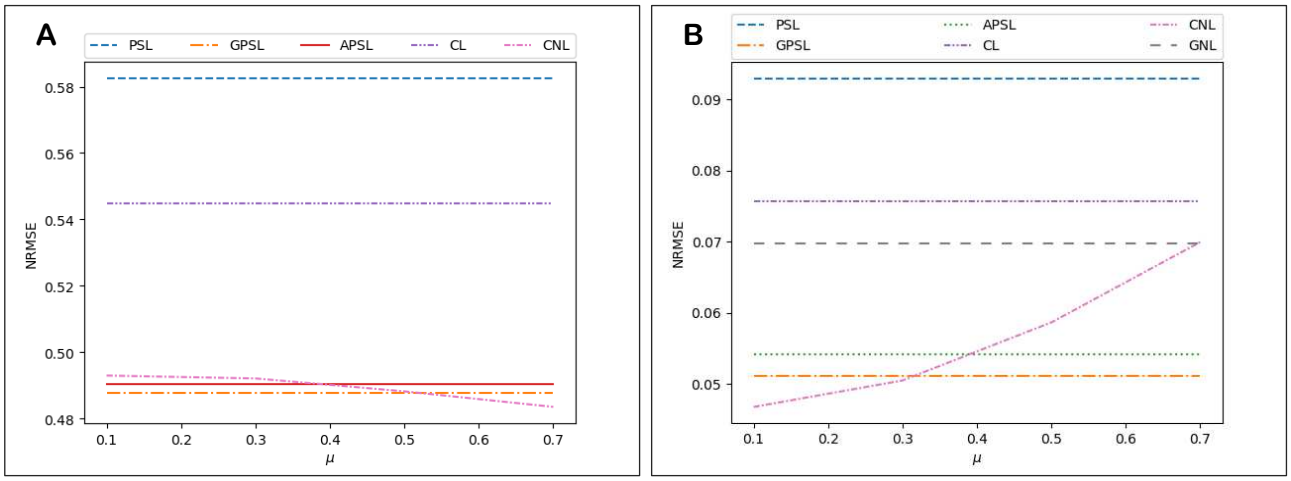

Fig. 12. Impact that varying the μ parameter has on choice set robustness for the CNL SUE model. **A:** Sioux Falls. **B:** Winnipeg.

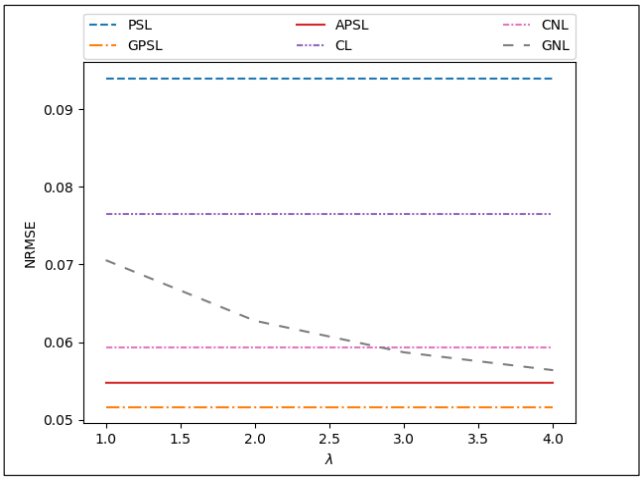

Fig. 13. Impact that varying the λ^{GNL} parameter has on choice set robustness for the GNL SUE model on the Winnipeg network.

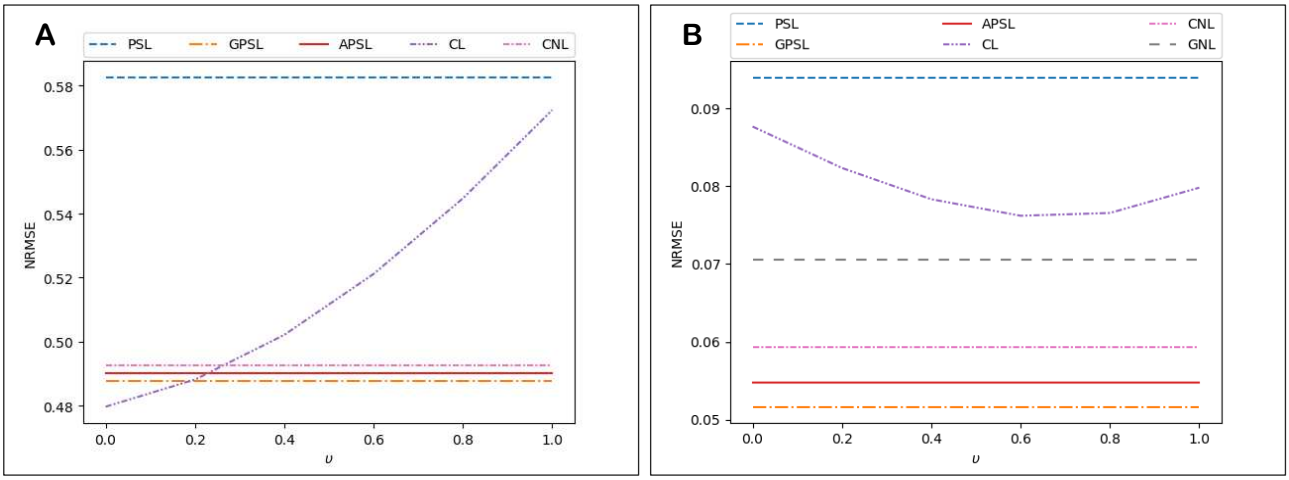

Fig. 14. Impact that varying the υ parameter has on choice set robustness for the CL SUE model. **A:** Sioux Falls. **B:** Winnipeg.

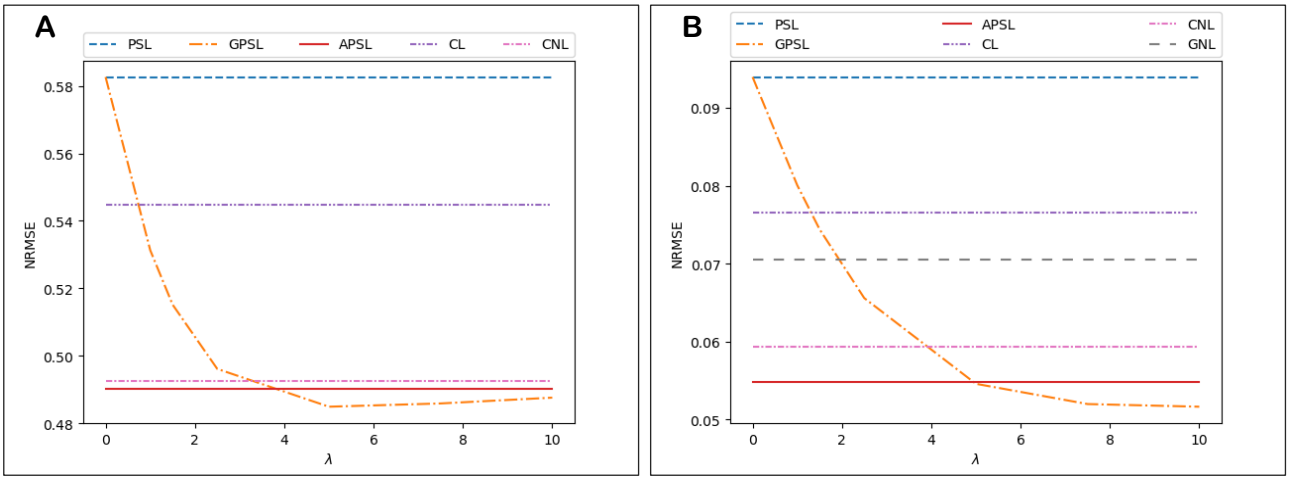

Fig. 15. Impact that varying the λ^{GPS} parameter has on choice set robustness for the GPSL SUE model. **A:** Sioux Falls. **B:** Winnipeg.

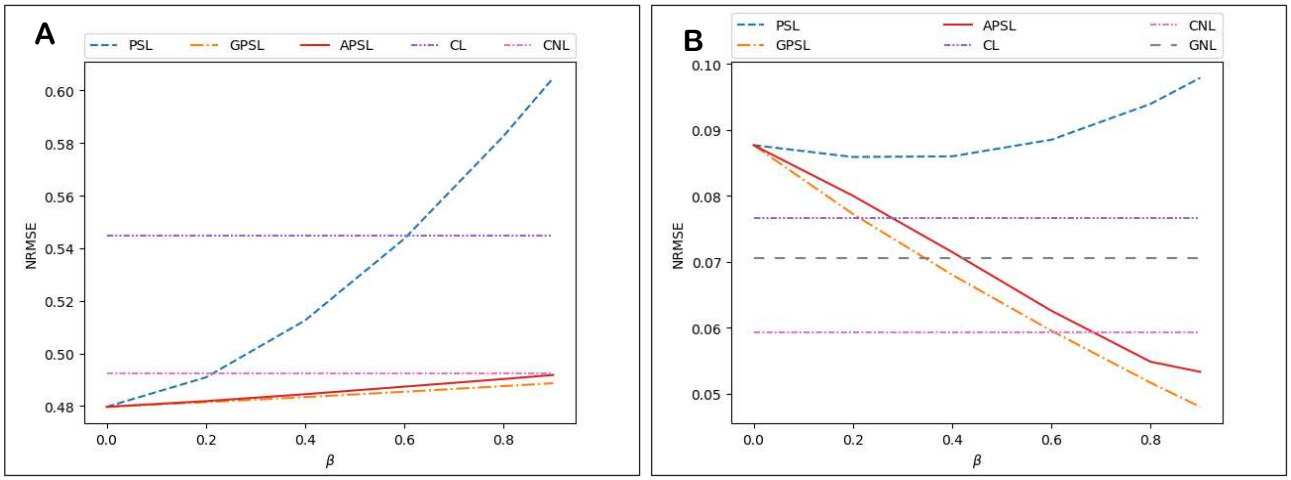

Fig. 16. Impact that varying the β parameter has on choice set robustness for the Path Size Logit SUE models. **A:** Sioux Falls. **B:** Winnipeg.

4.4 Internal Consistency

In this subsection, we conduct some numerical experiments to demonstrate the different types of internal consistency considered in this paper, and to show that internal consistency can make a significant difference to model output.

We begin by demonstrating the first type of internal consistency: the internal consistency of an SUE model in terms of employing the same definition of flow-dependent, generalised cost in all components of the specification. Fig. 17A-B display for the Sioux Falls and Winnipeg networks, respectively, how link-route prominence differs between flow-dependent and flow-independent versions of the PSL, GPSL, APSL, & CNL SUE models, for varying θ. For a given route flow solution $\boldsymbol{f}^*$ to one of these SUE models, we measure the difference in link-route prominence according to the following Proportional RMSE (PRMSE) measure:

$$PRMSE = \sqrt{\frac{1}{N}\sum_{m=1}^{M}\sum_{i\in R_m}\sum_{a\in A_{m,i}}\left(\frac{\left(\frac{l_a}{L_{m,i}} - \frac{t_a(\boldsymbol{\Delta f}^*)}{c_{m,i}\left(\boldsymbol{t}(\boldsymbol{\Delta f}^*)\right)}\right)}{\frac{1}{2}\left(\frac{l_a}{L_{m,i}} + \frac{t_a(\boldsymbol{\Delta f}^*)}{c_{m,i}\left(\boldsymbol{t}(\boldsymbol{\Delta f}^*)\right)}\right)}\right)^2},$$

where l_a and $L_{m,i}$ are the lengths of link $a \in A_{m,i}$ and route $i \in R_m$, respectively, and $t_a(\boldsymbol{\Delta f}^*)$ and $c_{m,i}\left(\boldsymbol{t}(\boldsymbol{\Delta f}^*)\right)$ are the flow-dependent, congested travel times of link $a \in A_{m,i}$ and route $i \in R_m$, respectively. The numerator is the difference in link-route prominence and the denominator is the mean value of the two link-route prominences. Therefore, the PRMSE provides a measure of how significant the differences are between the flow-dependent and flow-independent link-route prominences. It is clear to see from the PRMSE values in Fig. 17A-B that the differences for all models can indeed be significant. This is particularly the case for Sioux Falls where 0.6 seems a large average proportional difference. The differences between the models, in terms of their individual difference between flow-dependent and flow-independent link-route prominences, are more prominent for Winnipeg. This is likely due to the θ range being relatively large for Sioux Falls here and the travel cost components thus dominating the probability relations. As one can start to see, smaller ranges of θ on Sioux Falls will display greater differences (between models).

Fig. 18A-B display how the route flow result differences between the flow-dependent and flow-independent versions of the SUE models vary with θ. As shown, the route flow differences are also significant. Interestingly, PSL has the least similar link-route prominences but the most similar route flows. Clearly, the path size contribution factors for GPSL and APSL – which will also be different for the flow-dependent and flow-independent versions – also affect the flow results considerably. Since the GPSL flow results are so different compared to the other models, but relatively the link-route prominences are not as different, it is clear that the routes with the quickest/slowest travel times are not necessarily the shortest/longest routes.

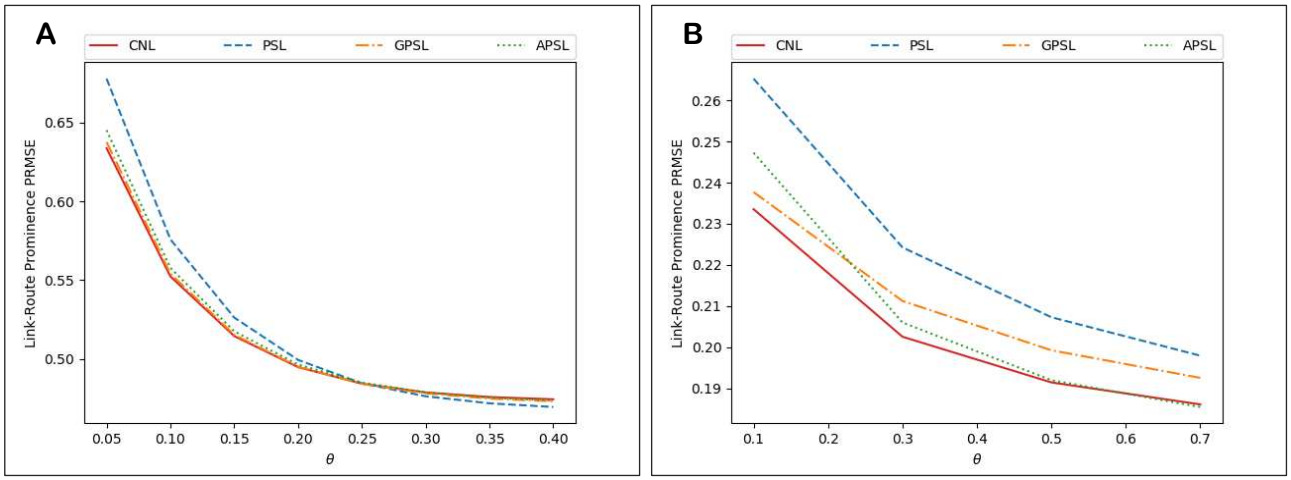

Fig. 17. The differences between the flow-dependent and flow-independent link-route prominence features for the different SUE models, for varying θ. **A:** Sioux Falls. **B:** Winnipeg.

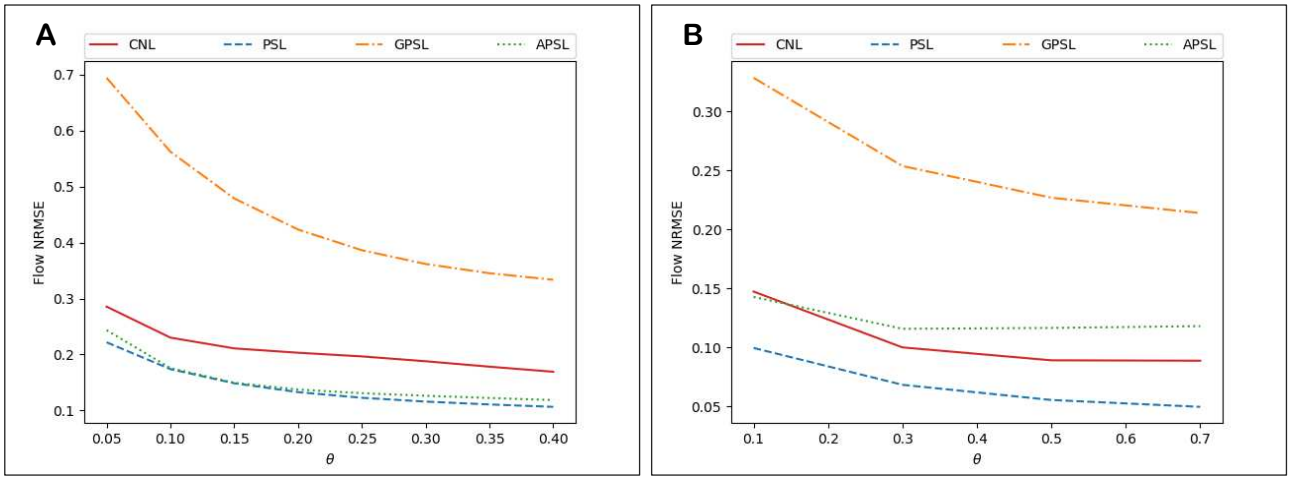

Fig. 18. The differences in flow results between the flow-dependent and flow-independent versions of the different correlation-based SUE models, for varying θ. **A:** Sioux Falls. **B:** Winnipeg.

Next, we demonstrate the second type of internal consistency: the internal consistency of a weighted contribution path size route choice model (e.g. GPSL, APSL) in terms of how the model's components define a route as (un)realistic (i.e. how the path size contribution factor defines a route as (un)realistic). As discussed throughout the paper, APSL is more internally consistent than GPSL in this way, as the APSL path size contribution factor is consistent with how the choice probability relation assesses route feasibility, i.e. according to choice probability rather than just travel cost. To demonstrate this in SUE context, we examine the differences in flow results between the different Path Size Logit SUE models.

Fig. 19A-B display for the Sioux Falls and Winnipeg networks, respectively, the impact the θ parameter has on the differences in SUE flow between the models. Most notably, in these ranges of θ, the flow differences between GPSL & APSL SUE decrease with θ (initially for Winnipeg) and the flow differences between PSL & APSL SUE increase with θ. The former is because as θ increases, the travel cost components within the APSL SUE path size contribution factors increase in contribution influence compared to the route distinctiveness components, and hence the factors increase in similarity to the GPSL SUE factors (which only consider travel cost), and thus the SUE route flows. The flows then begin to increase in difference as the θ parameter begins to accentuate the travel cost differences for APSL more than the λ parameter does for GPSL within the contribution factors. The latter occurs since for low θ routes are considered more evenly attractive and hence the APSL SUE path size contribution factors are closer to 1 (the PSL SUE factors), and increasing θ accentuates the travel cost differences within the factors moving them away from 1. A peak is reached and further increasing θ results in the travel cost components within the PSL & APSL probability relations dominating the distinctiveness components where the difference lies.

Fig. 20A-B display the impact of the β parameter. As shown, the flow differences all increase as β increases, which is logical since the differences between the SUE models are the different path size correction terms scaled by β. GPSL & APSL SUE are amongst the least different due to their similarity in adopting path size contribution weighting techniques. What is noticeable is that the differences between the APSL SUE flows and PSL/GPSL SUE flows increase significantly

for larger values of β. This is because distinctiveness increases significantly in contribution influence within the APSL SUE path size terms, moving the contribution factors away from 1 (PSL) and making the travel cost component less prominent (GPSL).

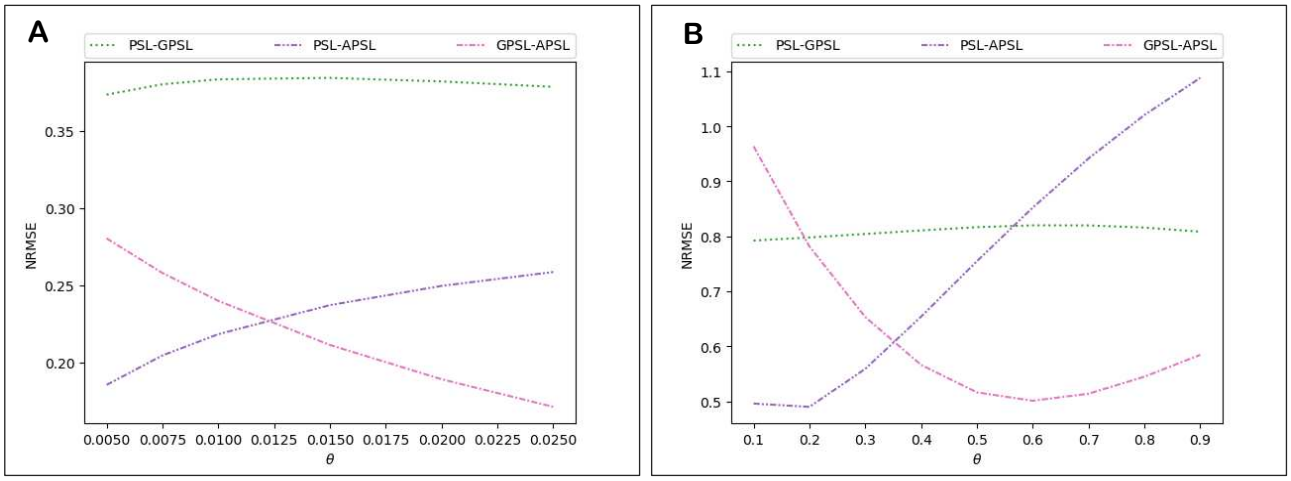

Fig. 19. Impact of the θ parameter on the differences in SUE flow between the Path Size Logit SUE models. **A:** Sioux Falls. **B:** Winnipeg.

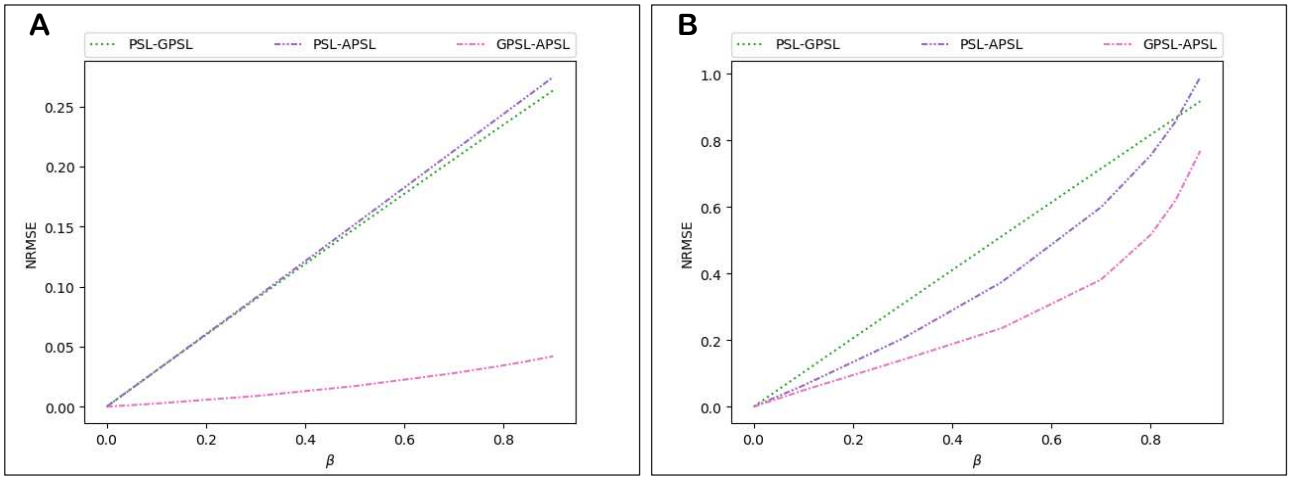

Fig. 20. Impact of the β parameter on the differences in SUE flow between the Path Size Logit SUE models. **A:** Sioux Falls. **B:** Winnipeg.

To explore the impact that varying the level of travel demand has on route choice (i.e. proportional route flow) for the Path Size Logit models, we measure the RMSE of the *route choice probabilities*, i.e. by dividing the flow results by the respective OD movement demands. The demand is scaled according to a parameter ω so that the demand for OD movement m is $\omega \cdot q_m, m = 1, \dots, M$. Fig. 21A-B display the impact different levels of travel demand have on the differences in choice probabilities between the Path Size Logit SUE models, with $\theta = 0.01$ for Sioux Falls. Most notably for Sioux Falls, the differences between the GPSL & APSL SUE probabilities decrease from being the most different as the demand level increases, while the PSL & APSL SUE probability differences increase from being the least different. At zero demand, the relatively low setting of θ given the zero flow link costs dampens the travel cost differences within the APSL path size contribution factors resulting in the PSL probabilities being closer and the GPSL probabilities further away to APSL. As demand increases however and the link costs increase in scale, the travel cost differences become less dampened and the APSL contribution factors consequently move away from 1 (PSL) and closer to the GPSL factors, where the travel cost differences are accentuated. For Winnipeg, due to the overall lower level of congestion, the effects are less significant; however, the flow differences between the GPSL & APSL SUE probabilities also decrease while the PSL & APSL SUE probability differences increase. This time though the GPSL & APSL SUE probabilities are the most similar, due to the similar path size contribution weightings given the scale of travel costs.

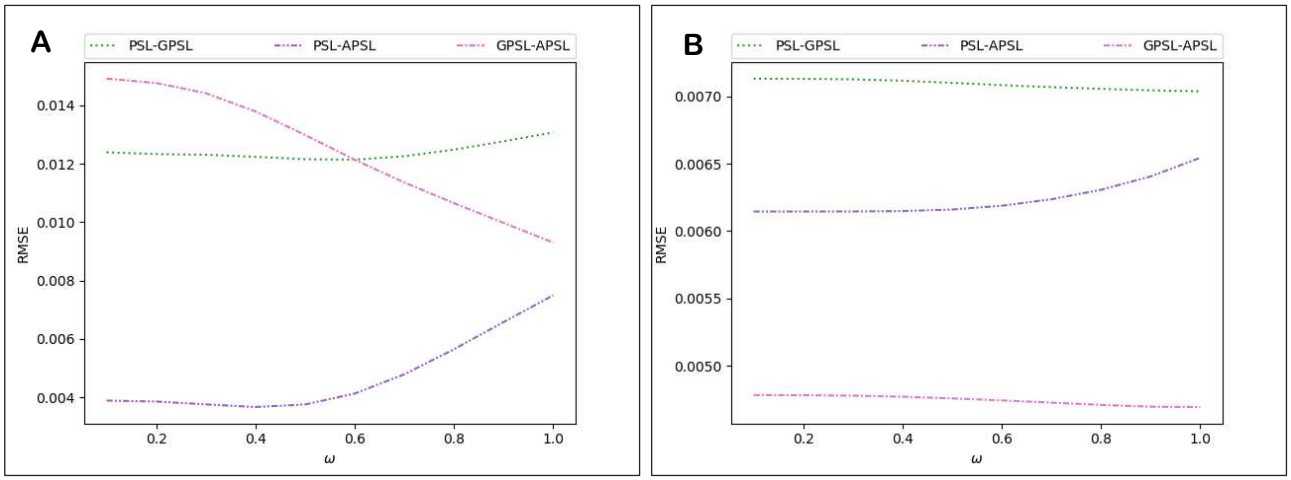

Fig. 21. Impact that different levels of demand has on the differences in choice probability between the Path Size Logit SUE models, demand scaled by ω. **A:** Sioux Falls. **B:** Winnipeg.

4.5 Uniqueness of Solutions

Zhou et al (2012) prove existence for the congestion-based CL SUE model, though uniqueness cannot be guaranteed. In a similar vein, solutions can be proven to exist for the other SUE models (as shown in Section 3.3), but it is expected that uniqueness can also not be guaranteed. This is because standard approaches for proving solution uniqueness require the SUE fixed-point function (i.e. $H_{m,i}$ in Section 3.3) to be monotonic, which is not necessarily the case with flow-dependent correction terms / correlation components.

Since standard approaches for proving solution uniqueness cannot be applied to the SUE models in this paper, the uniqueness of SUE solutions is investigated numerically. After experimenting on Sioux Falls and Winnipeg with different model parameters and initial conditions, we did not identify cases of multiple solutions for any of the models except from for APSL SUE. Further analysis is required to identify whether solutions are in fact guaranteed to be unique for the other SUE models e.g. establish a mathematical proof, or to identify uniqueness conditions, if they exist. For the APSL SUE model, however, since it is not guaranteed that even APSL probability solutions are unique, some attention is required. Due to the possibility of non-unique APSL probability solutions, before our research was conducted it was uncertain whether it would first even be possible to solve APSL SUE and second whether solutions would be unique. As our experiments found, however, uniqueness conditions appear to exist for the APSL SUE model: APSL SUE solutions are unique when APSL probability solutions are universally unique. For details of these experiments and methods for identifying the uniqueness conditions, see Supplementary Material C.

4.6 Findings of the Numerical Experiments

To summarise, the key findings of the numerical experiments were that:

a) GPSL/APSL SUE were generally more robust than PSL, CL, CNL, & GNL SUE to the inclusion of unrealistic routes to the choice set.

b) Internally consistent SUE formulations for the correlation-based models can have a significant impact on model outcome.

c) APSL SUE was more internally consistent than GPSL SUE in terms of dealing with unrealistic routes in the adopted choice sets, i.e. the theoretical consistency of the path size contribution factor.

d) Computing choice probabilities for the internally consistent SUE formulations of CL, CNL, GNL, & PCL was more computationally burdensome than for PSL & GPSL (considerably on the larger-scale Winnipeg network).

e) As such, typically, computation times were quickest for solving PSL & GPSL SUE, with the slowest being CL, CNL, GNL, then PCL SUE. (Convergence rates were similar).

f) Convergence rates for solving APSL SUE were similar to that for PSL & GPSL SUE, however the computational burden involved in computing the APSL choice probabilities for each FAA iteration resulted in much longer total computation times.

g) On-the-other-hand, the computational burden involved in computing the APSL′ choice probabilities was similar to that for PSL & GPSL (similarly closed-form), but the APSL′ SUE convergence rate was comparatively slow, and thus total computation times were also longer.

h) In general, the FPIM convergence parameter ξ (and thus the accuracy of the APSL choice probabilities) must be at a certain level for convergence of the FAA to the APSL SUE solution.

i) However, by utilising 'follow-on' initial FPIM conditions – where the initial conditions for solving the APSL probabilities at iteration n of the FAA are set as the route flow proportions from iteration $n-1$ – the FAA will converge to the APSL SUE solution regardless for all ξ.

j) There was a computational trade-off between solving APSL & APSL′ SUE: solving APSL SUE with low ξ and follow-on initial conditions simulated solving APSL′ SUE where the convergence rate was slow, while larger values of ξ resulted in comparatively quick convergence rates but lengthy computation times for the iterations.

k) There was an 'optimal' intermediate value of ξ for solving APSL SUE with follow-on initial FPIM conditions whereby a suitable SUE convergence rate meets suitable computation times for each iteration. Optimal values for the examples in this study were $\xi = 1$ for Sioux Falls and $\xi = 0$ for Winnipeg.

l) Another technique that improved APSL SUE computation times was to stipulate a set number of FPIM iterations to perform at each FAA iteration: optimal values were 3 and 2 FPIM iterations for Sioux Falls and Winnipeg, respectively.

m) Best computation times for solving APSL SUE were found when utilising a combination of a maximum number of FPIM iterations and an intermediate value of ξ: 3 FPIM iterations and $\xi = 5$ for Sioux Falls, 2 FPIM iterations and $\xi = 4$ for Winnipeg.

n) APSL SUE can thus be solved in feasible computation times – typically longer than PSL & GPSL SUE, but quicker than CL, CNL, GNL, & PCL SUE (significantly on the larger-scale Winnipeg network).

o) Uniqueness conditions appeared to exist for APSL SUE: for β in the range $0 \leq \beta \leq \bar{\beta}_{max}(\theta)$, where APSL probability solutions are unique.

p) $\bar{\beta}_{max,m}(\theta)$ values (uniqueness for OD movement m) in experiments were all close 1.

The 'optimal' values for the methods in k)-m) for solving APSL SUE are particular to the network, model, and algorithm specifications, e.g. model parameters, adopted step-size scheme, choice set sizes. However, by fixing the optimised values for a given specification, and then varying the specifications, it was shown that the method was robust in its effectiveness compared to solving APSL SUE in a standard way (i.e. where the APSL fixed-point probabilities are accurately solved with non-follow-on initial conditions). Future research could explore an intelligent, adaptive process whereby the optimal values of ξ and the maximum number of FPIM iterations to perform at each FAA iteration are learnt / worked out as the FAA progresses.

5 Conclusion

This paper explores internal consistency and choice set robustness for correlation-based Stochastic User Equilibrium (SUE) models. Internally consistent SUE formulations for GEV structure and correction term correlation-based route choice models (namely: Path Size Logit (PSL), C-Logit (CL), Cross-Nested Logit (CNL), Generalised Nested Logit (GNL), and Paired Combinatorial Logit (PCL)) are formulated, where the functional forms in the correlation components are based upon generalised, flow-dependent congested costs, rather than e.g. length / free-flow travel time as done typically. Without explicit mechanisms for dealing with unrealistic routes in the adopted choice sets, however, there are questions over how robust these models are to choice set mis-generation.

This paper thus also investigates the SUE application of the Generalised PSL (GPSL) and Adaptive PSL (APSL) route choice models. GPSL & APSL have explicit mechanisms for dealing with unrealistic routes: weighting the contributions of routes to path size terms with path size contribution factors. The integration of the APSL model within a SUE model is not straightforward, since the probabilities are a solution to a fixed-point problem. As explored in the paper, however, the requirement of solving fixed-point problems to compute APSL choice probabilities can be circumvented in SUE application, since at equilibrium the route flow proportions and choice probabilities equate.

Solutions are proven to exist for the internally consistent SUE models, but standard proofs for uniqueness of solutions could not be applied. Solution uniqueness is instead investigated numerically, where non-uniqueness was not found for any of the models except APSL. Experiments on the Sioux Falls and Winnipeg networks suggest that APSL SUE uniqueness conditions exist. These conditions are analogous to those for the uniqueness of APSL probability solutions, and APSL SUE solutions appear to be unique when APSL solutions are unique.

Computational performance and choice set robustness of the different internally consistent SUE models are analysed in numerical experiments on the Sioux Falls and Winnipeg network, where a flow-averaging solution algorithm with Method of Successive Weighted Averages step-size scheme is used. The key findings from the numerical experiments were that:

a) GPSL/APSL SUE are generally more robust than PSL, CL, CNL, & GNL SUE to the inclusion of unrealistic routes to the choice set.

b) APSL SUE is more internally consistent than GPSL SUE in terms of dealing with unrealistic routes in the adopted choice sets.

c) One can trade-off the accuracy of APSL probabilities (and thus computation times of each iteration) with rate of SUE convergence, and as such, APSL SUE can be solved in feasible computation times.

d) Typically, computation times are quickest for solving PSL & GPSL SUE, followed by APSL SUE, with the slowest being CL, CNL, GNL, & PCL SUE (considerably on the larger-scale Winnipeg network).

Scope for future research includes providing some empirical evidence to support the hypothesis that the internally consistent SUE formulations have greater behavioural realism than the original formulations, i.e. estimating/calibrating the correlation-based SUE models with flow-dependent and flow-independent correlation components and comparing goodness-of-fit. Choice set robustness could then also be explored in estimation, e.g. how variations to the adopted choice set affects parameter estimate values and goodness-of-fit.

Future research could also explore computational performances of the models under different averaging step-size schemes, such as the self-regulated averaging method (Liu et al, 2009), which has been applied with success in various SUE models (e.g. Yang et al, 2013; Xu & Chen, 2013; Kitthamkesorn & Chen, 2013,2014; Chen et al, 2014; Yao et al, 2014). It has not yet been explored whether similar techniques to those described in Section 4.2.1 for solving APSL SUE – where the APSL probabilities need not be computed accurately – are applicable for some 'inexact' step-size schemes, such as the self-adaptive method (e.g. Chen et al, 2012b, 2013; Xu et al, 2012; Zhou et al, 2012). Furthermore, future research could explore alternative algorithms, such as the New Self-Adaptive Gradient Projection algorithm (Chen et al, 2012a), which has been applied with success to solve SUE for the Congestion-based C-Logit SUE model (Zhou et al, 2012).

As mentioned at the end of the previous section, to further improve computation times solving APSL SUE, one could explore an intelligent, adaptive process whereby the required accuracy of the APSL choice probabilities is learnt / worked out as the algorithm progresses, perhaps in a similar way to the self-regulated averaging method (Liu et al, 2009). Moreover, future research could also explore utilising a different fixed-point algorithm (to the FPIM)) for computing the APSL probabilities within the SUE algorithm, or perhaps a combination of fixed-point algorithms could be used, e.g. Newton Raphson's Method for early iterations, Steffenson's Method for middle iterations, and the FPIM for latter iterations, as the initial conditions for the probabilities become closer to the solution through the use of follow-on initial conditions.

Lastly, as Marzano & Papola (2008) and Marzano (2014) find, the overall correlation between routes is smaller in a larger choice set. This may have implications for choice set robustness and internal consistency. For example, if choice set robustness worsens as the level of overall correlation increases, then given the above finding, generating larger choice sets should in theory result in greater choice set robustness between choice sets that size. This potentially supports the approach that is typically done in practice for large-scale networks, where choice sets are typically generated sufficiently large to minimise the possibility of excluding what might later turn out to be a realistic alternative. Moreover, if the overall route correlation is greater in smaller choice sets, then perhaps the need for internally consistent SUE formulations is greater. Further research could investigate these aspects.

6 Acknowledgements

We gratefully acknowledge funding provided by the University of Leeds by awarding the corresponding author with a University of Leeds Doctoral Scholarship for PhD research, and, the financial support of the Independent Research Fund Denmark to the project "Next-generation route choice models for behavioural realism and application in real-life models".

7 References

Azevedo J et al, (1993). An Algorithm for the ranking of shortest paths. European Journal of Operational Research, 69, p.97–106.

Baillon J & Cominetti R, (2008). Markovian traffic equilibrium. Mathematical Programming, 111(1-2), p.33-56.

Bekhor S & Prashker J, (1999). Formulations of extended logit stochastic user equilibrium assignments. In: Proceedings of the 14th International Symposium on Transportation and Traffic Theory, Jerusalem, Israel, p.351–372.

Bekhor S & Prashker J, (2001). Stochastic user equilibrium formulation for the generalized nested logit model. Transportation Research Record 1752, p.84–90.

Bekhor S, Toledo T, & Reznikova L, (2008a). A path-based algorithm for the cross-nested logit stochastic user equilibrium. Computer-Aided Civil and Infrastructure Engineering, 24(1), p.15–25.

Bekhor S, Toledo T, & Prashker J, (2008b). Effects of choice set size and route choice models on path-based traffic assignment. Transportmetrica 4(2), p.117-133.

Ben-Akiva M, & Ramming S, (1998). Lecture notes: discrete choice models of traveler behavior in networks. Prepared for Advanced Methods for Planning and Management of Transportation Networks. Capri, Italy.

Ben-Akiva M, & Bierlaire M, (1999). Discrete choice methods and their applications to short term travel decisions. In: Halled, R.W. (Ed.), Handbook of Transportation Science. Kluwer Publishers.

Bliemer M & Bovy P, (2008). Impact of Route Choice Set on Route Choice Probabilities. Transportation Research Record: Journal of the Transportation Research Board, 2076, p.10–19.

Bovy P, Bekhor S, & Prato C, (2008). The Factor of Revisited Path Size: Alternative Derivation. Transportation Research Record: Journal of the Transportation Research Board, 2076, Transportation Research Board of the National Academies, Washington, D.C., p.132–140.

Cantarella G & Binetti M, (2002). Stochastic assignment with gammit path choice models. Patriksson, M., Labbé's, M. (Eds.), Transportation Planning: State of the Art, p.53–68.

Cascetta E, Nuzzolo A, Russo F, & Vitetta A, (1996). A modified logit route choice model overcoming path overlapping problems: specification and some calibration results for interurban networks. In: Proceedings of the 13th International Symposium on Transportation and Traffic Theory, Leon, France, p.697–711.

Cascetta E, Russo F, & Vitetta A, (1997). Stochastic user equilibrium assignment with explicit path enumeration: comparison of models and algorithms. In: Proceedings of the international federation of automatic control: Transportation systems, Chania, Greece, p.1078–1084.

Chen A, Lo H, & Yang H, (2001). A self-adaptive projection and contraction algorithm for the traffic assignment problem with path-specific costs. European Journal of Operational Research, 135(1), p.27–41.

Chen A, Lee D-H, & Jayakrishnan R, (2002). Computational study of state-of-the-art path-based traffic assignment algorithms. Mathematics and Computers in Simulation, 59, p.509–518.

Chen A, Kasikitwiwat P, & Ji Z, (2003). Solving the overlapping problem in route choice with paired combinatorial logit model. Transportation Research Record 1857, p.65–73.

Chen A, Pravinvongvuth S, Xu X, Ryu S, & Chootinan P, (2012a). Examining the scaling effect and overlapping problem in logit-based stochastic user equilibrium models. Transportation Research Part A, 46, p.1343-1358.

Chen A, Zhou Z, & Xu X, (2012b). A self-adaptive gradient projection algorithm for the non-additive traffic equilibrium problem. Computers and Operations Research, 39(2), p.127–138.

Chen A, Xu X, Ryu S, & Zhou Z, (2013). A self-adaptive Armijo stepsize strategy with application to traffic assignment models and algorithms. Transportmetrica A: Transport Science, 9(8), p.695–712.

Chen A, S Ryu, Xu X, & Choi K, (2014). Computation and Application of the Paired Combinatorial Logit Stochastic User Equilibrium Problem. Computers and Operations Research, 43, p.68–77.

Connors R, Hess S, & Daly A, (2014). Analytic approximations for computing probit choice probabilities, Transportmetrica A: Transport Science, 10(2), p.119-139.

Daganzo C & Sheffi Y, (1977). On stochastic models of traffic assignment. Transportation Science, 11, p.253–274.

De La Barra T, Perez B, & Anez J, (1993). Multidimensional path search and assignment. Proceedings of the 21st PTRC summer annual meeting, Manchester, England, p.307–319.

Duncan L, Watling D, Connors R, Rasmussen T, & Nielsen O, (2020). Path Size Logit Route Choice Models: Issues with Current Models, a New Internally Consistent Approach, and Parameter Estimation on a Large-Scale Network with GPS Data. Transportation Research Part B, 135, p.1-40.

Duncan L, Watling D, Connors R, Rasmussen T, & Nielsen O, (2021). A bounded path size route choice model excluding unrealistic routes: Formulation and estimation from a large-scale GPS study. Transportmetrica A: Transport Science. DOI: 10.1080/23249935.2021.1872730.

Frejinger E, & Bierlaire M, (2007). Capturing correlation with subnetworks in route choice models. Transportation Research Part B, 41(3), p.363-378.

Hoogendoorn-Lanser S, van Nes R, & Bovy P, (2005). Path Size Modeling in Multimodal Route Choice Analysis. Transportation Research Record: Journal of the Transportation Research Board, 1921, p.27–34.

Isaacson E, & Keller H, (1966). Analysis of Numerical Methods. John Wiley & Sons, Inc., New York, USA.

Jayakrishnan R, et al., (1994). Faster path-based algorithm for traffic assignment. Transportation Research Record, 1443, p.75–83.

Kitthamkesorn S & Chen A, (2013). Path-size weibit stochastic user equilibrium model. Transportation Research Part B, 57, p.378-397.

Kitthamkesorn S & Chen A, (2014). Unconstrained weibit stochastic user equilibrium model with extensions. Transportation Research Part B, 59, p.1–21.

Knies A & Melo E, (2020). A Recursive Logit model with choice aversion and its application to route choice analysis. https://arxiv.org/pdf/2010.02398.pdf.

Liu H, He X, & He B, (2009). Method of successive weighted averages (MSWA) and self regulated averaging schemes for solving stochastic user equilibrium problem. Networks and Spatial Economics, 9(4), p.485–503.

Manzo S, Prato C & Nielsen O, (2015). How uncertainty in input and parameters influences transport model outputs: a four-stage model case-study. Elsevier, Transport Policy, 38, p.64-72.

Marzano V, (2014). A simple procedure for the calculation of the covariances of any Generalized Extreme Value model. Transportation Research Part B: Methodological, 70, p.151-162.

Marzano V & Papola A, (2008). On the covariance structure of the cross-nested logit model. Transportation Research Part B: Methodological, 42(2), p.83-98.

Prashker J & Bekhor S, (2004). Route choice models used in the stochastic user equilibrium problem: A review. Transport Reviews, 24, p.437-463.

Prato C, (2014). Expanding the applicability of random regret minimization for route choice analysis. Transportation, (41), p.351–375.

Ramming S, (2002). Network knowledge and route choice. Ph.D. Thesis, Massachusetts Institute of Technology, Cambridge, USA.

Rich J & Nielsen, O (2015). System convergence in transport models: algorithms efficiency and output uncertainty. European Journal of Transport Infrastructure Research (EJTIR), 15 (3), p.38-62.

Sheffi Y & Powell W, (1982). An algorithm for the equilibrium assignment problem with random link times. Network: An International Journal, 12(2), p.191-207.

Sheffi Y, (1985). Urban Transportation Networks: Equilibrium Analysis with Mathematical Programming Methods. Prentice-Hall.

Watling D, Rasmussen T, Prato C, & Nielsen O, (2015). Stochastic user equilibrium with equilibrated choice sets: Part I – Model formulations under alternative distributions and restrictions. Transportation Research Part B (77), p.166-181.

Watling D, Rasmussen T, Prato C, & Nielsen O, (2018). Stochastic user equilibrium with a bounded choice model. Transportation Research Part B, 114, p.254-280.

Xu X, Chen A, Zhou Z, & Behkor S, (2012). Path-based algorithms for solving C-logit stochastic user equilibrium assignment problem. Transportation Research Record, 2279, p.21–30.

Xu X, & Chen A, (2013). C-logit stochastic user equilibrium model with elastic demand. Transportation Planning and Technology, 36(5), p.463–478.

Xu X, Chen A, Kitthamkesorn S, Yang H, & Lo H, (2015). Modeling absolute and relative cost differences in stochastic user equilibrium problem. Transportation Research Part B, 81, p.686-703.

Yang C, Chen A, & Xu X, (2013). Improved partial linearization algorithm for solving the combined travel-destination-mode-route choice problem. Journal of Urban Planning and Development, 139(1), p.22–32.

Yao J, Chen A, Ryu S, & Shi F, (2014). A general unconstrained optimization formulation for the combined distribution and assignment problem. Transportation Research Part B, 59, p.137–160.

Zhou Z, Chen A, & Bekhor S, (2012). C-logit stochastic user equilibrium model: formulations and solution algorithm. Transportmetrica, 8(1), p.17–41.

8 Supplementary Material

8.1 Supplementary Material A – Effectiveness of the APSL SUE* Solution Technique

Fig. 22A-B display for the Sioux Falls and Winnipeg networks, respectively, how the computation time for APSL SUE* as well as for solving APSL SUE with follow-on and fixed initial FPIM conditions, varies as the β parameter is increased. Fig. 23A-B display how the average number of FPIM iterations per OD movement per FAA iteration and how the total number of FAA iterations vary as β is increased. As shown, for APSL SUE follow-on & fixed, while the number of FAA iterations do not vary considerably, the average number of FPIM iterations increases exponentially with β and hence so do computation times. For APSL SUE*, the number of SUE iterations increases as β increases, while the average number of FPIM iterations remains low (decreasing slightly due to more SUE iterations), resulting in the technique significantly improving in effectiveness as β increases.

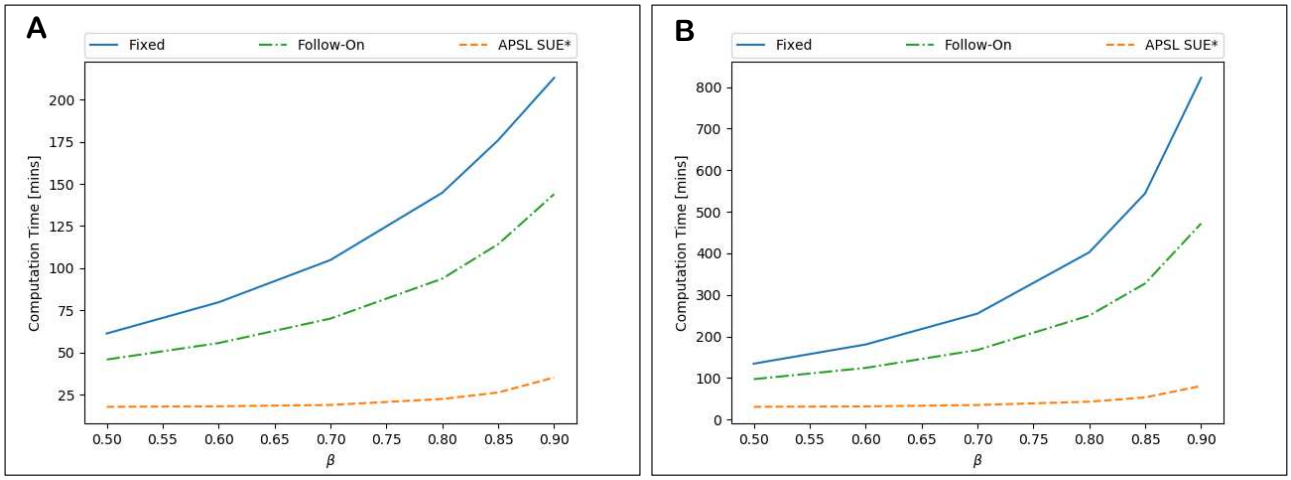

Fig. 22. Computation time for APSL SUE*, APSL′ SUE, and solving APSL SUE with follow-on and fixed initial FPIM conditions as β is increased. **A:** Sioux Falls. **B:** Winnipeg.

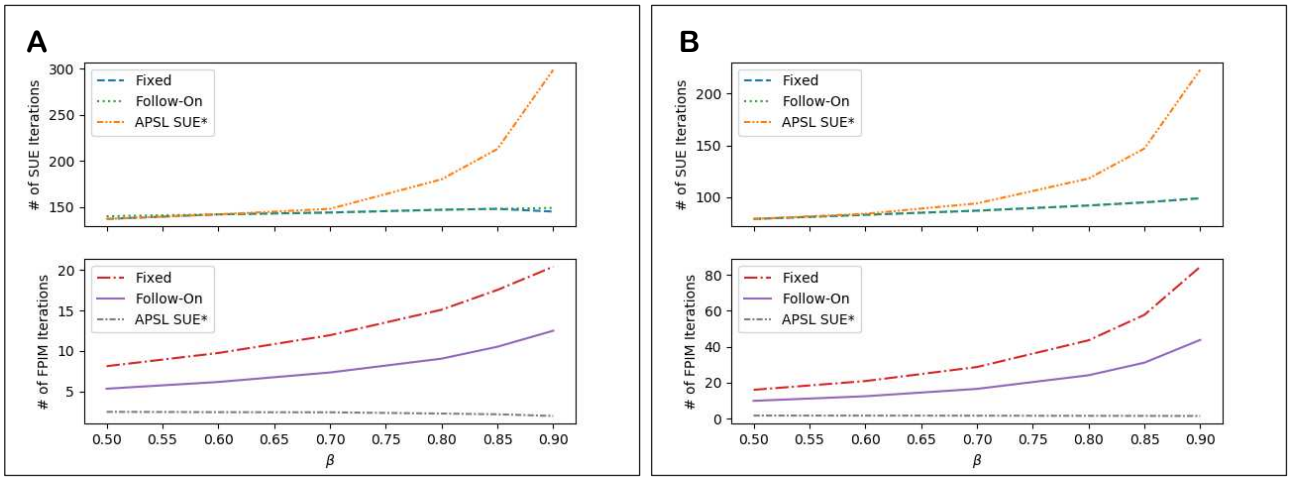

Fig. 23. Number of FAA iterations, and average number of FPIM iterations for APSL SUE*, APSL′ SUE, and solving APSL SUE with follow-on and fixed initial FPIM conditions as β is increased. **A:** Sioux Falls. **B:** Winnipeg.

Fig. 24A-B display for the Sioux Falls and Winnipeg networks, respectively, how the computation time for APSL SUE* as well as for solving APSL SUE with follow-on and fixed initial FPIM conditions, varies as the choice set sizes are increased. Fig. 25A-B display how the average number of FPIM iterations per OD movement per FAA iteration and how the total number of FAA iterations vary. The choice sets are obtained by generating all routes (from the master generated choice sets used throughout this section) with a free-flow travel time less than φ times greater than the free-flow travel time on the quickest generated route for each OD movement. As shown, computation times increase as the choice sets are expanded. The greater number of routes to capture the correlation between means that more FPIM iterations are required for APSL probability convergence, which, combined with a greater number of FAA iterations required for SUE convergence, results in increasing computation times (more SUE iterations that each take longer on average). It is also shown again how effective APSL SUE* can be.

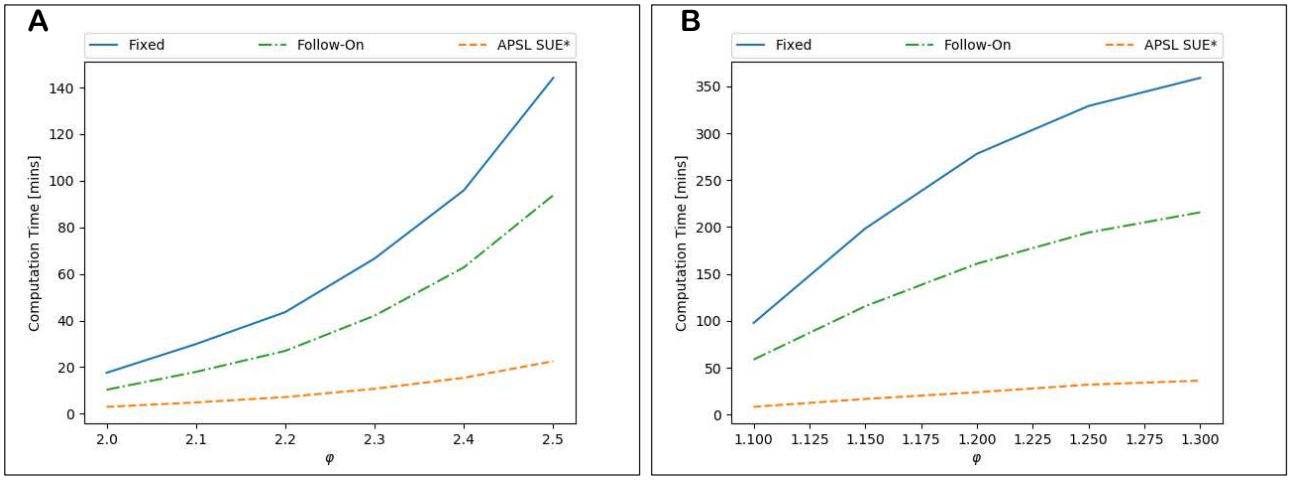

Fig. 24. Computation time for APSL SUE* and solving APSL SUE with follow-on and fixed initial FPIM conditions the choice set sizes are increased, scaled by φ. **A:** Sioux Falls. **B:** Winnipeg.

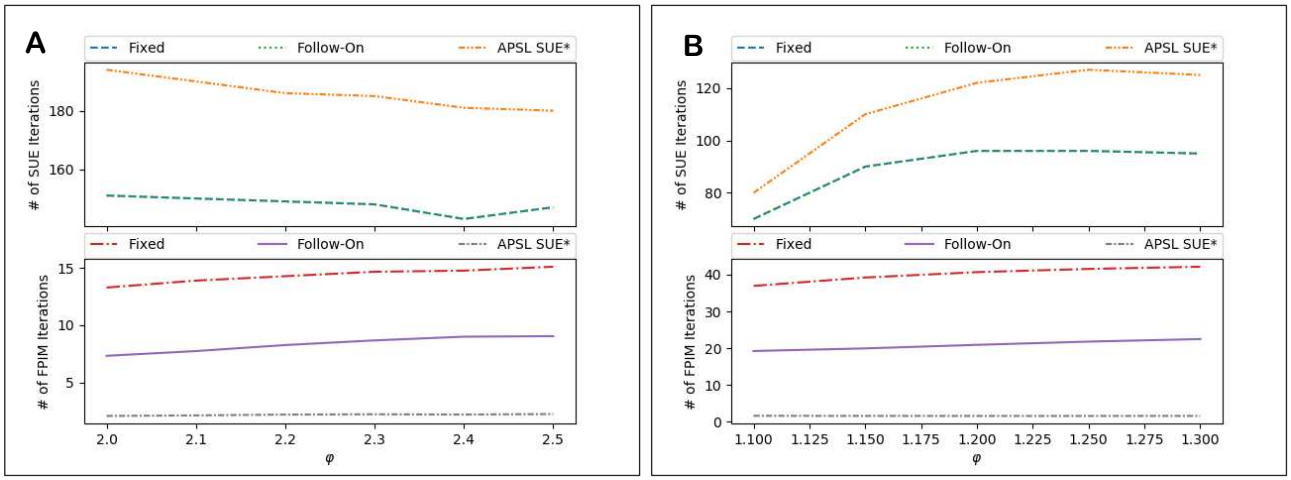

Fig. 25. Number of FAA iterations, and average number of FPIM iterations for APSL SUE* and solving APSL SUE with follow-on and fixed initial FPIM conditions the choice set sizes are increased, scaled by φ. **A:** Sioux Falls. **B:** Winnipeg.

8.2 Supplementary Material B – Computational Performance Sensitivity Analysis

We investigate here for all SUE models, how total computation times and number of FAA iterations vary according to different sizes of choice sets, levels of travel demand, and model parameters. Since we do not have calibrated model parameters, we perform sensitivity analysis by investigating the effects of choice set size and demand level on computational performance for fixed parameter settings, then explore how varying the parameters effects results (with fixed choice sets / demand).

Fig. 26A-B display for the Sioux Falls and Winnipeg networks, respectively, how the total computation times for the different SUE models vary as the choice set sizes are increased. Fig. 27A-B display how the required number of FAA iterations varies. As shown, for Sioux Falls, although the number of iterations required for convergence decreases for most of the models, computation times increase due to additional burden involved in computing choice probabilities / working with more routes. For APSL SUE, computation times increase significantly due also to the more burdensome fixed-point problems (i.e. Fig. 24/Fig. 25). For Winnipeg, the number of iterations requited for SUE convergence increases, increasing to the computational burden of larger choice sets.

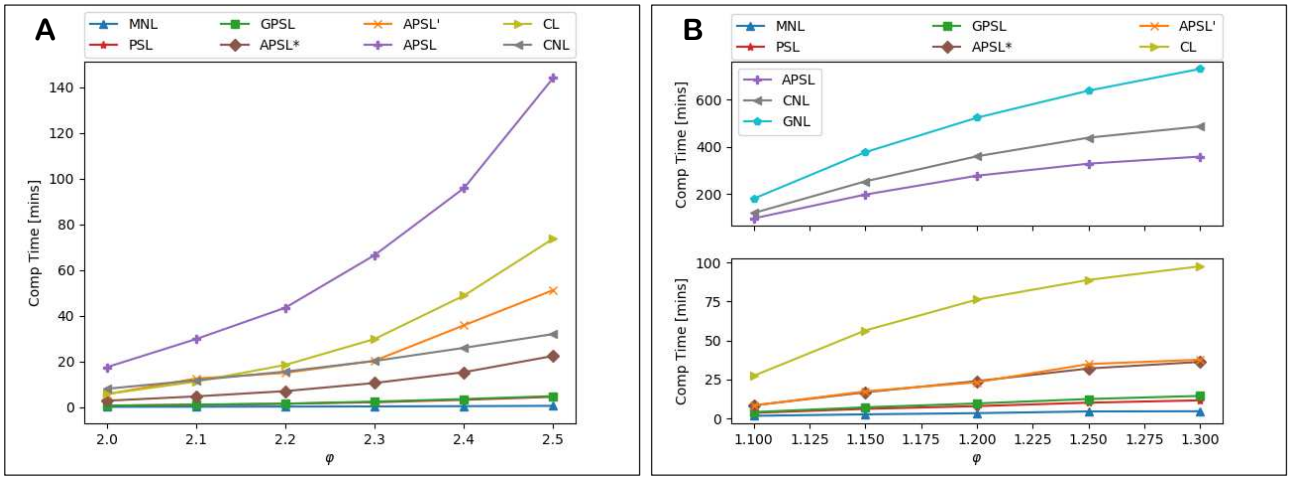

Fig. 26. Computation times for solving the SUE models as the choice set sizes are increased, scaled by φ. **A:** Sioux Falls. **B:** Winnipeg.

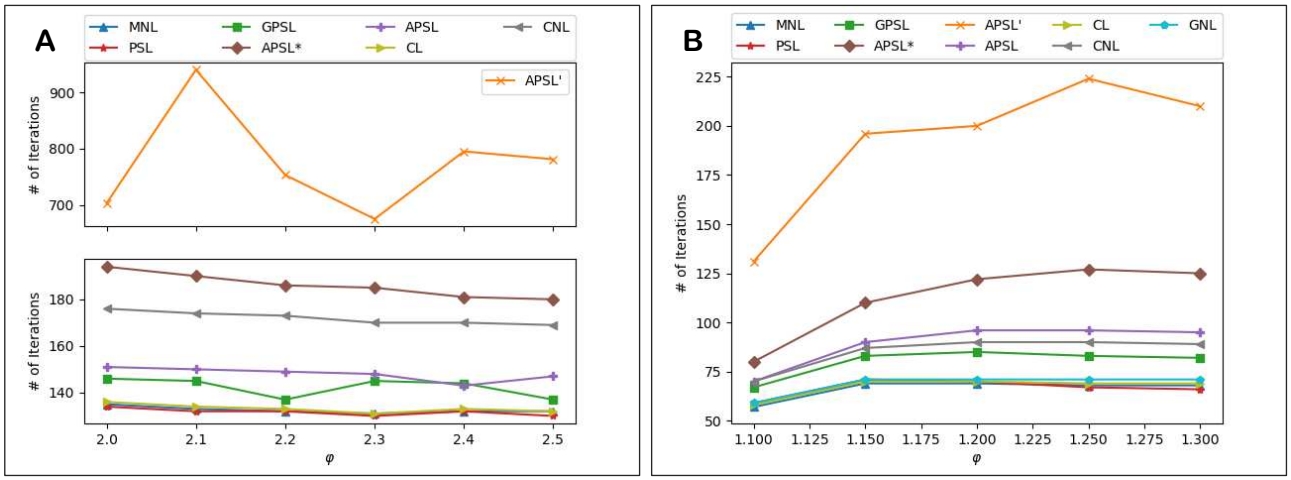

Fig. 27. Number of iterations required for convergence for the SUE models as the choice set sizes are increased, scaled by φ. **A:** Sioux Falls. **B:** Winnipeg.

Fig. 28A-B display for the Sioux Falls and Winnipeg networks, respectively, how the total computation times vary for the different SUE models as the level of travel demand is varied. Fig. 29A-B display how the required number of FAA iterations varies. The demand is scaled according to the parameter ω so that the demand for OD movement m is $\omega \cdot q_m$, $m = 1, \dots, M$. As shown, and as expected (due to logic and results from e.g. Chen et al (2012b,2014) for the non-additive traffic equilibrium problem and flow-independent PCL SUE model, respectively), the number of iterations required for convergence increases for all SUE models as the level of demand increases, thus increasing total computation times. APSL′ SUE experiences a significant increase for large demand.

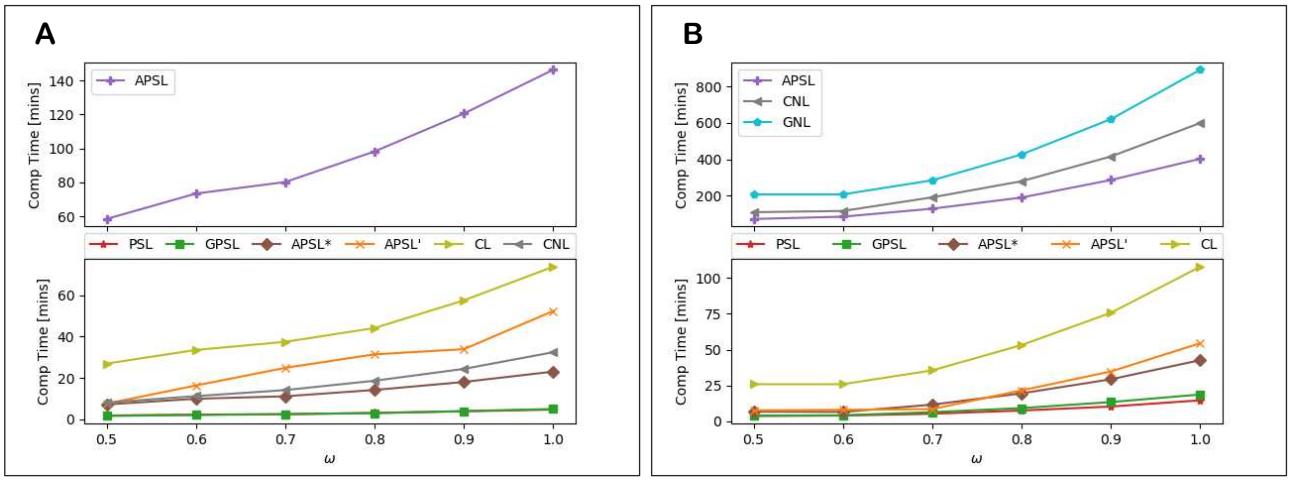

Fig. 28. Computation times for solving the SUE models as the level of travel demand is increased, scaled by ω. **A:** Sioux Falls. **B:** Winnipeg.

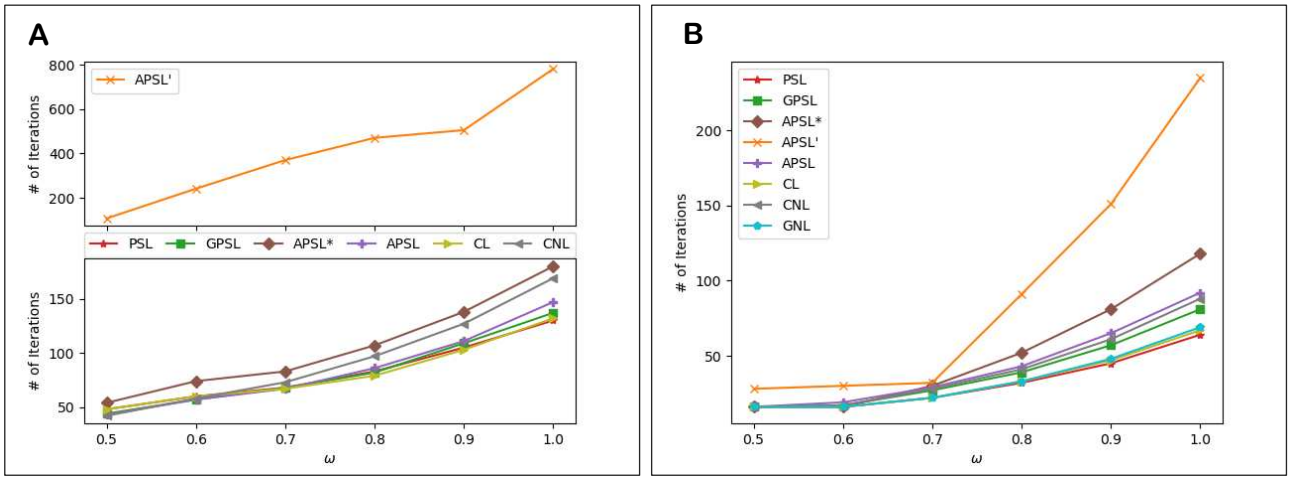

Fig. 29. Number of iterations required for convergence for the SUE models as the level of travel demand is increased, scaled by ω. **A:** Sioux Falls. **B:** Winnipeg.

Fig. 30A-B display for the Sioux Falls and Winnipeg networks, respectively, how the total computation times vary for the different SUE models as the common θ parameter is varied. Fig. 31A-B display how the required number of FAA iterations varies. As shown, apart from for APSL′ SUE on the Sioux Falls network, convergence for the SUE models generally gets slower as θ increases and the route cost differences are accentuated more resulting in greater flow fluctuations. Note that for the flow-dependent C-Logit SUE model, this is the same result found by Zhou et al (2012), Xu et al (2012).

Fig. 32A-B and Fig. 33A-B display how total computation times / number of iterations vary, respectively, for the CNL SUE model as the μ parameter is varied. As shown, for both networks, the number of iterations (and thus computation time) required for convergence decreases for greater values of μ, i.e. as CNL SUE increases in similarity to MNL SUE. This is a typical finding for CNL SUE models, e.g. Bekhor et al (2008a).

Fig. 34A-B display results for the GNL SUE model as the λ^{GNL} parameter is varied. As shown, the number of iterations (and thus computation time) required for convergence decreases for greater values of λ^{GNL}. Note that for $\lambda^{GNL} = 0$, GNL SUE is equivalent to MNL SUE (since $\lambda^{GNL} = 0$ results in $\mu_m = 1, m = 1, \dots, M$).

Fig. 35A-B and Fig. 36A-B display results for the GPSL SUE model as the λ^{GPS} parameter is varied. As shown, the number of iterations (and thus computation time) required for convergence increases for greater values of λ^{GPS}, where greater fluctuations occur within the path size contribution factors.

Fig. 37A-B and Fig. 38A-B display results for the PSL/GPSL/APSL SUE models as the common β parameter is varied. As shown, for APSL′ SUE and APSL SUE*, the number of FAA iterations increases exponentially with β. For the other models however, the effects are not as significant, though for APSL SUE – as also shown in Fig. 22/Fig. 23– total computation times increase exponentially with β due to the fixed-point probability computation.

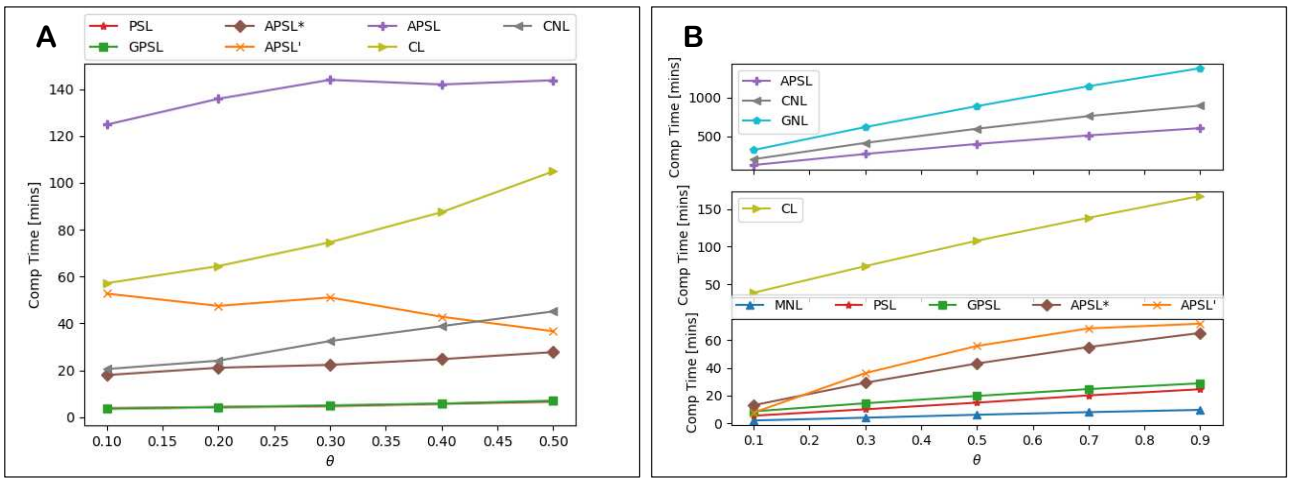

Fig. 30. Computation times for SUE convergence as θ is varied. **A:** Sioux Falls. **B:** Winnipeg.

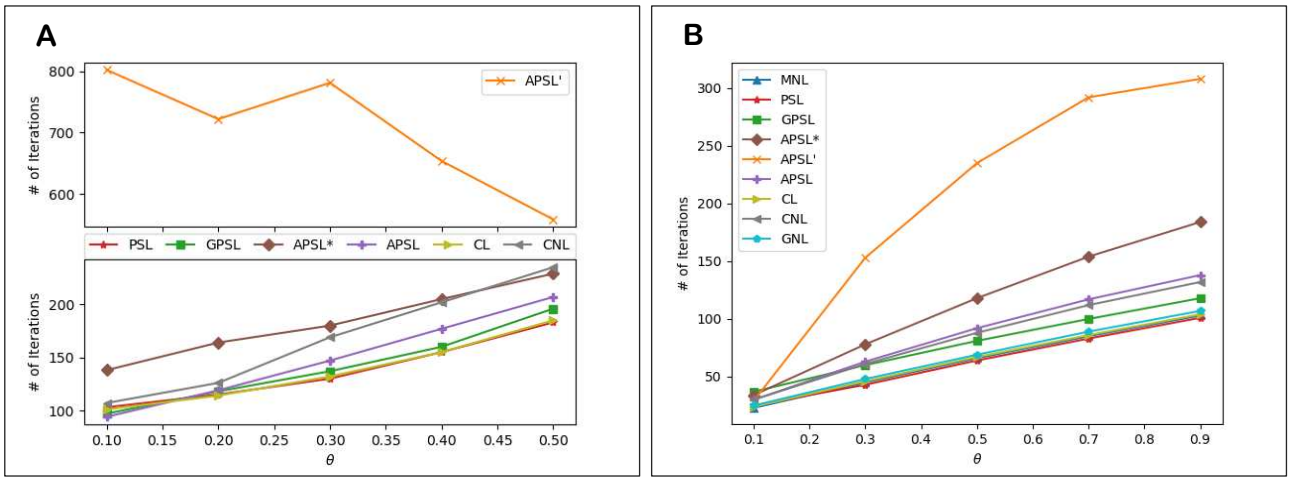

Fig. 31. Number of iterations required for SUE convergence as θ is varied. **A:** Sioux Falls. **B:** Winnipeg.

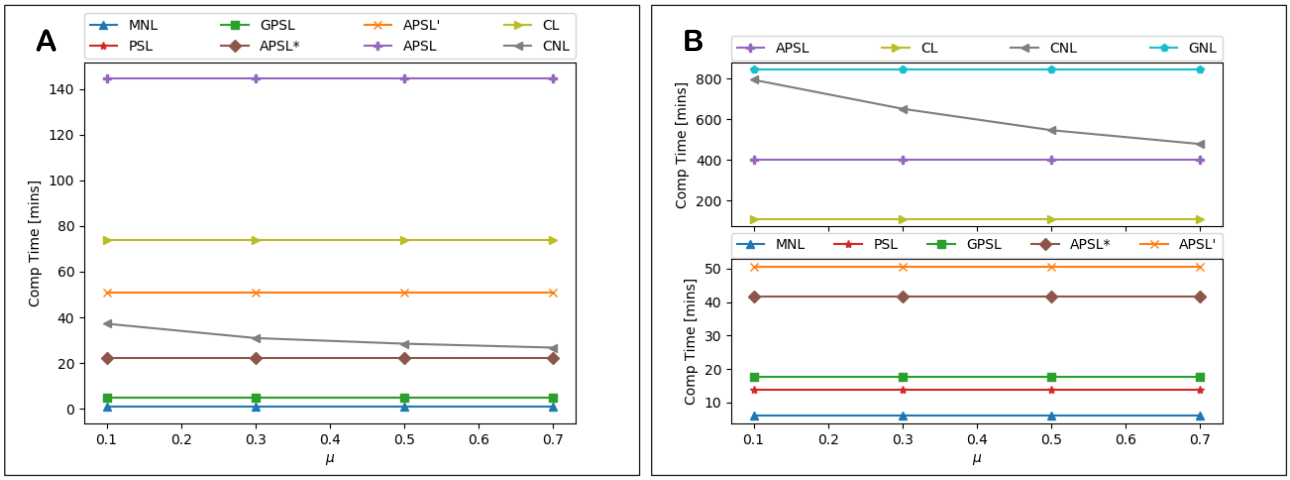

Fig. 32. Computation times for CNL SUE convergence as μ is varied. **A:** Sioux Falls. **B:** Winnipeg.

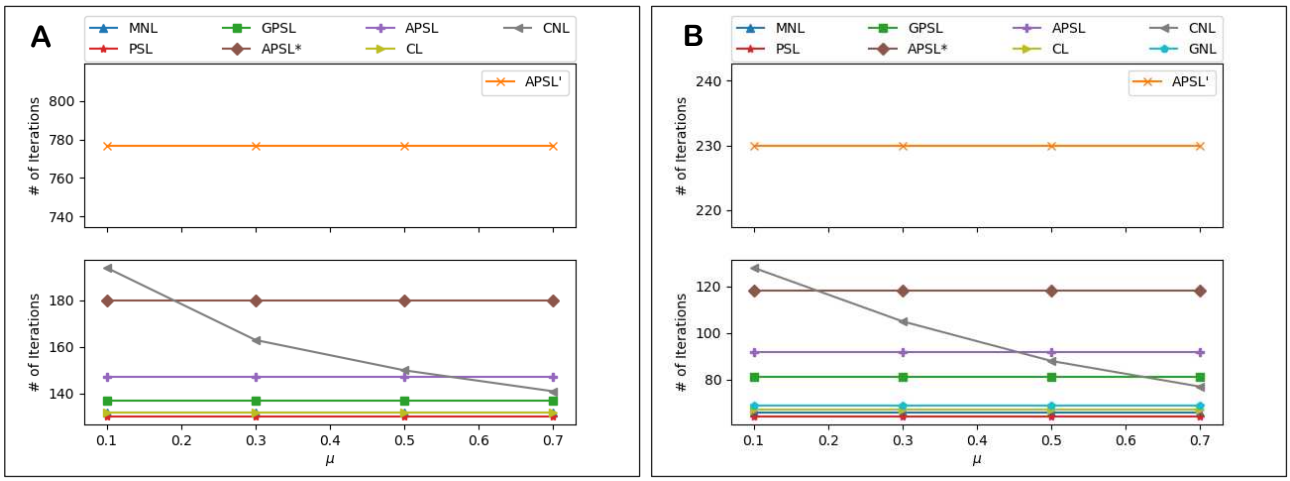

Fig. 33. Number of iterations required for CNL SUE convergence as μ is varied. **A:** Sioux Falls. **B:** Winnipeg.

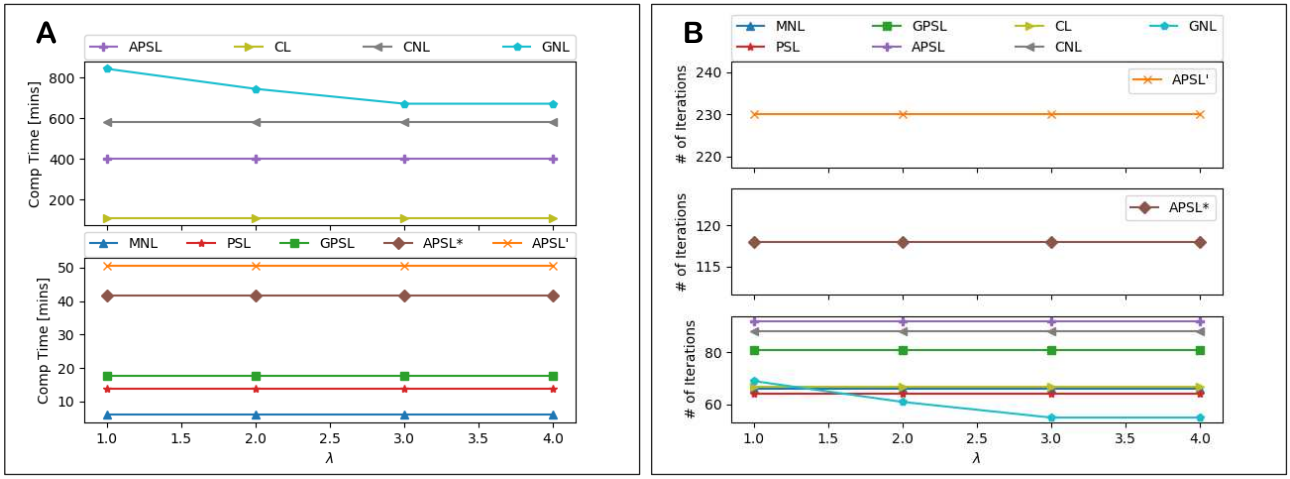

Fig. 34. Winnipeg: GNL SUE convergence as λ^{GNL} is varied. **A:** Computation time [mins]. **B:** Number of iterations.

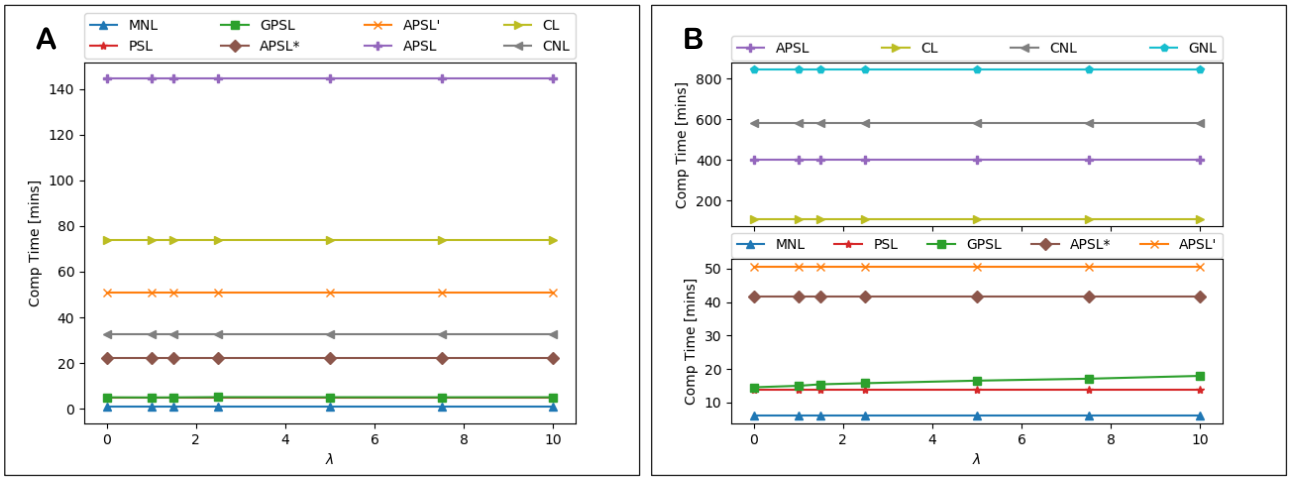

Fig. 35. Computation times for GPSL SUE convergence as λ^{GPS} is varied. **A:** Sioux Falls. **B:** Winnipeg.

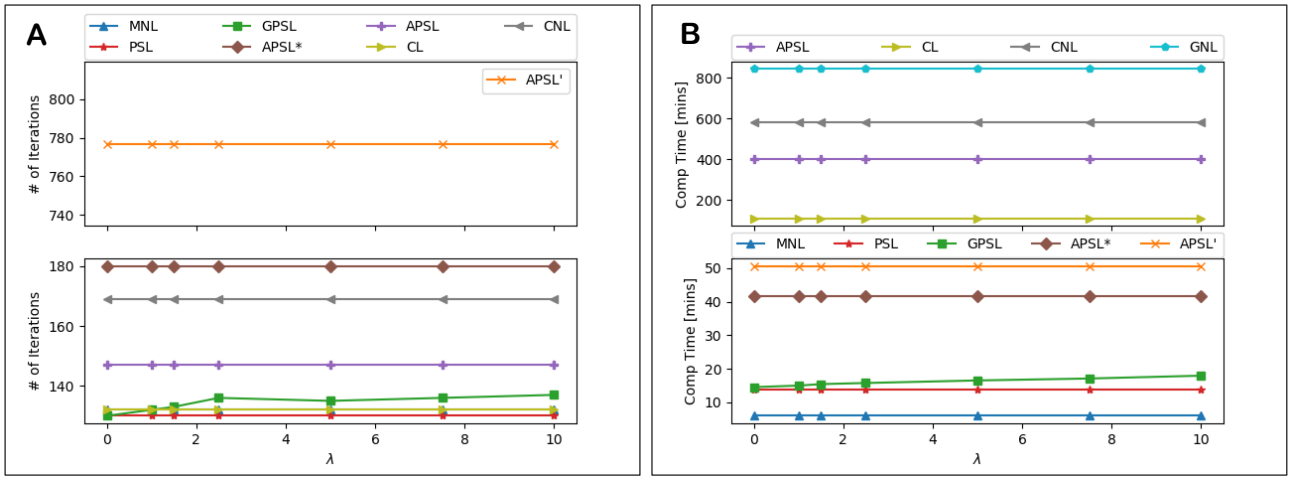

Fig. 36. Number of iterations required for GPSL SUE convergence as λ^{GPS} is varied. **A:** Sioux Falls. **B:** Winnipeg.

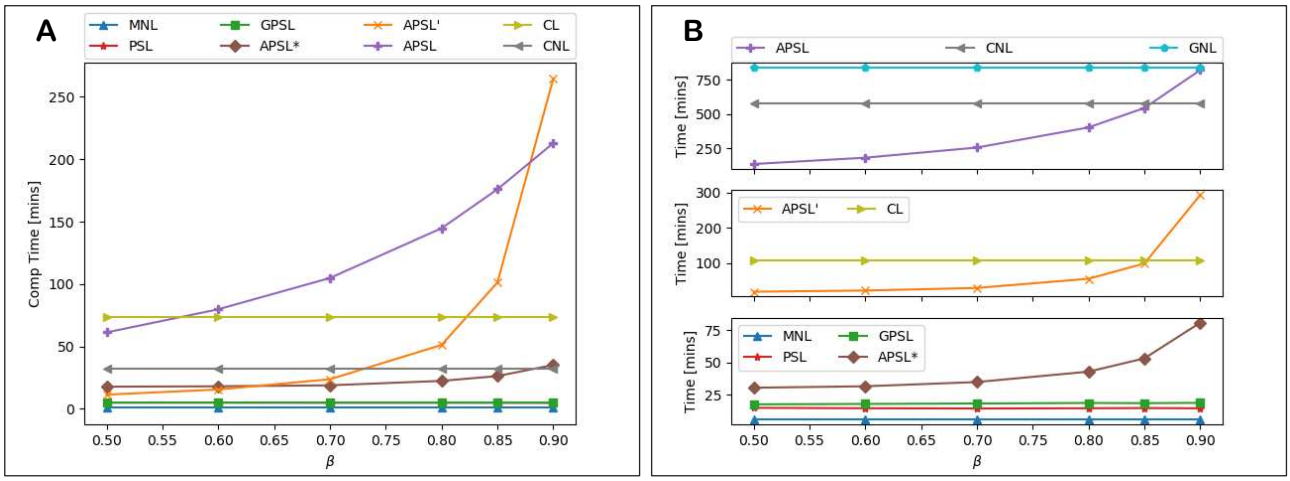

Fig. 37. Computation times for convergence for the Path Size Logit SUE models as β is varied. **A:** Sioux Falls. **B:** Winnipeg.

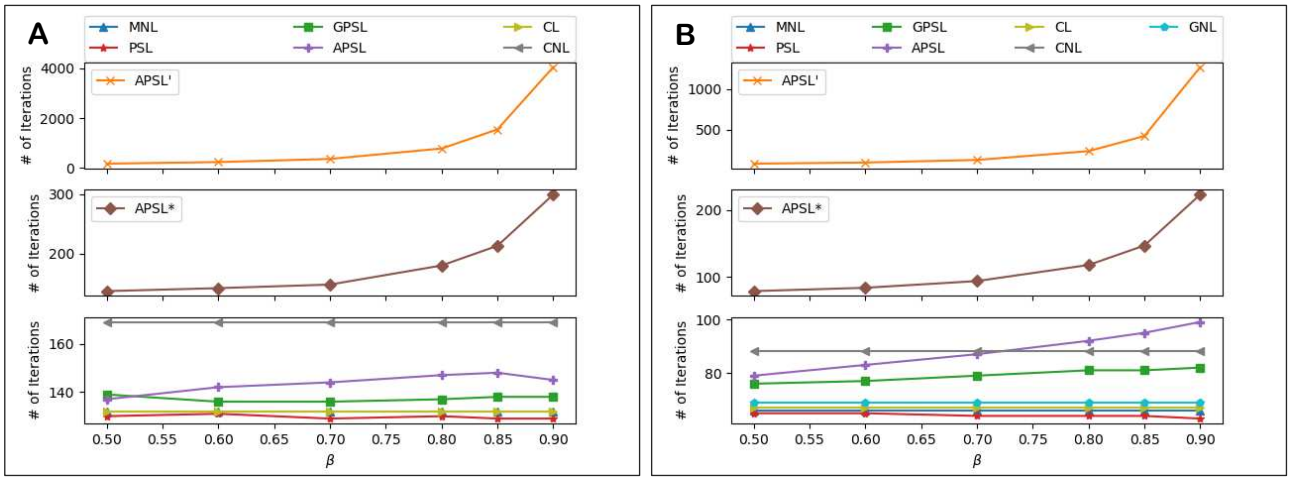

Fig. 38. Number of iterations required convergence for the Path Size Logit SUE models as β is varied. **A:** Sioux Falls. **B:** Winnipeg.

Lastly, Fig. 39A-B display for the Sioux Falls and Winnipeg networks, respectively, and for the different SUE models, how the number of iterations required for convergence varies for different settings of the MSWA parameter d. For MNL, PSL, GPSL, & APSL SUE, $d = 5$ and $d = 10$ provide roughly the best convergence for Sioux Falls and Winnipeg, respectively. As shown, for APSL′ SUE and APSL SUE*, convergence improves significantly with greater values of d, though for APSL SUE* the number of FPIM iterations and ξ value has been 'optimised' for $d = 15$.

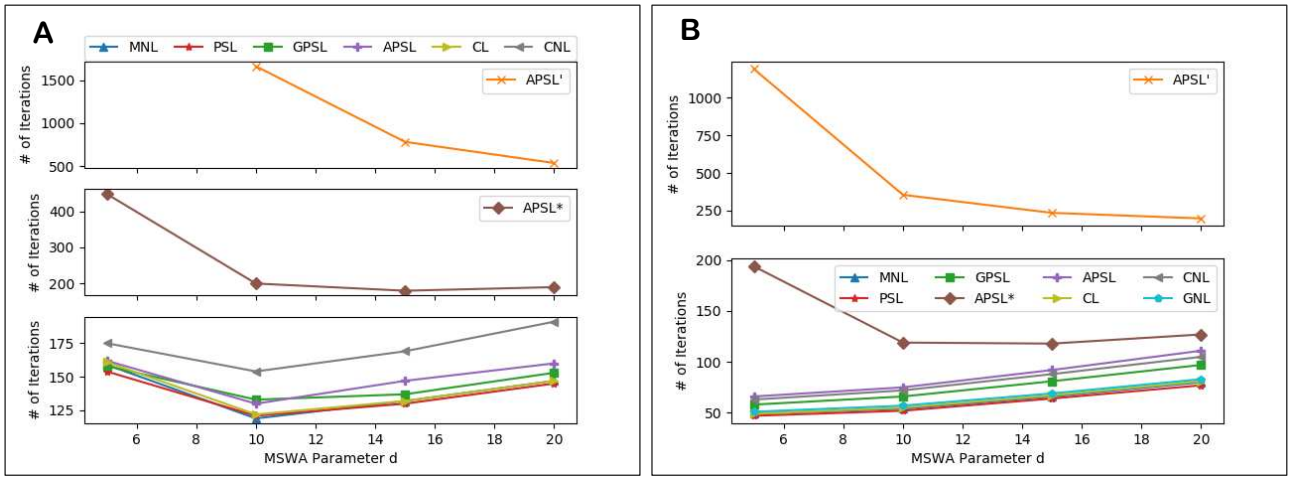

Fig. 39. Number of iterations required for SUE convergence for varying settings of the MSWA parameter d. **A:** Sioux Falls. **B:** Winnipeg.

8.3 Supplementary Material C – Uniqueness of APSL SUE Solutions

In this section, we explore the uniqueness of APSL SUE solutions. For some of the experiments, we consider a small example network (Fig. 40) that consists of 3 nodes, 4 links, and 1 OD movement (with demand 200). The BPR function parameters are $D = 0.15$, $B = 4$, $K_a = 100$ for all links, and $T_{0,a}$ for each link is shown in Fig. 40. The working choice set utilises all 4 routes, where the routes are Route 1: $1 \rightarrow 3$, Route 2: $1 \rightarrow 4$, Route 3: $2 \rightarrow 3$, Route 4: $2 \rightarrow 4$.

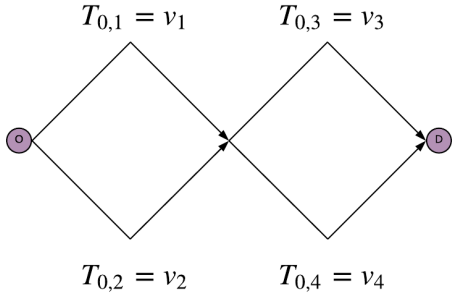

Fig. 40. Small example network.

As demonstrated in Duncan et al (2020), for a given setting of the link costs $\boldsymbol{t}$ and θ value, a β value exists, $\beta_{max,m}(\boldsymbol{t},\theta) > 0$, for OD movement m such that APSL choice probability solutions are unique for all β in the range $0 \leq \beta \leq \beta_{max,m}(\boldsymbol{t},\theta)$. This means that a β value exists, $\beta_{max}(\boldsymbol{t},\theta) > 0$, such that solutions are unique for all OD movements for all β in the range $0 \leq \beta \leq \beta_{max}(\boldsymbol{t},\theta)$, i.e. $\beta_{max}(\boldsymbol{t},\theta) = \min\left(\beta_{max,m}(\boldsymbol{t},\theta)\right)$. And, assuming the link costs are bounded, i.e. they have a maximum and minimum value (for example due the fixed demands), for a given θ value, a β value exists, $\bar{\beta}_{max}(\theta) > 0$, such that APSL solutions are unique for all OD movements and for all feasible flow vectors (and thus costs) for all β in the range $0 \leq \beta \leq \bar{\beta}_{max}(\theta)$. Obviously, $\bar{\beta}_{max}(\theta) \leq \beta_{max}(\boldsymbol{t},\theta) \leq \beta_{max,m}(\boldsymbol{t},\theta)$.

While it is not guaranteed that in all cases APSL SUE solutions will be unique when APSL probabilities are universally unique, i.e. for β in the range $0 \leq \beta \leq \bar{\beta}_{max}(\theta)$, as we show below, it appears from numerical experiments that this is often the case.

Fig. 41A-B plot, for two runs, the small example network route flows at each iteration of the FAA when the initial conditions for the FPIM computing the APSL probabilities are randomly generated, for $\beta = 0.9$ and $\beta = 1.1$, respectively, $v_1 = 2$, $v_2 = v_3 = v_4 = 1$, $\theta = 1$, $\xi = 8$. The step-size is set as $\eta_n = 1$ ($n = 1,2,\ldots$) and the algorithm is stopped after 20 iterations if convergence is not reached. As shown, for $\beta = 0.9$, because the APSL probabilities are unique for the route costs (from the flows) at each iteration, the route flows on both runs converge in the same way to the same APSL SUE solution. For $\beta = 1.1$, however, as demonstrated clearly at iteration 1, there are multiple APSL probabilities for the route costs at each iteration, and hence due to the step-size the flows fluctuate randomly and do not converge. This suggests that APSL probability solutions are universally unique for $\beta = 0.9$, but not for $\beta = 1.1$, and hence that $0.9 \leq \bar{\beta}_{max}(1) < 1.1$.

Fig. 42A-B plot for $\beta = 0.9$ and $\beta = 1.1$, respectively, and for multiple runs, the flows at each iteration of the FAA utilising follow-on initial conditions for the FPIM computing the APSL probabilities, where the initial SUE conditions are randomly generated, $v_1 = 2$, $v_2 = v_3 = v_4 = 1$, $\theta = 1$, $\xi = 8$. As shown, for $\beta = 0.9$, all initial conditions lead to the same solution, whereas for $\beta = 1.1$, two solutions are found with different initial conditions. Fig. 43A-B plot the flows at each iteration of the FAA for solving APSL′ SUE. As shown, for $\beta = 0.9$, all initial conditions again lead to the same solution, whereas for $\beta = 1.1$, two solutions are found.

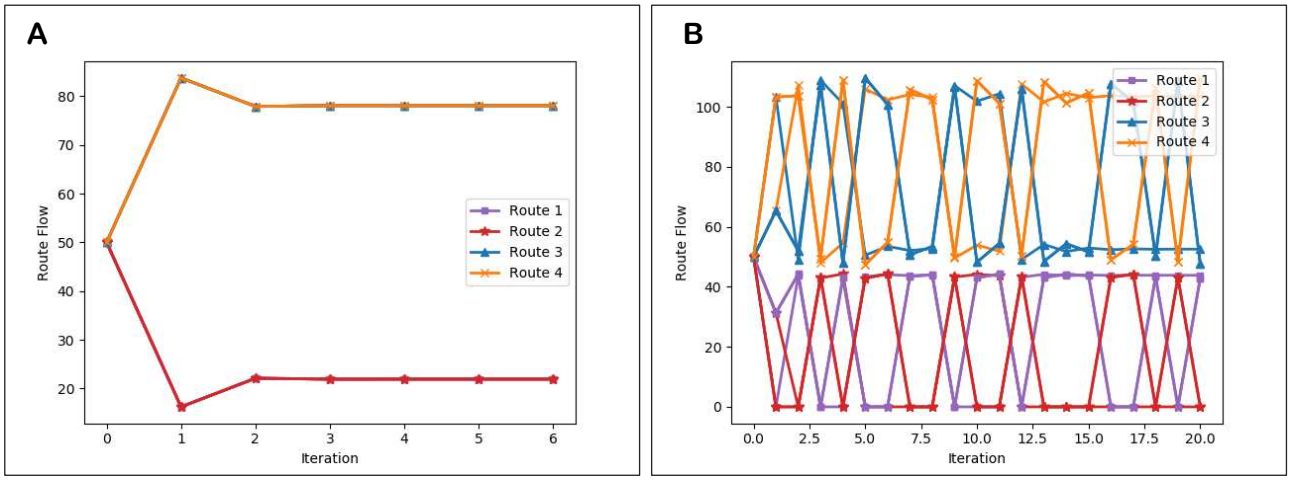

Fig. 41. Small example network: APSL SUE route flows at each iteration of the FAA with randomly generated initial FPIM conditions, two runs ($v_1 = 2$, $v_2 = v_3 = v_4 = 1$, $\theta = 1$, $\xi = 8$). **A:** $\beta = 0.9$. **B:** $\beta = 1.1$.

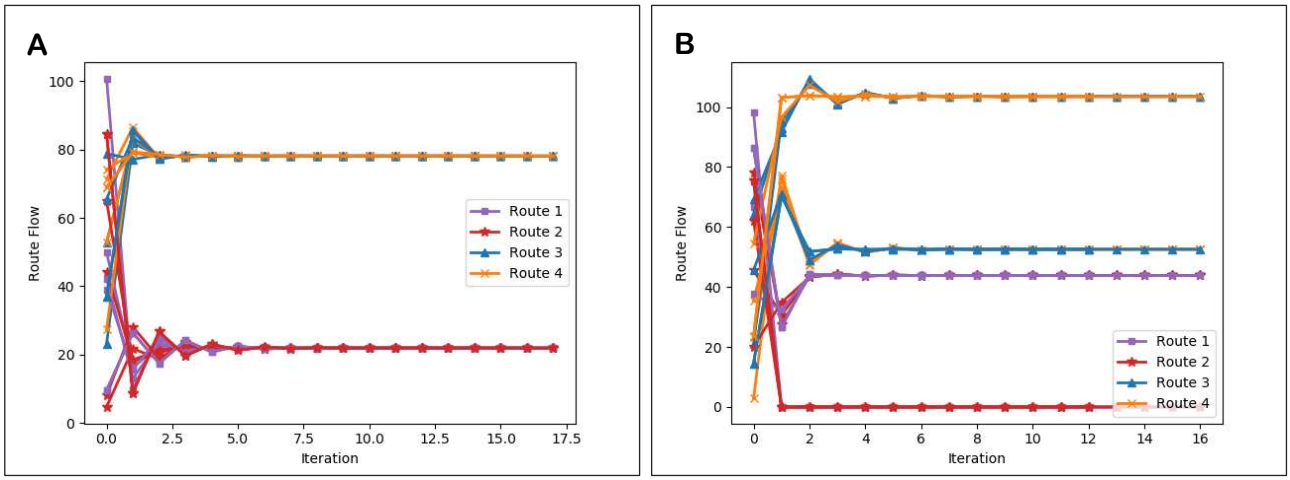

Fig. 42. Small example network: APSL SUE route flows at each iteration of the FAA with follow-on FPIM initial conditions and randomly generated initial SUE conditions, multiple runs ($v_1 = 2$, $v_2 = v_3 = v_4 = 1$, $\theta = 1$, $\xi = 8$). **A:** $\beta = 0.9$. **B:** $\beta = 1.1$.

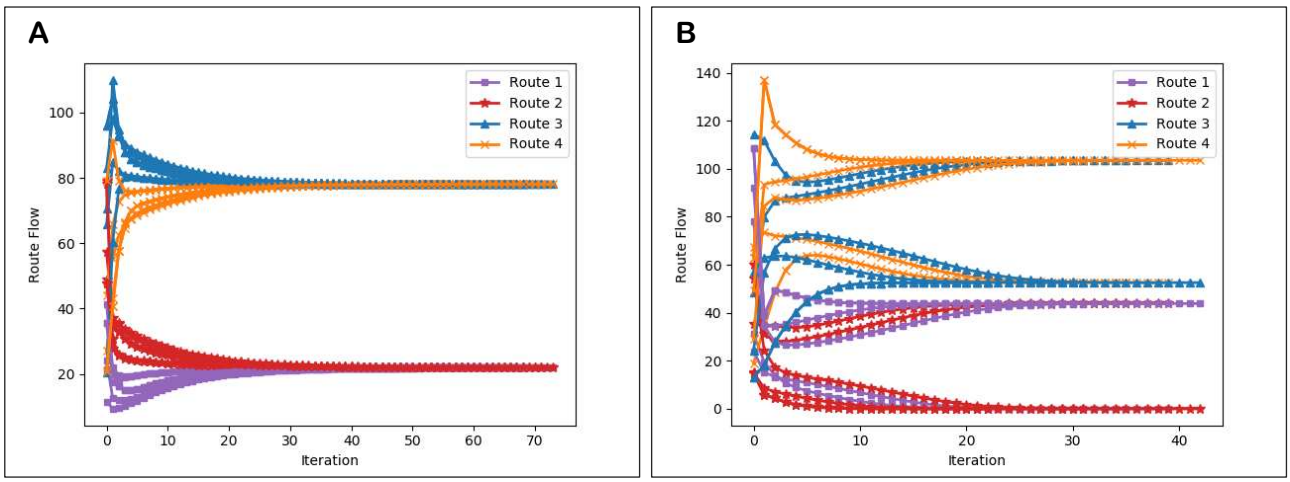

Fig. 43. Small example network: APSL′ SUE route flows at each iteration of the FAA with randomly generated initial SUE conditions, multiple runs ($v_1 = 2$, $v_2 = v_3 = v_4 = 1$, $\theta = 1$). **A:** $\beta = 0.9$. **B:** $\beta = 1.1$.

Fig. 42 & Fig. 43 suggest that the APSL SUE solution is unique for $\beta = 0.9$, and solutions are non-unique for $\beta = 1.1$, and Fig. 41 suggests that this due to the APSL choice probability solutions being universally unique for $\beta = 0.9$, but not for $\beta = 1.1$. One can imply from this that $0.9 \leq \bar{\beta}_{max}(1) < 1.1$, and potentially that APSL SUE solutions are unique for β in the range $0 \leq \beta \leq 0.9 \leq \bar{\beta}_{max}(1)$.

Duncan et al (2020) demonstrate how APSL choice probability solutions for OD movement m are unique for β in the range $0 \leq \beta \leq \beta_{max,m}(\boldsymbol{t}, \theta)$. Here, we utilise a similar method to that described in Section 4.4 of Duncan et al (2020) for the APSL model, to attempt to identify $\bar{\beta}_{max,m}(\theta)$ values and thus $\bar{\beta}_{max}(\theta) = \min\left(\bar{\beta}_{max,m}(\theta): m = 1, \dots, M\right)$ for the APSL SUE model, where the costs are not fixed. $\bar{\beta}_{max,m}(\theta)$ is estimated by plotting trajectories of APSL SUE solutions for OD movement m for varying β, and identifying where a unique trajectory of solutions ends and multiple trajectories begin. A simple method for obtaining trajectories of APSL SUE solutions is as follows:

Step 1. Identify a suitably large value for β (where it is predicted that solutions will be non-unique).

Step 2. Solve APSL SUE for this large β with a randomly generated SUE initial condition.

Step 3. Decrement β and obtain the next APSL SUE solution with the SUE initial condition set as the solution for the previous β.

Step 4. Continue until a suitably low value of β (where it is predicted that solutions will be unique).

By plotting the route flows for OD movement m at each decremented β, and repeating this method several times, one can determine where non-unique solution trajectories end and hence estimate $\bar{\beta}_{max,m}(\theta)$. If after several repetitions (with different randomly generated initial conditions) only a single trajectory of solutions is shown, then the initial large β value is increased. Similarly, if only multiple trajectories are shown, the stopping low β value is decreased. However, one can test beforehand whether the initial and stopping β values are suitable by solving for each a few times with

random initial conditions and observing whether there are different solutions for the initial β value and the same solution for the stopping β. In the experience of the authors, the $\bar{\beta}_{max,m}(\theta)$ values typically range between 0.9 and 1.1 (usually around 1). If in large-scale networks it is computationally burdensome to solve APSL SUE once at a time for each decremented value of β, then one can instead (by possibly harnessing parallel processing) solve for different β values simultaneously, each with randomly generated initial conditions. This should also identify where solutions are and are not unique. Moreover, one can plot flow trajectories for all OD movements simultaneously, so the method does not need to be repeated for each OD movement. We illustrate the approach graphically here, but there is no need to draw graphs for general networks. One can instead observe the route flow values, where a finer grained decrement of β will provide a more accurate estimation of $\bar{\beta}_{max,m}(\theta)$.

In the case of the small example network where there is a single OD movement, we estimate $\bar{\beta}_{max}(1)$ using the above method. Fig. 44 displays trajectories of APSL SUE route flow solutions as the β parameter is varied for $v_1 = 2$, $v_2 = v_3 = v_4 = 1$, $\theta = 1$, $\xi = 8$. β was decremented by 0.005 and the initial large β value was 1.2. The solution trajectory plotting was repeated until multiple trajectories were shown. As shown, there is a unique trajectory of route flow solutions up until $\beta = \bar{\beta}_{max}(1)$ where there then becomes multiple trajectories. The estimated $\bar{\beta}_{max}(1)$ value is 0.995. While two APSL SUE solutions were found for $\beta = 1.1$ in Fig. 42B & Fig. 43B, Fig. 44 shows that there are three solutions.

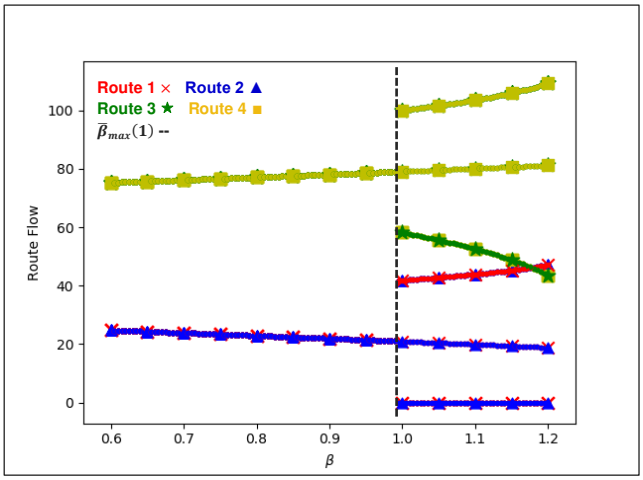

Fig. 44. Small example network: Trajectories of APSL SUE solutions as β is varied ($v_1 = 2$, $v_2 = v_3 = v_4 = 1$, $\theta = 1$, $\xi = 8$).

We use the same technique of plotting flow trajectories to estimate the APSL SUE uniqueness conditions for the Sioux Falls and Winnipeg networks. Fig. 45 displays for Sioux Falls the maximum route flow from three trajectories of APSL SUE solutions as the β parameter is varied for four different randomly chosen OD movements. β was decremented by 0.005, and the initial large β and stopping small β values were $\beta = 1.1$ and $\beta = 0.9$, respectively. As shown, the $\bar{\beta}_{max,m}(0.01)$ values for these OD movements appear to be close to 1. Fig. 46 display results for the Winnipeg network (two trajectories are plotted), where the $\bar{\beta}_{max,m}(0.5)$ values also appear to be close 1.

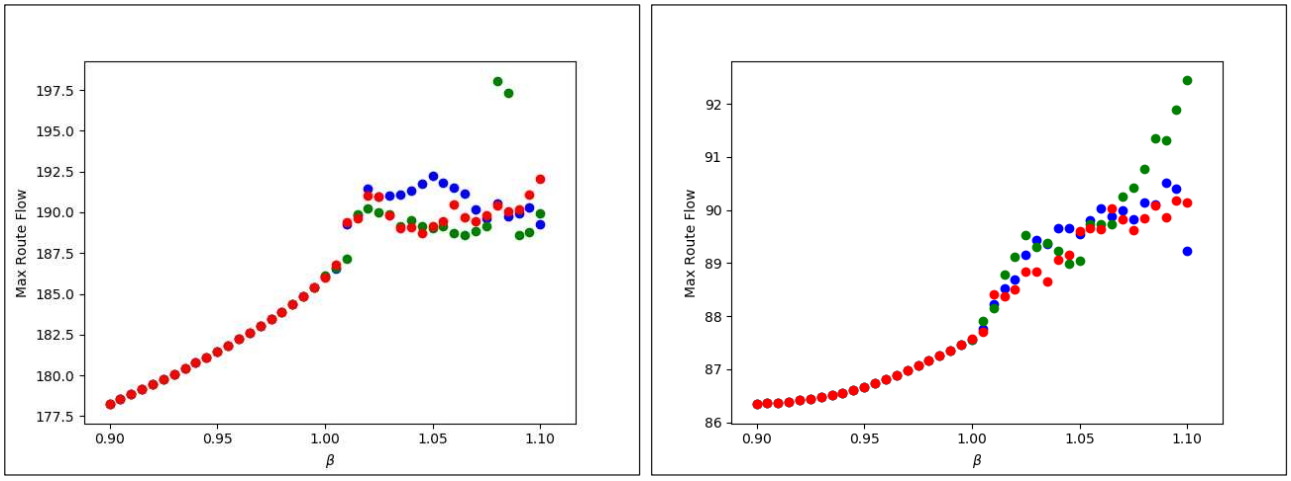

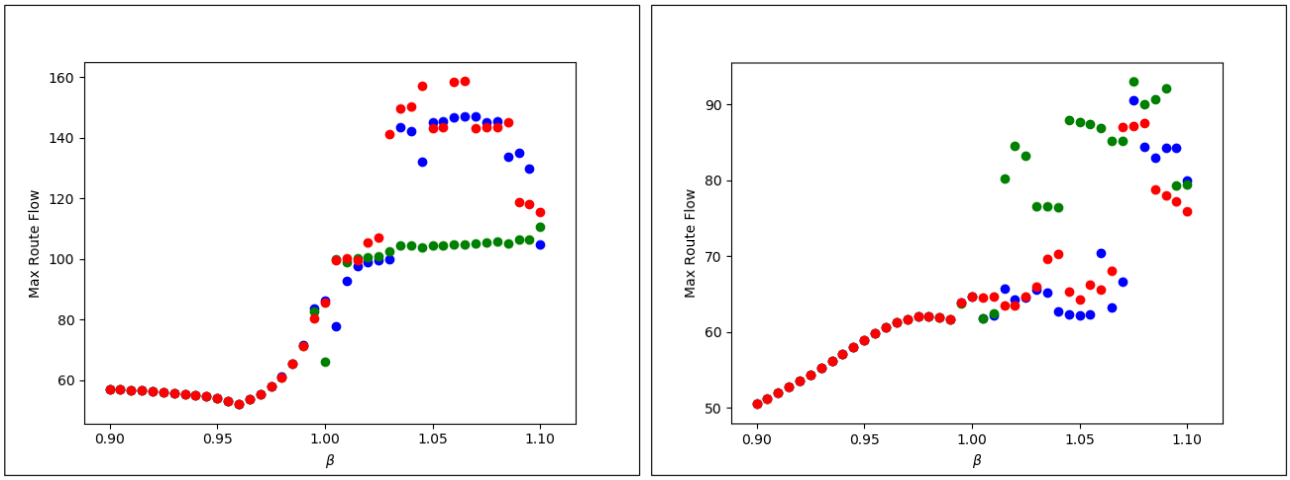

Fig. 45. Sioux Falls: Maximum route flow for four different OD movements from three trajectories of APSL SUE solutions as β is varied.

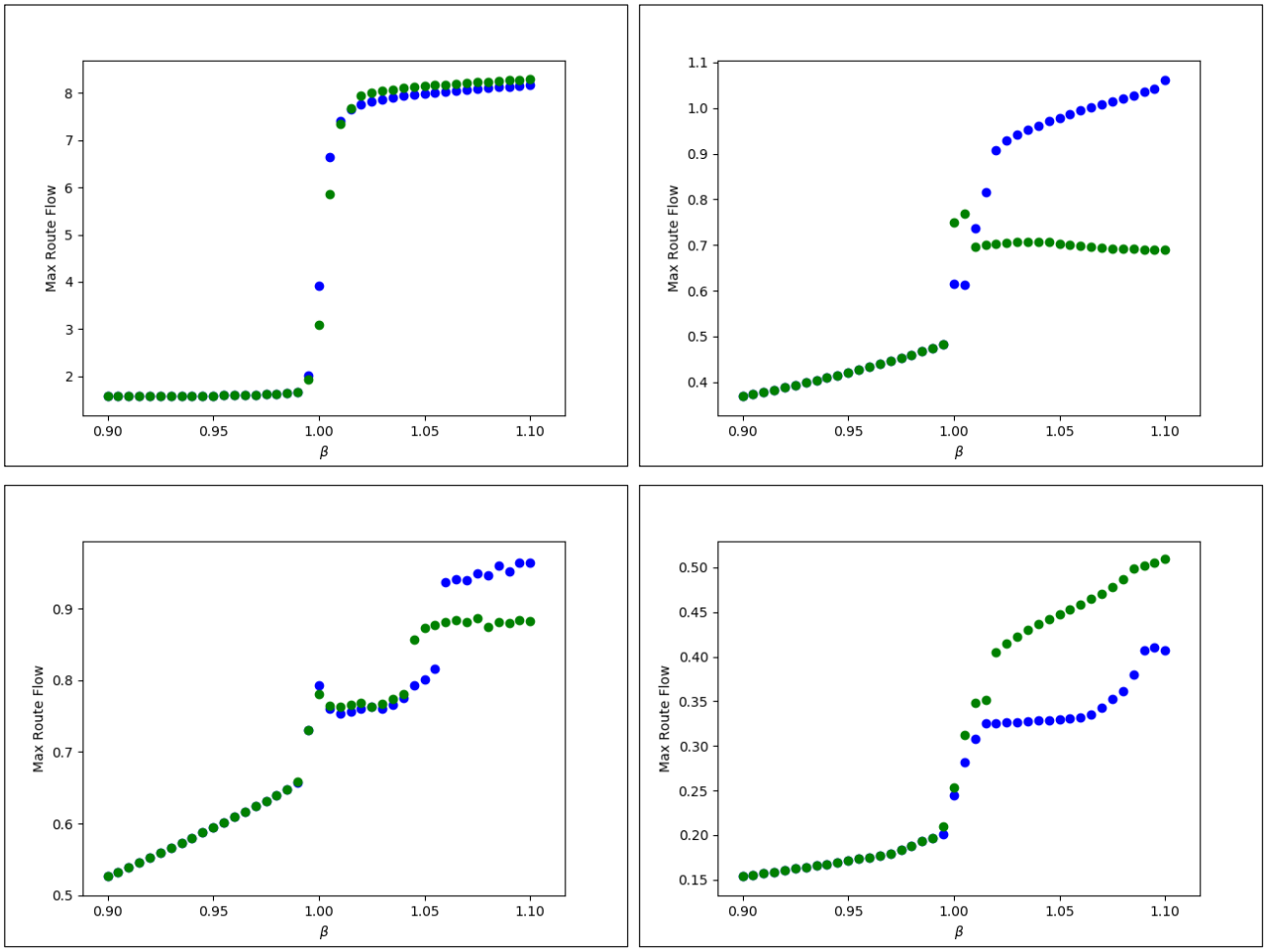

Fig. 46. Winnipeg: Maximum route flow for four different OD movements from two trajectories of APSL SUE solutions as β is varied.

In our experience, the ranges of β that exist for the uniqueness of APSL and APSL SUE solutions provide enough scope for fitting to behaviour, where typical β_{max} values range between 0.9 and 1.1. Duncan et al (2020) experienced no difficulties in estimating APSL on a real-life large-scale network, and obtained a maximum likelihood estimate of $\beta = 0.84$, where it was verified that this was within the uniqueness range. Although there are obvious differences in the models, we note that this 'safe' range for β for APSL uniqueness also includes values for β reported in empirical studies with PSL & GPSL (e.g. Ramming, 2002, Bovy et al, 2008, Hoogendoorn-Lanser et al, 2005; Frejinger & Bierlaire, 2007; Prato, 2013), where estimated values have been reported in the range 0.6 to 0.93. We also emphasise that, as per Duncan

et al (2020), the recommendation is that the APSL model is only used when solutions are unique. Thus, since we are not concerned with APSL when solutions are non-unique, and the uniqueness range provides enough scope for fitting to behaviour, it is an important and encouraging finding that APSL SUE solutions are unique when APSL solutions are unique.